Study on Shear Strengthening of RC Structures by Bonding Ultra High Strength Fiber Reinforced Concrete Panels

Wang, Jian

(Degree)
博士（工学）

(Date of Degree)
2015-03-25

(Date of Publication)
2017-03-25

(Resource Type)
doctoral thesis

(Report Number)
甲第6429号

(URL)
https://hdl.handle.net/20.500.14094/D1006429

Doctoral Dissertation

Study on Shear Strengthening of

RC Structures by Bonding Ultra High Strength

Fiber Reinforced Concrete Panels

（超高強度繊維補強コンクリートパネル接着による

鉄筋コンクリート構造物のせん断補強に関する研究）

January 2015

Graduate School of Engineering

Kobe University

Jian Wang

Contents

Acknowledgements

CHAPTER 1

Introduction

1.1.   BACKGROUND

Concrete as one of the most important construction materials has been studied for centuries. Especially since Reinforced Concrete (RC) was patented by Joseph Monier in 1849, the development of concrete material has stepped into a new age. With the countries' tremendous economic growth and rapid development, a large amount of RC bridges have been built since 1960s. As time went on, those RC bridges have been aging or deteriorated, which leads to an increase of the accident risks. Now, how to deal with these aging or deteriorated RC bridges becomes a very urgent issue.

In recent decades, many researchers have been working on how to upgrade the capabilities of the aging or deteriorated RC bridges. Some methods have been proposed to strengthen the flexural capacity of RC bridges, such as strengthening with Fiber Reinforced Polymer (FRP)[1-4]. However, some of aging RC bridges were poorly designed and/or poorly constructed, and the concrete strength is comparatively low or even lower

than the design value. At the end of the bridge girder, since the rainwater can not be drained in short order, it is easy to cause the corrosion in the rebars there (especially stirrups), then the shear capacity and the bond performance of rebars may be degraded[5]. Considering both factors of the low concrete strength and the deteriorated rebars (especially stirrups) in the aging RC bridges, the possibility of shear failure would be higher than that of flexural failure. As a dangerous brittle failure mode, more attention should be paid on the shear failure, and the corresponding strengthening methods should be further investigated and developed.

Fig. 1.1 shows one of the aging bridges built in 1960s in Japan. Due to the low concrete strength and the heavy load, the shear cracks have already occurred in the girder end of this bridge. To ensure the transportation security as well as to meet the transport demand, the shear capability of this aging bridge (shown in Fig. 1.1) should be strengthened. Till

Fig. 1.1. Girder end of an aging bridge built in 1960s in Japan.

now, some materials have been investigated to be used to strengthen the shear capability in RC bridges, such as the steel plate[6-10] and FRP[11-15]. The safety and effectiveness of the shear strengthening performance using these materials have also been evaluated on RC bridges. However, there exist some limitations of those materials. For example, the steel plate is low corrosion/chemical resistances and the workability is still insufficient due to the heavy weight. On the other hand, FRP is limited by its comparatively low strengthening effectiveness and the possibility of unpredictable debonding failure[16]. Thus, further investigation and improvement of the shear strengthening materials are still needed. An ideal shear strengthening material should be capable of overcoming these limits mentioned above and also meeting the requirements of high durability, workability, efficiency and reliability. Here, a substitute strengthening material, Ultra High Performance Fiber Reinforced Concrete (UHPFRC), was considered to improve the shear capability and safety of the aging RC bridges.

1.2.   OBJECTIVE

In order to meet the requirements of high durability, efficiency, reliability, short-duration and low-cost, Ultra High Strength Fiber Reinforced Concrete (UFC), a type of UHPFRC products was developed in France in 1990s with the high compressive strength (up to 750MPa) and high tensile strength (up to 100 MPa)[17]. In this study, a new shear strengthening method, bonding the panels made of UFC on the girder end of aging RC bridges, was proposed. The principle of the proposed shear strengthening method is to retard the opening and propagation of cracks around the ends of the RC beams by bonding UFC panels. There exist amounts of causes to rise worse structural performance for RC structures, such as physical damage and chemical deterioration. The strengthening effectiveness of bonding UFC panels on the RC structures with concrete degradation problem, such as the initial defect (low concrete strength), chloride attack and Alkali-Silica Reaction (ASR) damage will be discussed in this study.

3

1.3.   LITERATURE REVIEW

Fiber Reinforced Concrete (FRC) as a type of modern reinforced concrete was proposed in the middle of last century, where uniformly dispersed and randomly oriented short discrete fibers were mixed, aiming at ameliorating either the brittle failure or shrinkage cracking[18-20]. Later, to find a proper mix and to achieve a high performance effect on the RC, different types of fiber, volume fraction and additive compositions were explored[21-26]. Moreover, to find out a proper way to determine the FRC properties such as tensile, compressive and flexural behaviors, numerous types of testing methods were developed[27-30]. Based on the above fundamental studies, FRC has been applied in the structural practices as the supplementary structural members[31]. Also, FRC was considered to be used in the precast concrete to increase the strength and ductility in real structures[32,33].

Due to the excellent properties of FRC, such as high durability, workability, and corrosion resistance, FRC has been considered for repairing or strengthening the aging or damaged RC structures. Mesbah et al. applied FRC to strengthen the flexural behavior of RC beams, where RC beams were strengthened under different compositions and their flexure properties were tested[34]. The results showed that the load bearing capacity of damaged RC beams could be restored and the thinner cracks were observed in the repaired RC beams strengthened by FRC. More strengthening studies using FRC have been conducted on the low strength concrete beams and a remarkable improvement of strength and ductility have been demonstrated[35,36] (Boscato et al., 2009; Martinola et al., 2010; Rosignoli et al., 2012). On the other hand, FRC was also treated as a repair material to replace the damaged materials in the aging structures, such as the Ductile Fiber Reinforced Cementitious Composite (DFRCC), which is a high performance cementitious composite with superior strain capacity[37]. However, in Kim's study[37], the shear behavior of the RC specimens repaired by DFRCC had not been improved, as compared to the RC specimens without DFRCC strengthening.

With the development of technology, a new type of FRC product named as UHPFRC is attracting high attention and has already been applied in some projects[38-41]. UHPFRC is

of good qualities in terms of compression, ductility and reliability[42-50]. Recently, based on the superior properties of UHPFRC, some researchers proposed some repairing methods by using UHPFRC products. Tayeh et al. used UHPFRC as newly overlay repair material for the interfacial bonding between the deteriorated concrete structures, and the results showed the overlay technique using UHPFRC gained high bond strength. In other words, UHPFRC could be a good alternative to the usual overlay materials[51]. Iskhakov et al. proposed a repairing method to raise the flexural capacity and the ultimate deformations by casting the Steel Fibered High Strength Concrete (SFHSC) in the compressed zone[52]. The experimental results showed an effective ductile behavior up to failure. However, the unexpected de-bonding between concrete layers led this method to be unreliable and to be hard to be applied in some existing RC structures. On the other hand, considering the ultra-high strength, UHPFRC was also expected to strengthen the RC structures. For example, UFC is a type of UHPFRC products, with a high compressive strength (up to 750 MPa) and high tensile strength (up to 100 MPa). Wang and Lee proposed to strengthen the interior RC beam-column joint sub-assemblages by using UFC, where the improvement of the ductility and the formation of plastic hinges in the beams were demonstrated[53]. In the case of strengthening RC beams, Martinola et al.[54] and Wirojjanapirom et al.[55] both pointed out that the strengthening technique using UHPFRC jacket can strengthen the shear capacity of RC members. But the UHPFRC jacket or the adhesive concrete has to be placed on the site and the concrete has to be cured when the UHPFRC jacket method is applied for the shear strengthening. Thus, the labor cost would increase and the progress would be delayed.

A new shear strengthening method was proposed by bonding the panels made of UFC on the girder end of the aging RC bridges. Since the UFC was cast into a panel shape, the method of bonding UFC panels shows the outstanding characteristics of workability, efficiency, reliability, short-duration and low-cost. Other advantages of this product include outstanding corrosion resistance, reduced maintenance costs, chemical resistances and environmental resistances (such as freeze and thaw, salt water and so on) In this study, the proposed shear strengthening method through bonding UFC panels is to retard the opening cracks to propagate around the ends of the RC beams. Besides, a strong epoxy glue was used to bond UFC panels.

1.4.　OUTLINE OF THE THESIS

In Chapter 2, a new shear strengthening technique, bonding the UFC panels on the girder end of aging RC bridges, was proposed. Two groups of specimens, Group 1 and Group 2, were used to evaluate the effects of the shear strengthening of UFC panels under different shear-span ratios (a/d = 2.5, 1.5). As there were many RC bridges reinforced with round rebars in 1960s, round rebars in tension were used and the influence of rebar type was investigated in this study. Besides, due to the poor design and/or construction, some of the aging RC bridges exists the problem of the initial defect (low concrete strength), thus the method of bonding UFC panels on RC beams with low concrete strength were conducted. In addition, the aim of this experiment is to evaluate the shear strengthening performance for aging or damaged RC bridges. For this objective, RC beams were designed to break down in shear failure and few shear reinforcement stirrups were set. In Group 1, one control beam and five strengthened beams were included, and two strengthened schemes (B type and DB type) were designed. Experimental investigations were implemented in terms of the upgrading of shear capacity and the failure mode. In Group 2, two control beams and two strengthened beams were included, and the strengthening effect with low shear span ratio was explored.

In Chapter 3, to investigate the influence of UFC panel strengthening on the shear resisting mechanism and rebar bond-slip properties of RC beams with low shear-span ratio, experiments were conducted. For better understanding of the influence of UFC panel strengthening on the shear resisting mechanism in RC beams, the numerical analyses were also conducted. When analyzing the shear resisting mechanism of the strengthened RC beams, it is essential to investigate the material properties of UFC and the influence of UFC panel on the rebar bond-slip properties. So far, there are lots of investigations on the evaluation of the material properties of UFC. However, the influence of UFC panel on the rebar bond-slip properties has not been studied by now. According to the previous research results, the rebar bond-slip model affects the accuracy of

6

analytical results. Thus, in the investigations in this study, the rebar bond-slip properties was studied by conducting the rebar bond-slip tests. Furthermore, two types of rebar bond-slip models were compared through numerical analyses.

In Chapter 4, the patch repair has been widely used to locally replace the deteriorated concrete, remove the rust and implement the corrosion protection, rehabilitating the pervious functions of repairing objects. The patch repair method was carried out on the RC beams to study its effects on the shear resisting mechanism. The strengthening effectiveness of bonding UFC panels on the patch repaired RC beams is evaluated. And the factors of shear-span ratio, patch repair and strengthening of UFC panels are also discussed in this chapter. RC beams were designed to fail in shear and few shear reinforcement stirrups were set. Two groups of specimens, Group 1 and Group 2, were used to evaluate the effects of the shear strengthening of UFC panels under different shear-span ratios (a/d = 2.5, 1.5).

Chapter 5 presented how to evaluate the degradation states of RC members which were deteriorated by ASR for 1 year and 3 years exposure tests, and investigated the influence of the strengthening measures on the load-bearing capacity and failure mode. Two series (A and B) of RC beams were cast to simulate the ASR affected bridge girder and T-shaped RC pier beam, respectively. Except the control beams, the slow reactive aggregates and alkali additives were added to induce ASR. Also, they were exposed in exterior environment for years and watered regularly to keep the suitable humidity. In the T-shaped RC pier beam, the tensile rebars were located on the top which were easy to contact the rainwater. Thus, the beams in Series B were overturned to keep the tensile rebars on the top. As the accidents that the anchor of tensile rebars fractured due to ASR have been reported recently, the influence of fractured rebars on the load bearing of ASR affected structures was also investigated here. The non-destructive inspections, loading tests, and strengthening evaluations were conducted to evaluate the influence of the ASR damage and the strengthening effects on the degradation states and load-bearing mechanism. Moreover, in order to investigate the

influence of those strengthening methods on the load bearing mechanism, some of the beams were strengthened by bonding CFRP sheets and some others were strengthened by bonding UFC panels. In addition, the nonlinear Finite Element (FE) analyses were used to help better understanding of the ASR damage, and an analysis model was proposed to simulate the expansion caused by ASR.

In Chapter 6, the practical study on shear strengthening of RC beams using UFC panels was conducted. To evaluate the influence of concrete strength, tensile rebar type, shear-span ratio and patching repair on the strengthening effects and the shear resisting mechanism, the experimental investigations of the UFC panels strengthening on RC beams with 1/4 scale depth of real bridge girder were conducted in previous chapters. However, whether the similar shear strengthening effects can be gained on the existing bridge girder, becomes an important problem. To realize the practical application, the influence of the factors in terms of size effect and UFC panel thickness has to be evaluated. In this chapter, the experimental investigations were conducted to evaluate the strengthening performance of bonding UFC panels on the large specimens and to evaluate the influence of the factors in terms of size effect and UFC panel thickness. JSCE recommendation equation was verified to be able to give a reasonable prediction to the shear strength carried by UFC panels.

REFERENCES

1 Valivonis, J., and Skuturna, T., Cracking and strength of reinforced concrete structures in flexure strengthened with carbon fibre laminates, Journal of Civil Engineering and Management, 13(4), pp. 317-323, 2007.

2 Yeong-soo, S., and Chadon, L., Flexural behavior of reinforced concrete beams strengthened with carbon fiber-reinforced polymer laminates at different levels of sustaining load, Structural Journal, 100(2), pp. 231-239, 2003.

3 Ashour, A.F., El-Refaie, S.A., and Garrity, S.W., Flexural strengthening of RC continuous beams using CFRP laminates, Cement and Concrete Composites, 26, pp. 765-775, 2004.

4 Esfahani, M., Kianoush, M., and Tajari, A., Flexural behaviour of reinforced concrete beams strengthened by CFRP sheets, Engineering Structures, 29(10), pp. 2428-2444, 2007.

5 Chao, S.H., Naaman, A.E., and Montesinos, G.J.P., Bond behaviour of reinforcing bars in tensile strain hardening fibre reinforced cementitious composites, Structural Journal, 106(06), pp. 897-906, 2009.

6 CEB Bulletin d'Information 162, *Assessment of concrete structures and design procedures for upgrading (redesign)*, Losanne: CEB, 1983.

7 Sharif, A.M., Al-Sulaimani, G.J., and Hussain, M., Strengthening of shear damaged RC beams by external plate bonding of steel plates, *Magazine of Concrete Research*, 47(173), pp. 329-334, 1995.

8 Swamy, R.N., Jones, R., and Charif, A., Contribution of externally bonded steel plate reinforcement to the shear resistance of reinforced concrete beams, *ACI Special Publication*, 165, pp. 1-24, 1996.

9 Subedi, N.K., and Baglin, P.S., External plate reinforcement for concrete beams, *Journal of Structural Engineering*, 124(12), pp. 1490-1495, 1998.

10 Adhikary, B.B., Mutsuyoshi, H., and Sano, M., Shear strengthening of reinforced concrete beams using steel plates bonded on beam web: experiments and analysis, *Construction and Building Materials*, 14(5), pp. 237-244, 2000.

11 Chajes, M.J., Januska, T.F., Mertz, D.R., Thomson, Jr T.A., and Finch Jr, W.W., Shear strengthening of reinforced concrete beams using externally applied composite fabrics, *ACI Structural Journal*, 92(3), pp. 295-303, 1995.

12 Norris, T., Saadatmanesh, H., and Ehasani, M.R., Shear and flexural strengthening of RC beams with carbon fiber sheets, *Journal of Structural Engineering*, 123(7), pp. 903-911, 1997.

13 Triantafillou, T.C., Shear strengthening of reinforced concrete beams using epoxy bonded FRP composites, *Structural Journal*, 95(2), pp. 107-115, 1998.

14 Challal, O., Nollet, M.J., and Perraton, D., Shear strengthening of RC beams by externally bonded side CFRP strips, *Journal of Composites for Construction*, 2(2), pp. 111-113, 1998.

15 Adhikary, B.B., and Mutsuyoshi, H., Behavior of concrete beams strengthened in shear with carbon-fiber sheets, *Journal of Composites for Construction*, 8(3), pp. 258-264, 2004.

16 Oehlers, D.J., Development of design rules for retrofitting by adhesive bonding or bolting either FRP or steel plate to RC beams or slabs in bridges and building, *Composites Part A: Applied Science and Manufacturing*, 32(9), pp. 1345-1355, 2001.

17 Behloul, M., HPFRCC field of applications: Ductal recent experience, in: Proceedings of the international RILEM workshop High performance fiber reinforced cement composites, pp. 213-222, 2007.

18 Romualdi, J.P., and Batson, G.B., Mechanics of crack arrest in concrete, ASCE *Journal of Engineering Mechanics Division*, 89(EM3), pp. 147-168, 1963.

19 Romualdi, J.P., and Mandel, J.A., Tensile strength of concrete affected by uniformly distributed and closely spaced short lengths of wire reinforcement, *Journal Proceedings*, 61(6), pp. 657-672, 1964.

20 Shah, S.P., and Rangan, V.B., Fiber reinforced concrete properties, *Journal Proceedings*, 68(2), pp. 126-137, 1971.

21 Brandt, A.M., Fibre reinforced cement-based (FRC) composites after over 40 years of development in building and civil engineering, *Composite Structures*, 86(1-3), pp. 3-9, 2008.

22 Rossi, P., High performance multimodal fibre reinforced cement composite (HPMFRCC): the LCPC experience, *Materials Journal*, 94(6), pp. 478-83, 1997.

23 Morin, V., Cohen-Tenoudji, F., Feylessoufi, A., and Richard, P., Evolution of the capillary network in a reactive powder concrete during hydration process, *Cement and Concrete Research*, 32(12), pp. 1907-1914, 2002.

24 Sarkar, S.L., and Aïtcin, P.C., Dissolution rate of silica fume in very high strength concrete, *Cement and Concrete Research*, 17(4), pp. 591–601, 1987.

25 Chung, D.D.L., Review: improving cement-based materials by using silica fume, *Journal of Materials Science*, 37(4), pp. 673-682, 2002.

26 Goldman, A., and Bentur, A., Properties of cementitious systems containing silica fume or nonreactive micro fillers, *Advanced Cement Based Materials*, 1(5), pp. 209-215, 1994.

27 Sivakumar, A., and Santhanam, M., Mechanical properties of high strength concrete reinforced with metallic and non-metallic fibers, *Cement and Concrete Composites*, 29(8), pp. 603-608, 2007.

28 British Standards Institute Staff, *Test method for metallic fibre concrete. Measuring the flexural tensile strength (limit of proportionality (LOP), residual)*, British Standards Institution, 2005.

29 Ahmed, S.F.U., Maalej, M., Paramasivam, P., Flexural responses of hybrid steel polyethylene fiber reinforced cement composites containing high volume fly ash, *Construction and Building Materials*, 21(5), pp. 1088-1097, 2007.

30 BS EN 12390-5. *Testing hardened concrete. Flexural strength of test specimens*, British Standards Institution, 2009.

31 Di Prisco, M., and Toniolo, G., Structural applications of steel fibre reinforced concrete, *Proceedings of the International Workshop*, Milan (Italy), April 4, 2000.

32 Failla, C., Toniolo, G., and Ferrara, L., Structural design of prestressed precast roof elements made with steel fibre reinforced concrete, *BIBM 2002 International Conference*, 2002 (proceedings in CD-ROM).

33 Caratelli, A., Meda, A., Rinaldi, Z., and Romualdi, P., Structural behaviour of precast tunnel segments in fiber reinforced concrete, *Tunnelling and Underground Space Technology*, 26(2), pp. 284-291, 2011.

34 Mesbah, H.A., Yahia, A., and Khayat, K.H., Flexural performance of reinforced concrete beams repaired with fiber-reinforced SCC, *5th International RILEM Symposium on Self-Compacting Concrete*, pp.637-643, 2007.

35 Boscato, G., and Russo, S. Experimental investigation on repair of RC pavements with SFRC, *Concrete Repair, Rehabilitation and Retrofitting II – Alexander et al (eds)*, pp. 1285–1289, 2009.

36 Rosignoli, D., Simonelli, F., Meda, A., and Rosignoli, R., High-performance fiber-reinforced concrete jacketing in a seismic retrofitting application, *Concrete Repair Bulletin*, pp. 26-31, 2012.

37 Kim, J.H.J., Lim, Y.M., Won, J.P., Park, H.G., Lee, K.M., Shear capacity and failure behavior of DFRCC repaired RC beams at tensile region, *Engineering Structures*, 29, pp. 121-131, 2007.

38 Buitelaar, P., Ultra high performance concrete: developments and applications during 25 years, *Plenary Session International Symposium on UHPC*, pp. 1-25, 2004.

39 Denarié, E., Structural rehabilitations with Ultra-High Performance Fibre Reinforced Concretes (UHPFRC), in: M. Alexander, H.D. Beushausen, F. Dehn, P. Moyo (Eds.), *Proceedings International Conference on Concrete Repair, Rehabilitation and Retrofitting (ICCRRR05)*, Taylor and Francis, London, 2005.

40 Minelli, F., Cominoli, L., Meda, A., Plizzari, G.A., and Riva, P., Full-scale Tests on HPSFR Prestressed Roof Elements Subjected to Longitudinal Flexure, *RILEM PRO 49 International Rilem Workshop on High Performance Fiber Reinforced Cementitious Composites (HPFRCC) in Structural Applications*, pp. 1-8, 2006.

41 Behloul, M., HPFRCC field of applications: Ductal recent experience, *Proceedings of the international RILEM workshop High performance fiber reinforced cement composites*, pp. 213-222, 2007.

42 Kamal, M.M., Safan, M.A., Etman, Z.A., and Salama, R.A., Behavior and strength of beams cast with ultra high strength concrete containing different types of fibers, *HBRC Journal*, 10(1), pp. 55-63, 2014.

43 de Larrard, F., and Sedran, T., Optimization of Ultra-High-Performance Concrete by the use of a packing model, *Cement and Concrete Research*, 24 (6), pp. 997–1009, 1994.

44 Morin, V., Cohen Tenoudji, F., Feylessoufi, A., and Richard, P., Super plasticizer effects on setting and structuration mechanisms of Ultra High-Performance Concrete, *Cement and Concrete Research*, 31(1), pp. 63–71, 2001.

45 Habel, K., Viviani, M., Denarie, E., and Bruhwiler, E., Development of the mechanical properties of an Ultra-High Performance Fiber Reinforced Concrete (UHPFRC), *Cement and Concrete Research*, 36(7), pp. 1362-1370, 2006.

46 Rossi, P., Influence of fibre geometry and matrix maturity on the mechanical performance of ultra-high-performance cement-based composites, *Cement and Concrete Composites*, 37, pp. 246-248, 2013.

47 Park, S.H., Kim, D.J., Ryu, G.S., and Koh, K.T., Tensile behaviour of Ultra-High Performance Hybrid Fibre Reinforced Concrete, *Cement and Concrete Composites*, 34, pp. 172–184, 2012.

48 El-Dieb, A.S., Mechanical, durability and microstructural characteristics of ultra-high-strength self-compacting concrete incorporating steel fibres, *Materials & Design*, 30, pp. 4286-4292, 2009.

49 Tayeh, B.A., Abu Bakar, B.H., Megat Johari, M.A., and Voo, Y.L., Mechanical and permeability properties of the interface between normal concrete substrate and ultra-high performance fibre concrete overlay, *Construction and Building Materials*, 36, pp. 538–548, 2012.

50 Hassan, A.M.T., Jones, S.W., and Mahmud, G.H., Experimental test methods to determine the uniaxial tensile and compressive behaviour of ultra-high performance fibre reinforced concrete (UHPFRC), *Construction and Building Materials*, 37, pp. 874-882, 2012.

51 Tayeh, B.A., Abu Bakar, B.H., Megat Johari, M.A., and Voo, Y.L., Mechanical and permeability properties of the interface between normal concrete substrate and ultra high performance fiber concrete overlay, *Construction and Building Materials*, 36, pp. 538-548, 2012.

52 Iskhakov, I., Ribakov, Y., Holschemacher, K., and Mueller, T., High performance repairing of reinforced concrete structures, *Materials and Design*, 44, pp. 216-222, 2013.

53 Wang, Y.C., and Lee, M.G., Ultra-high strength steel fiber reinforced concrete for strengthening of RC frames, *Journal of Marine Science and Technology*, 15(3), pp. 210-218, 2007.

54 Martinola, G., Meda, A., Plizzari, G.A., and Rinaldi, Z., Strengthening and repair of RC beams with fiber reinforced concrete, *Cement and Concrete Composites*, 32(9), pp. 731-739, 2010.

55 Wirojjanapirom, P., Matsumoto, K., Kono, K., and Niwa, J., Shear Resistance Mechanisms of RC Beams Using U-Shaped UFC Permanent Formwork with Shear Keys and Bolts, *Proceedings of 3rd International Conference on Sustainable Construction Materials and Technologies*, e-35, pp. 1-10, 2013.

CHAPTER 2

Basic Investigations on Shear Strengthening Effects of

Bonding UFC Panels on RC Beams with Low Concrete Strength

2.1. INTRODUCTION

In this chapter, the strengthening issues using UFC panels were studied on the RC structures with the initial defect (low concrete strength). The proposed shear strengthening method through bonding UFC panels is to retard the opening cracks to propagate around the ends of the RC beams. Besides, a strong epoxy glue was used to bond UFC panels. The validity of the epoxy glue has been investigated in the previous researches[1,2]. Here, the proposed shear strengthening method was used to strengthen the low-strength RC beams. Two experimental groups were conducted to evaluate the strengthening performance and to analyze the influence of various factors such as rebar type, strengthening position, shear-span ratio (a/d) and UFC panel thickness.

15

2.2. METHODOLOGY

2.2.1. Material properties

In this chapter, a new shear strengthening method is proposed to reinforce low strength RC structures, aiming at retarding the extension of cracks around the ends of the RC beams by bonding with UFC panels. Two groups of specimens, Group 1 and Group 2, were used to evaluate the effects of the shear strengthening of UFC panels under different shear-span ratios (a/d = 2.5, 1.5). As there were many RC bridges reinforced with round rebars in 1960s, round tensile rebars were used and the influence of rebar type was investigated in this study. In addition, the emphasis of this experiment is placed on the evaluation of the shear strengthening performance for aging or damaged RC bridges. For this objective, RC beams were designed to fail in shear and few shear reinforcement stirrups were provided.

The lists of specimens are shown in Table 2.1 and Table 2.2. Ten identical RC beams were used in the experiments, loading with a four point bending configuration. All the beams were cast in steel molds and were cured in the molds under a wet hessian for two days. To evaluate the strengthening performance after bonding UFC panels, two experimental groups were formed with different shear-span ratios. For Group 1, beams were designed to have a shear-span ratio of 2.5, since all sorts of failure modes would occur when the shear-span ratio is equal to 2.5. The purpose of this group was to investigate the strengthening effects under different UFC panels bonding schemes. For

Table 2.1. List of specimens in loading tests (Group 1).

Specimen	Concrete strength (MPa)	Tensile rebar	UFC panel	CFRP sheet	a/d	Beam depth (mm)
2.5RNN	19.2	φ16	-	-	2.5	240
2.5RDN	19.2	φ16	DB type	-	2.5	240
2.5RBN	19.2	φ16	B type	-	2.5	240
2.5DDN	19.2	D16	DB type	-	2.5	240
2.5RNS	19.2	φ16	-	O	2.5	240
2.5RDS	19.2	φ16	DB type	O	2.5	240

Table 2.2. List of specimens in loading tests (Group 2).

Specimen	Concrete strength (MPa)	Tensile rebar	UFC panel	a/d	Beam depth (mm)
1.5RNN	18.5	φ16	-	1.5	240
1.5RDN	18.5	φ16	DB type	1.5	240
1.5RN1/4	24.6	φ16	-	1.5	240
1.5RDA	24.6	φ16	DB type	1.5	240

Group 2, beams were designed to have a shear-span ratio of 1.5, simulating the girder end of a strengthened RC bridge or the RC deep beam girder. The purpose of this group was to compare the strengthening influence under different shear-span ratios. In Group 2, the strengthening scheme selected from Group 1 was implemented.

▪ **Group 1**: There were total six beams including one control specimen 2.5RNN and five strengthened beams by bonding the UFC panels or CFRP sheets. Fig. 2.1 shows the details of RC beams. In some of the RC beams, the round rebars φ16 were used as the tensile longitudinal bar. The longitudinal reinforcement consisted of three φ16 tensile bars and two D13 compressive bars. The tensile strength of them were 439 MPa and 587 MPa respectively, and the yield strength of them were 316 MPa and 406 MPa, respectively. The shear reinforcement consisted of φ6 (round bar) with the yield strength of 324 MPa. For the beam 2.5DDN, the tension part of RC beam was reinforced by deformed D16 rebars with the tensile strength of 499 MPa and the yield strength of 359 MPa.

▪ **Group 2**: There were total four beams including two control RC beams and two strengthened beams strengthened by bonding the UFC panels. All the beams had the same shear-span ratio (=1.5). Fig. 2.2 shows the details of RC beams. The longitudinal reinforcement consisted of three φ16 for tension and two D13 for compression. The tensile strength of them were 465 MPa and 564 MPa, and the yield strength of them were 333 MPa and 385 MPa. The shear reinforcement consisted of φ6 with the yield strength of 548 MPa.

(a) 2.5RNN

(b) 2.5RBN

(c) 2.5RDN or 2.5DDN

(d) 2.5RDS
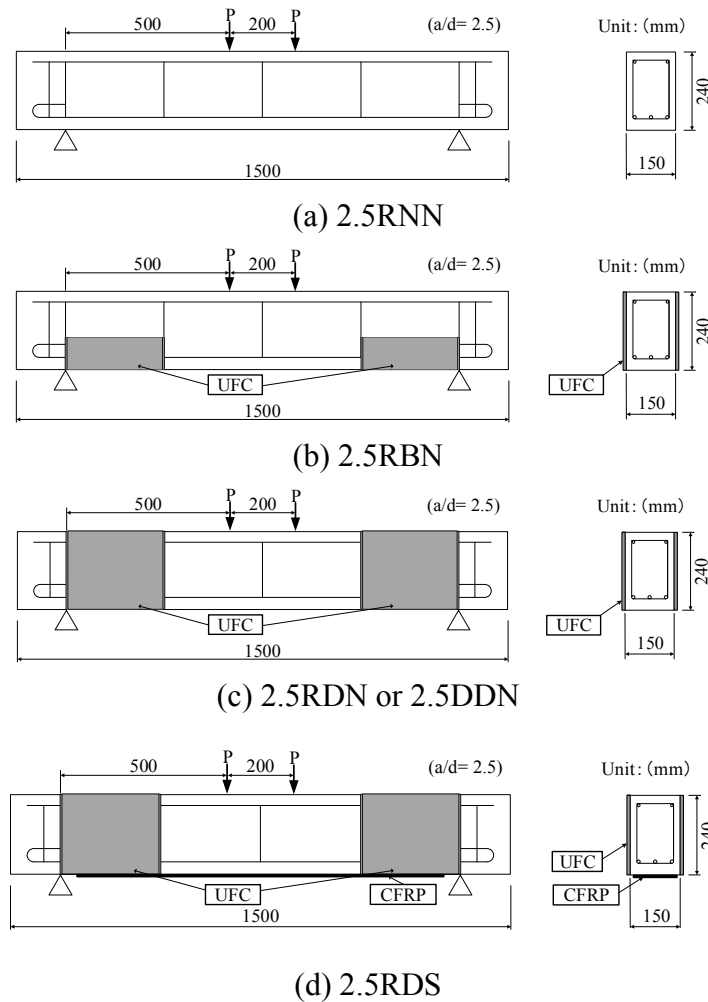
Fig. 2.1. Dimensions of RC beams and Locations of UFC panel (Group 1).

2.2.2. UFC properties

In the experiment, the UFC was molded into panels. The volume of mixed steel fibers was set at around 5%, and the steel fibers had the diameter of 0.1~0.25 mm, the length of 10~20 mm and the tensile strength of 2×10^3 MPa. The water-cement ratio was below 0.24. And other components were silica fume, ground quartz, super-plasticizer, and high amount of Portland cement (up to 1000 kg/m³). The thickness of UFC panels was set as 7 mm. The reason is to ensure a good cohesion between concrete matrix and UFC panel. To prevent the stress concentration, the edge of UFC panel was molded to be a 45° taper. The properties of the UFC panel are specified in Table 2.3 and one of the used UFC panels is shown in Fig. 2.3.

18
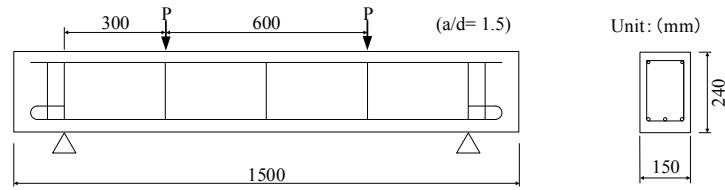
(a) 1.5RNN & 1.5RN1/4
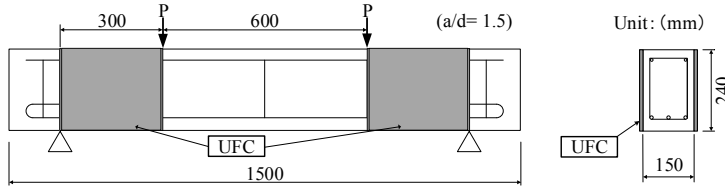
(b) 1.5RDN
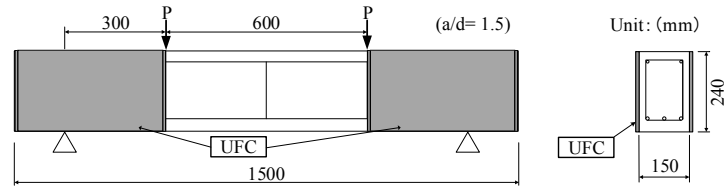
(c) 1.5RDA

Fig. 2.2. Dimensions of RC beams and Locations of UFC panel (Group 2).

Table 2.3. Material properties of UFC panel.

Compressive strength (MPa)	Flexural strength (MPa)	Tensile strength (MPa)	Elastic modulus (GPa)
210	43	10.8	54

2.2.3. UFC panel bonding

The surfaces of concrete matrix and UFC panel were polished and roughed by disk grinder firstly, and then the UFC panels were fixed by anchor bolts at the designed strengthening positions. Fig. 2.4 shows the positions of the anchoring holes where no rebar passes through. During anchoring, the washers of 3 mm thickness were interposed between concrete matrix and UFC panel. The gaps around the panels were sealed except the injection side (preparing for injection of the epoxy resin). Table 2.4 shows the material properties of the adhesive epoxy resin.

19

2.2.4. CFRP sheets bonding

To study the shear strengthening effect on the loading-bearing capacity and to prevent the unexpected flexural failure, a flexural strengthening method was conducted by bonding the CFRP sheets. The procedure of bonding the CFRP sheets was explained below. Firstly, the bonding surface of RC beams was polished by the disc sander. Secondly, the putty with the thickness of 1 mm was applied after the day of the surface coating with epoxy primer. On the putty, CFRP sheet was impregnated and bonded with epoxy resin and deaerated by roller. Thirdly, the surface was covered with a release sheet and was flatted, and then was cured for days. The properties of CFRP sheet are given in Table 2.5.

Table 2.4. Material properties of adhesive epoxy resin.

Compressive strength (MPa)	Tensile strength (MPa)	Tensile modulus (GPa)
73.5	23.5	3.7

Table 2.5. Material properties of CFRP sheet.

Fiber weight per unit area (g/m^2)	Design thickness (mm)	Tensile strength (MPa)	Tensile modulus (GPa)
600	0.333	4490	263

Fig. 2.3. Photo of UFC panel used.

Fig. 2.4. Setting of UFC panel.

2.3. EXPERIMENTAL RESULTS (GROUP 1)

2.3.1. Specimen conditions

Total six specimens were tested in this group, which included the control beam 2.5RNN and the strengthening beams (2.5RDN, 2.5RBN and 2.5DDN). Below, the loading testing results were validated and discussed. To assess the strengthening effect by bonding the UFC panels, two strengthening schemes were proposed. One strengthening scheme was named as B type (tested in 2.5RBN as shown in Fig. 2.1(b)), and another scheme was named as DB type (tested in 2.5RDN and 2.5DDN as shown in Fig. 2.1(c, d)). In B type, the rectangle of UFC panels was bonded along the longitudinal steel bars so as to restrict the shear tension failure. In DB type, the UFC panels were bonded in the whole shear region of RC beam in order to obtain the deep beam effect upgrading the shear strength. Also, the influence of tensile rebar type on the load-bearing capacity was investigated.

2.3.2. Investigations of strengthening schemes

The loading testing results and the load-deflection relationships are shown in Table 2.6 and Fig. 2.5, respectively. The shear strength and flexural strength were evaluated based on Standard Specifications for Concrete Structures. P_{max} presents the applied maximum load, $N_{V,cal}$ indicates the load-bearing capacity based on the calculated shear strength, and $N_{Mu,cal}$ indicates the load-bearing capacity based on the calculated flexural strength. As shown in Table 2.6, it is seen that the control beam 2.5RNN resulted in the shear tension failure, the strengthened beam 2.5RBN resulted in the shear compression failure, and the strengthened beam 2.5RDN failed in flexural failure. Furthermore, Fig. 2.5 shows a greater strengthening effect was gained in strengthened beams using the DB type. Due to the difference of the employed tensile rebars, different performances were observed in 2.5DDN and 2.5RDN. In beam 2.5DDN, the load dropped immediately after the load reached at about 140kN. While in the beam 2.5RDN, the ductile failure was obtained in the beam with round rebars. It is considered that for 2.5RNN, the beam failed in the flexural failure when the load was raised beyond the flexural capacity of the substrate concrete. The loading testing results confirmed that the tensile rebar type would affect the load-bearing mechanism.

22

Table 2.6. Loading test results.

| Specimen | Calculated results | | Experimental results | | | | |
	$N_{V,cal}$ (kN)	$N_{Mu,cal}$ (kN)	P_{max} (kN)	Effective-ness	Stiffness at 30kN (kN/mm)	Effective-ness	Failure mode
2.5RNN	116.0	133.0	128.2	-	91.5	-	Shear tension failure
2.5RDN	-	133.0	144.0	12.3%	94.3	3.1%	Flexural failure
2.5RBN	-	133.0	133.4	4.1%	96.7	5.7%	Shear compression failure
2.5DDN	-	146.0	143.4	-	105.1	-	Shear compression failure
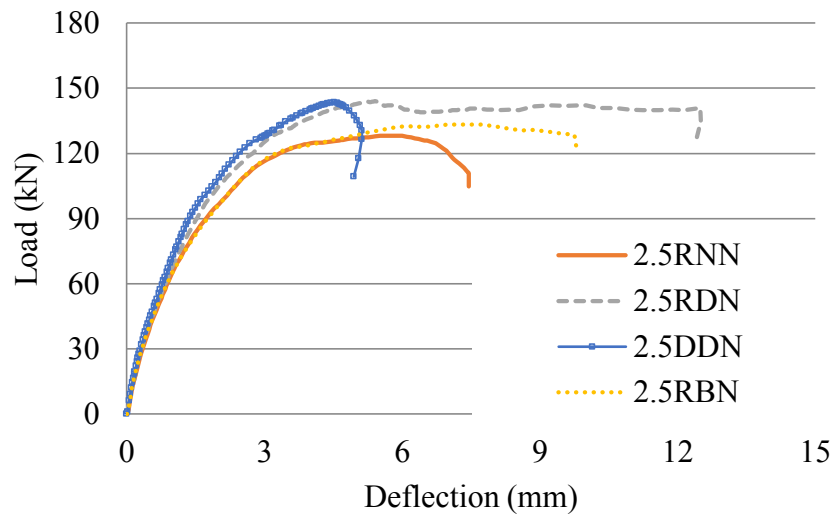
Fig. 2.5. Load-deflection relationships.

The observed crack patterns obtained during the loading testing are shown in Fig. 2.6. In the control beam 2.5RNN, the flexural cracks opened firstly. Then, the shear flexural cracks appeared and developed in two directions: toward the loading points and along the tensile rebar. Finally, the control beam broke down in the shear tension failure. On the other hand, in the strengthened beams, the cracks along tensile rebars were restrained because of the strengthening effect by bonding the UFC panels. In the strengthened beams, the main cracks were confined in the area between UFC panels. The beam 2.5RDN with round tensile rebars finally failed in flexural mode due to the main flexural crack. The beam 2.5DDN with deformed tensile rebars failed in shear

23

mode, where the flexural cracks were dispersed to lots of small cracks, and then the shear cracks dominated the failure.

The results indicated that the failure mode and the load-bearing capacity were both improved with the strengthening effect by bonding the UFC panels. Comparing to the B type, a greater strengthening effects were gained in the strengthened beams by using DB type. One reason is that the cracks were restricted in the mid-span between the UFC panels in DB type strengthening scheme. Comparing different types of tensile rebars (2.5RDN and 2.5DDN), the results show that a greater strengthening effect and a significant ductility were obtained in the beam with round tensile rebars (2.5RDN). In summary, a good performance can be expected once the DB type strengthening scheme (bonding RC beams with round tensile rebars) is applied in the practical applications. But, the load-bearing capacity was raised beyond the flexural strength, so on earth how much the load-bearing capacity can be upgraded by UFC panels is unsure. The influence of flexural failure should be eliminated and the flexural strengthening was introduced.

(a) 2.5RNN

(b) 2.5RDN

(c) 2.5RBN

(d) 2.5DDN

Fig. 2.6. Crack patterns.
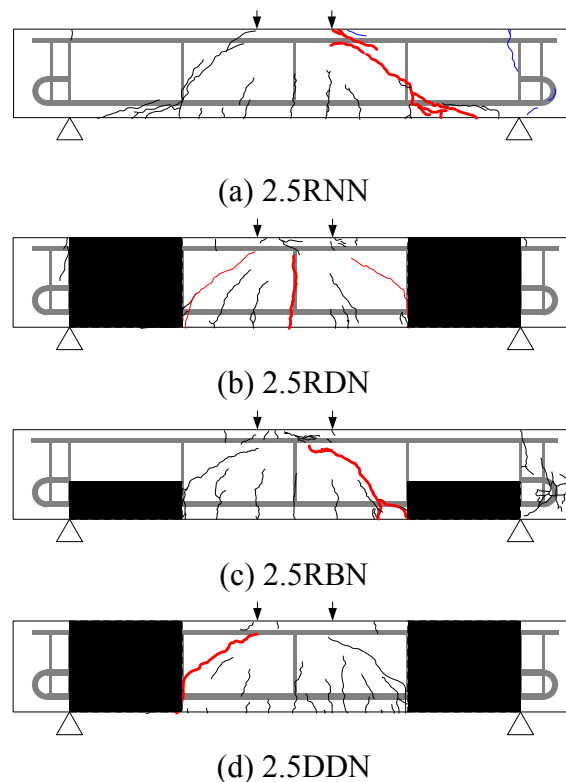
2.3.3. Investigations of shear strengthening effect on load-bearing capacity

To study the influence of flexural strengthening on the resisting mechanism of RC beams strengthened by UFC panels and to prevent the unexpected flexural failure, a flexural strengthening was introduced by bonding the CFRP sheets onto the bottom of RC beams. There were two beams (2.5RNS and 2.5RDS) which were strengthened by CFRP sheets. In 2.5RDS, the DB type scheme of bonding the UFC panels was implemented as well.

The loading testing results were shown in Table 2.7. Compared with the control beam 2.5RNN, the flexural strengthening method for 2.5RNS failed to upgrade the maximum load, where the maximum load was 127.1kN. In the beam 2.5RDS, the load-bearing capacity was significantly upgraded because of the strengthening effect by bonding the UFC panels. As the flexural capacity was improved by bonding the CFRP sheets, an approximated upgrading of the shear strength was inferred from the experiments (23%).

The observed crack patterns obtained during the loading testing are shown in Fig. 2.7. In both of the beams 2.5RNN and 2.5RNS, the splitting cracks along the tensile rebars were observed. The failure mode did not change after bonding the CFRP sheets. On the other hand, as the splitting cracks along the tensile rebars were confined by bonding the UFC panels, the shear cracks in the mid-span of RC beam spread and led the beam to fail in shear compression.

Table 2.7. Loading test results.

Specimen	Calculated results		Experimental results				
	$N_{V,cal}$ (kN)	$N_{Mu,cal}$ (kN)	P_{max} (kN)	Effective-ness	Stiffness at 30kN (kN/mm)	Effective-ness	Failure mode
2.5RNN	116.0	133.0	128.2	-	91.5	-	Shear tension failure
2.5RNS	116.0	133.0	127.1	-0.9%	110.4	20.7%	Shear tension failure
2.5RDS	-	133.0	157.6	22.9%	111.4	21.7%	Shear compression failure

The relationships between load and deflection are illustrated in Fig. 2.8. Comparing the beams 2.5RNN and 2.5RNS, the stiffness of 2.5RNS was greater than that of 2.5RNN at the early stage. When the load reached at 90kN, the stiffness of 2.5RNS declined and dropped immediately, which showed the brittleness after bonding the CFRP sheets. While in beam 2.5RDS, a high stiffness was observed and the ductility was kept even after the maximum load reached.

(a) 2.5RNN

(b) 2.5RNS

(c) 2.5RDS
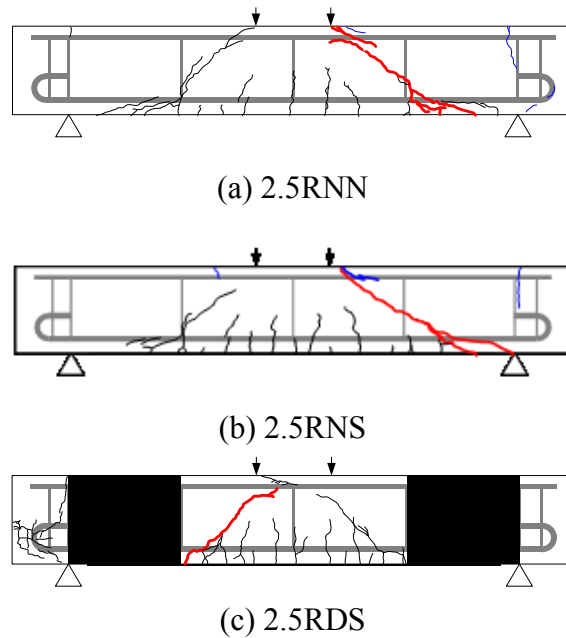
Fig. 2.7. Crack patterns.
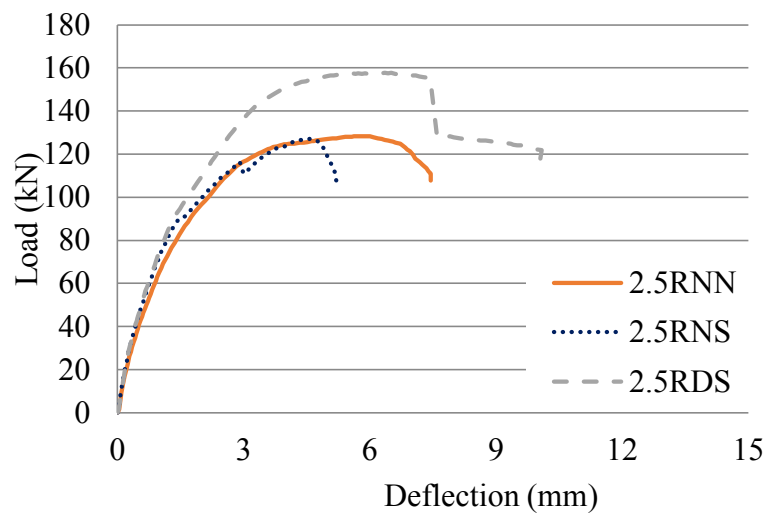
Fig. 2.8. Load-deflection relationships.

Fig. 2.9 shows the rebar strain distribution. Similar features can be seen in both of the beams 2.5RNN and 2.5RNS. The debonding occurred at the end of the tensile rebars and also occurred at a similar load value. But, the intense debonding in 2.5RNS occurred at about 120kN. The reason is that the splitting failure occurred and led to the failure of RC beam. On the other hand, in the beam 2.5RDS, the strain of the tension rebar was restrained at a low level until the concrete failed in compression.

The results show that bonding CFRP sheets did not affect the load bearing capacity. In the beam 2.5RNS, the brittle failure occurred. On the contrary, for the beam 2.5RDS, because of the strengthening effect by bonding the UFC panel, the shear strength was upgraded (about 23%) and the ductile failure mode was obtained.

(a) 2.5RNN

(b) 2.5RNS

(c) 2.5RDS
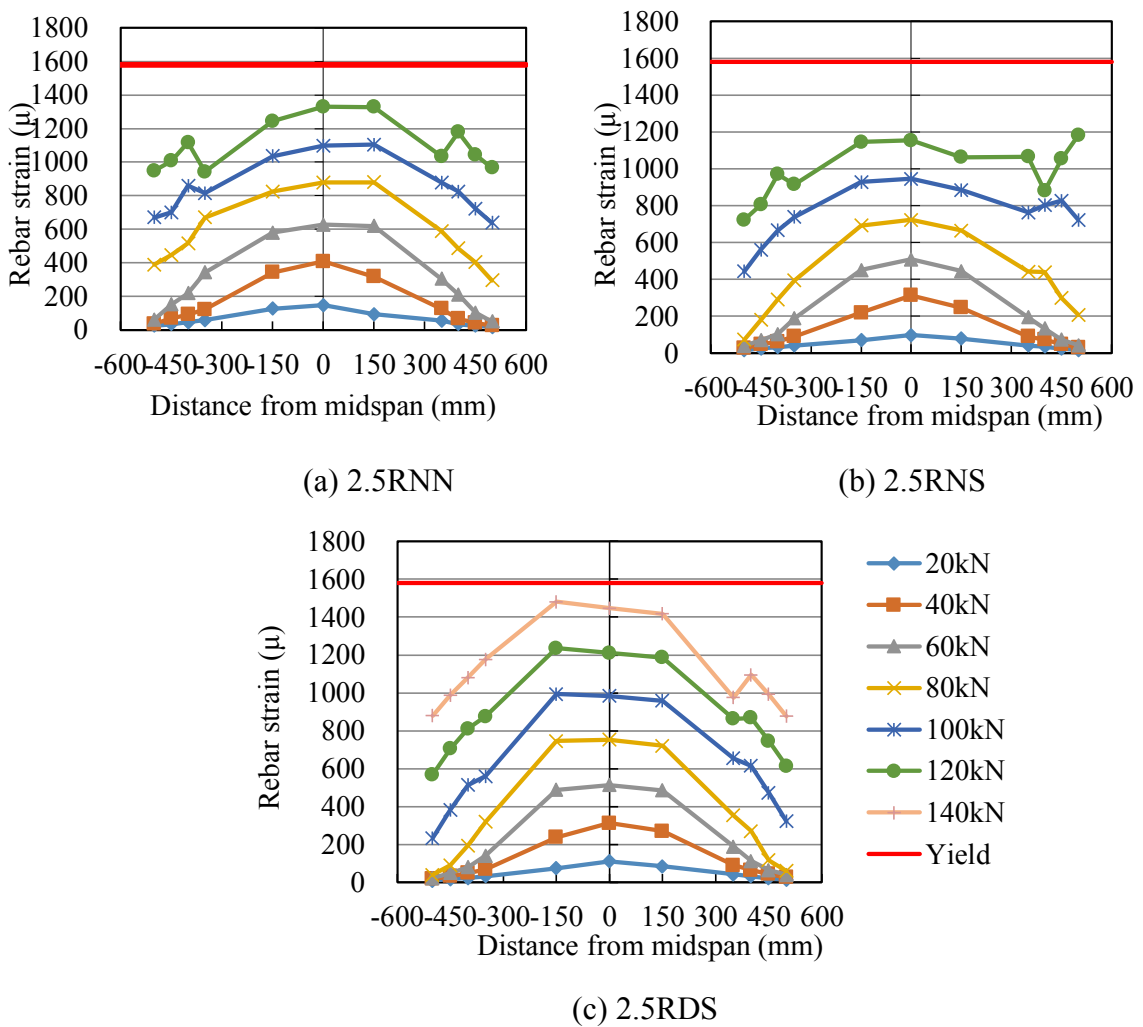
Fig. 2.9. Rebar strain distribution.

2.4. EXPERIMENTAL RESULTS (GROUP 2)

2.4.1. Specimen conditions

In Group 1, the experimental results showed that the load-bearing capacity and the failure mode were significantly improved by bonding the UFC panels. By using the DB type strengthening scheme, the shear strength was improved by 23%. On the other hand, with a consideration of the RC deep beam girders or RC bridges suffering excessive shear force on the girder end (e.g., over-loading), the proposed strengthening method by bonding the UFC panels is also expected to raise the shear capacity or enhance the ductility. In Group 2, the strengthening effect on the RC beams with relatively small shear span ratio was evaluated. Moreover, the DB type strengthening scheme was also conducted in Group 2.

2.4.2. Experimental results

The loading testing results of Group 2 are given in Table 2.8. The shear strength and flexural strength were evaluated based on Standard Specifications for Concrete Structures. P_{max} presents the applied maximum load, $N_{V,cal}$ indicates the load-bearing capacity based on the calculated shear strength, and $N_{Mu,cal}$ indicates the load-bearing capacity based on the calculated flexural strength. For the RC beam 1.5RDN, the DB type strengthening scheme (bonding UFC panels) was applied only in the shear span region except the anchorage region of 1.5RDN (refer to Fig. 2.2(b)). In the loading testing results, an un-predictable failure mode, anchorage splitting failure, occurred in the beam 1.5RDN. The reason is that the anchorage section cannot provide sufficient bond strength due to the low concrete strength. Fig. 2.10 shows the crack patterns obtained in specimens 1.5RNN and 1.5RDN. For the control beam 1.5RNN, two main shear cracks occurred in each side. The first shear crack occurred near the mid-span, and then extended along the tensile rebars and formed splitting cracks. Due to the dominant shear crack occurred between the loading point and the end anchorage section, the beam finally broke down in the shear failure (arch action). For the strengthened beam 1.5RDN, the development of shear cracks in the shear region was restricted because of bonding the UFC panels. However, the dominant cracks in the end of anchorage section led the beam to fail in an

Table 2.8. Loading test results.

Specimen	Calculated results		Experimental results				
	$N_{V,cal}$ (kN)	$N_{Mu,cal}$ (kN)	P_{max} (kN)	Effective-ness	Stiffness at 30kN (kN/mm)	Effective-ness	Failure mode
1.5RNN	147.7	236.6	196.1	-	124.6	-	Shear compression failure
1.5RDN	-	-	206.2	5.2%	132.4	6.3%	Anchorage splitting failure
1.5RN1/4	148.4	243.5	173.5	-	153.3	-	Shear failure (arch action)
1.5RDA	-	243.5	242.9	40.0%	138.9	-9.4%	Flexural failure

un-predictable anchorage splitting failure. Fig. 2.11 shows the load-deflection relationships. As shown in the figure and Table 2.8, the ultimate load and initial stiffness of 1.5RDN increased by only 5% and 6%, respectively, from those of 1.5RNN. The results showed that strengthening of the anchorage section should also be taken into account when strengthening the RC beams with round tensile rebars and small shear span ratio. Therefore, an anchorage reinforcement method was proposed. In this new method, the bonding region of UFC panel was extended to the anchorage section to prevent the anchorage splitting failure. Two beams (control beam 1.5RN1/4 and strengthened beam 1.5RDA) were cast in this experiment to verify the improved strengthening method (refer to Fig. 2.2).

The load-deflection relationships of 1.5RN1/4 and 1.5RDA are shown in Fig. 2.11(b). As shown in the figure, the brittle failure occurred in the control beam 1.5RN1/4 in which the load declined immediately after it reached at the peak. On the other hand, because of the anchor reinforcement and shear strengthening, a significant upgrading effect on the bearing capacity was obtained for 1.5RDA and the maximum load was enhanced by about 40%. Moreover, the failure mode was also ameliorated, and the measured load-deflection curve demonstrated the outstanding ductility at the last stage.

Fig. 2.12 shows the rebar strain distribution. For the control beam 1.5RN1/4, the debonding occurred at the early stage (load = 90kN). On the other hand, because of the UFC panels strengthening and the anchorage reinforcement, the strain value of end region of tensile rebars at ends of beam 1.5RDA stayed at a low level, and the debonding was restricted until the beam broke down.

Fig. 2.13 shows the crack patterns. For the control beam 1.5RN1/4, the shear cracks and the compression cracks can be observed in the shear span region, and the beam resulted in the shear compression failure. On the contrary, because of the anchorage reinforcement, the anchorage splitting cracks did not occur in the beam 1.5RDA that failed in flexural failure. The experimental results demonstrated that the ultimate load-bearing capacity and the failure mode were ameliorated because of the anchorage reinforcement.
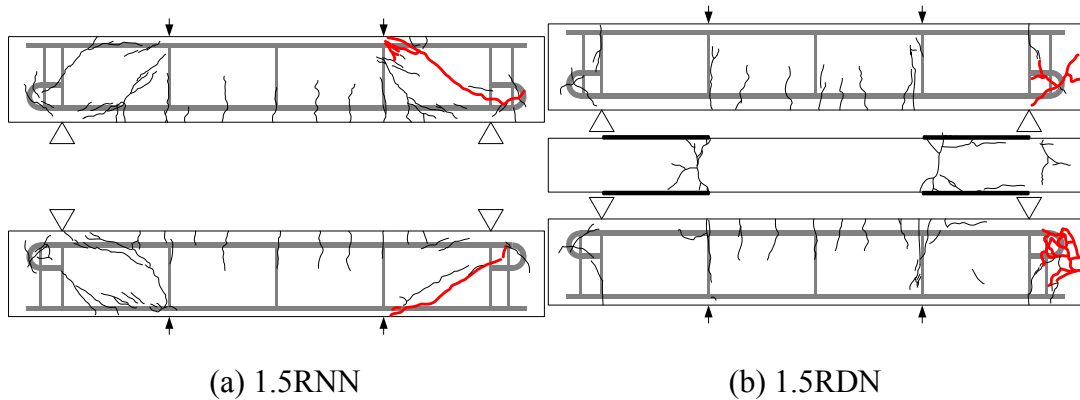

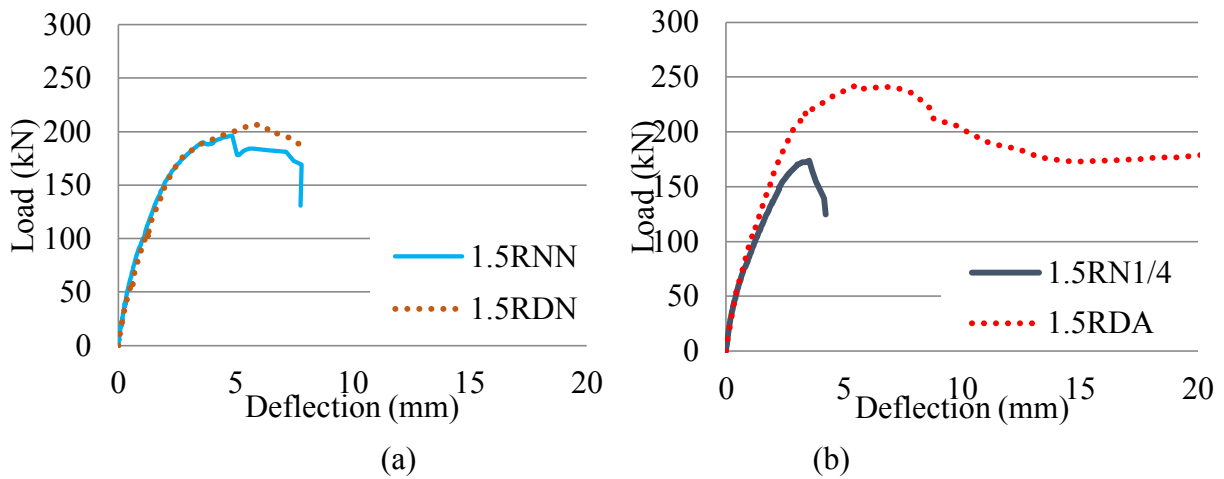(a) 1.5RNN (b) 1.5RDN

Fig. 2.10. Crack patterns.
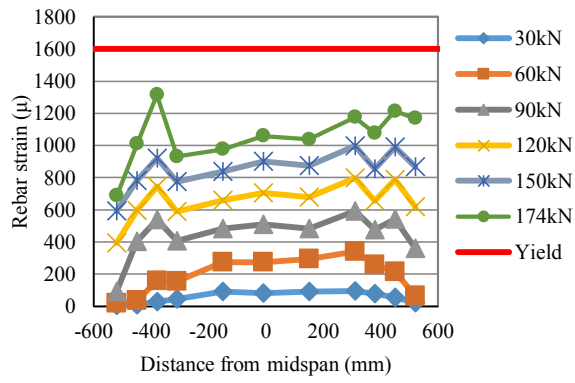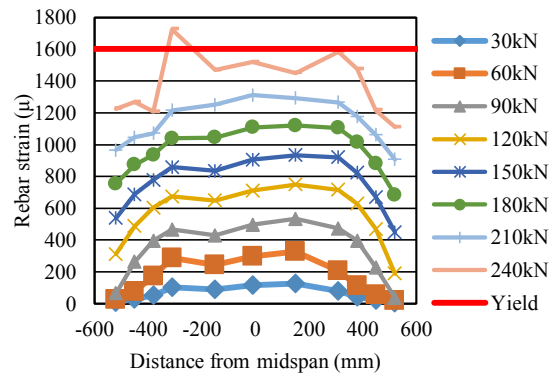

(a) (b)

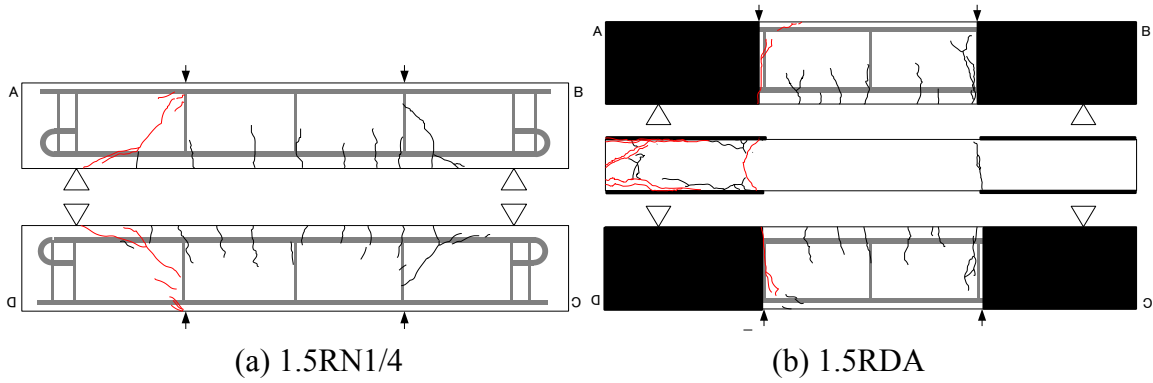Fig. 2.11. Load-deflection relationships.

(a) 1.5RN1/4 (b) 1.5RDA

Fig. 2.12. Rebar strain distribution.

(a) 1.5RN1/4 (b) 1.5RDA

Fig. 2.13. Crack patterns.

2.5. DISCUSSION

2.5.1. DB type strengthening scheme of UFC panels

According to the loading test results, all the dominant cracks occurred in the region between the UFC panels. Fig. 2.14 shows the principal strain distribution at the load of 50kN, where the principal strain value was calculated based on the data from the strain gauges. Compared with the control beam, the value of principal strain between the UFC panels increased significantly and the stress concentration formed in the mid-span. Consequently, bonding the UFC panels substantially relieved the stress in the shear region. In addition, since the round tensile rebars with low bond strength were used here, it was easy to form the arch mechanism to resist the shear. Due to the strengthening effect of bonding the UFC panels on the shear span section of RC beams, the sufficient tensile force in the rebar ends was sustained by UFC panels until the rebars yielded. Therefore the greater bearing capacities and the ductile failure mode were gained when the DB type strengthening method were adopted.

2.5.2. Influence of shear span ratio on strengthening effects

With respect to the normal shear span ratio (a/d = 2.5), the upgrading of bearing capacity (23% for 2.5RDS) and the ameliorating of failure mode were confirmed. However, in the case of low shear span ratio (a/d = 1.5), the intensive strengthening on the shear region caused the unexpected failure: the destruction of the anchorage section. Once the anchorage reinforcement that extends the bonding region of UFC panel to the anchorage section was applied, the desired results were gained. Fig. 2.15 shows the load-strain relationships of the anchorage section. L and R mean the left side and right side, respectively. For the control beam 1.5RN1/4, the strain started rising abruptly when the load reached at about 100kN. On the contrary, because of the anchorage reinforcement, the value of strain in beam 1.5 RDA was restricted until the load reached at 150kN and increased gradually. The strengthening effects of anchorage reinforcement were confirmed in the loading tests. At last, the strengthening by UFC panels raised the bearing capacity (40% for 1.5RDA). It demonstrated that the greater strengthening effects can be gained in RC beams with small shear span ratio.
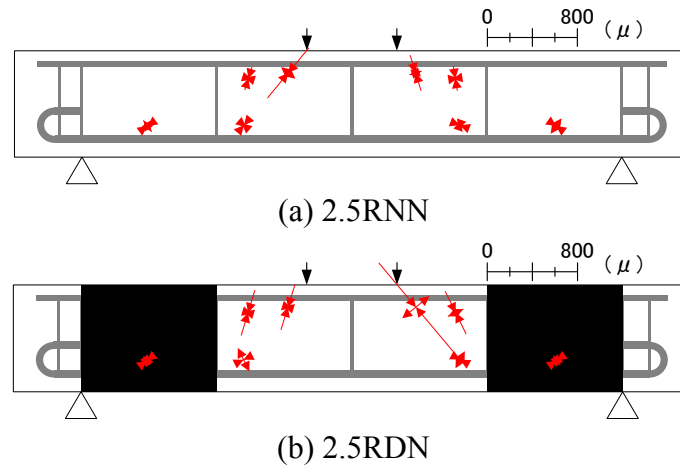
(a) 2.5RNN

(b) 2.5RDN

Fig. 2.14. Principal strain distribution at the load of 50kN.
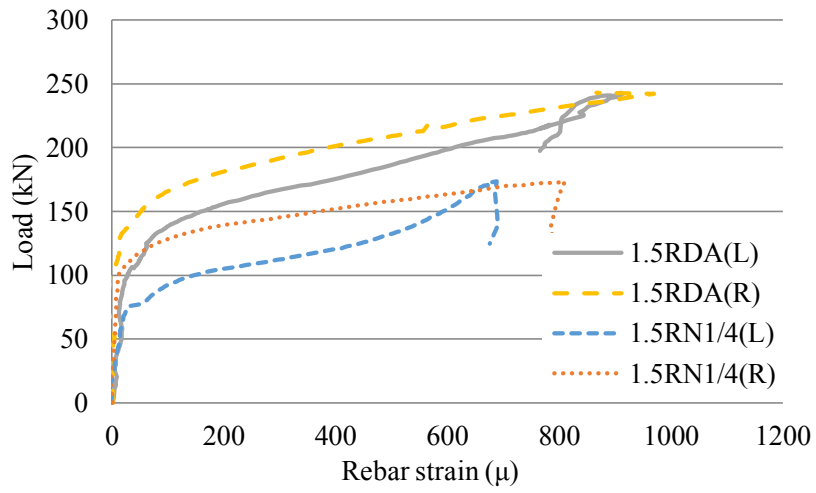
Fig. 2.15. Load-strain relationships in the anchorage section.

33

2.6. CONCLUSIONS

This chapter proposed a strengthening method using UFC panels to upgrade the shear capacity and ameliorate the failure mode in the aging or damaged RC structures. Taking the factors of rebar type, strengthening position, shear-span ratio and anchorage reinforcement as main experimental variables, the experimental investigations were conducted. The results are summarized below.

1. When a/d is equal to 2.5, the shear capacity of RC beams was enhanced and the failure mode was ameliorated by bonding the UFC panels. Especially when the DB type strengthening (bonding RC beams with round tensile rebars) was applied, the improvement of the structural performance of RC beams was confirmed. It is because the cracks in the shear zone were mostly restricted. Moreover, comparing different types of tensile rebars, the results showed that a greater strengthening effectiveness and significant ductility were obtained in the beam with round tensile rebars. A good performance can be expected when the DB type strengthening scheme is applied in the practical applications.

2. The influence of CFRP sheet strengthening on the load bearing capacity was also investigated. The results presented that the bonding CFRP sheets could reduce the structural performance, especially the ductility. On the other hand, the combination of UFC panels and CFRP sheets did upgrade the shear capacity of RC beams (a/d = 2.5) by about 23%.

3. When strengthening the RC beams with low shear span ratio, an un-predictable failure mode (anchorage splitting failure) was observed. Thus, the anchorage reinforcement method was necessary to extend the bonding region of UFC panel to the anchorage section. Based on the test results, the improvement on the shear strength (40%) and the destruction energy absorption were demonstrated, when the anchorage reinforcement method was applied.

4. From the comparisons between Group 1 and Group 2, it is inferred that the strengthening effect varies with the shear span ratios. For Group 2, the strengthening method by bonding the UFC panels raised the shear capacity (40%). It demonstrated that greater strengthening effects can be gained in RC beams with small shear span ratio.

REFERENCES

1 Fink, J.K., *Chapter 3 – Epoxy Resins, Reactive Polymers Fundamentals and Applications (Second Edition)*, pp. 95-153, 2013.

2 Morikawa, H., and Kawaguchi, T., Strengthening effect of UFC panels bonded to web panel of plate girders, *Memoirs of Construction Engineering Research Institute*, pp. 11-19, 2011 (in Japanese).

CHAPTER 3

Investigations on Strengthening by UFC Panels on RC Beams

with Low Shear-span Ratio

3.1. INTRODUCTION

In previous chapter, the strengthening issues using UFC panels were studied on the RC structures with the initial defect (low concrete strength). The influence on the strengthening effectiveness was also investigated in terms of the tensile rebar type, strengthening position, shear-span ratio (a/d) and flexural strengthening (bonding CFRP sheets). The test results demonstrated that this strengthening method achieved significantly positive effects. This chapter focuses on the strengthening of RC beams with low shear-span ratio (a/d = 1.5).

For better understanding of the influence of UFC panel strengthening on the shear resisting mechanism in RC beams, the numerical analyses were also conducted. When analyzing the shear resisting mechanism of the strengthened RC beams, it is essential to investigate the material properties of UFC and the influence of UFC panel on the bond-slip properties of rebars. So far, there are lots of investigations on the evaluation of the material properties of UFC[1-3]. However, the influence of UFC panel on the bond-slip properties of rebars has not been studied by now. According to the previous

research results, the bond-slip model affects the accuracy of analytical results. Thus, in this study, the bond-slip properties were evaluated by conducting the bond-slip tests of rebars. Furthermore, two types of bond-slip models were compared through numerical analyses.

3.2. EXPERIMENTS (LOADING TEST)

3.2.1. Material properties

In this experiment, UFC was molded into panels. The volume of mixed steel fibers was set at about 5%, with the diameter of 0.1~0.25 mm, the length of 10~20 mm and the tensile strength of 2×10^3 MPa. In addition, the water-cement ratio was below 0.24, and the other components were silica fume, ground quartz, super-plasticizer, and high amount of Portland cement (up to 1000 kg/m³). According to the previous research results, the thickness of UFC panels was set as 7 mm to ensure the good cohesion between concrete matrix and UFC panel. To prevent the stress concentration, the edge of UFC panel was molded to be a 45° taper. The properties of the UFC panel are specified in Table 3.1 and Fig. 3.1 shows one of the used UFC panels.

Table 3.1. Material properties of UFC panel.

Density (g/cm³)	Compressive strength (N/mm²)	Flexural strength (N/mm²)	Tensile strength (N/mm²)	Elastic modulus (kN/mm²)
2.55	210	43	10.8	54

Fig. 3.1. The photo of UFC panel used.

3.2.2. UFC panel bonding

The surfaces of concrete matrix and UFC panel were polished and roughed by disk grinder firstly, and then the UFC panels were fixed to the designed strengthening positions. Fig. 3.2 shows the positions of the anchoring holes where no rebar passes through. During anchoring, the washers of 3 mm thickness were interposed between concrete matrix and UFC panel. The gaps around the panels were sealed except the injection side (preparing for the injection of the epoxy resin). Table 3.2 shows the material properties of the adhesive epoxy resin.

3.2.3. Loading test introduction

The details of specimens and the position of strain gauges are shown in Fig. 3.3, and the list of specimens is given in Table 3.3. In the experiments, six RC beams were divided into three groups based on the difference of concrete strength and tensile rebar type. For each group, one RC beam was kept as the control beam, and another RC beam was strengthened by UFC panels on the shear region. They were all cast in the same dimensions in 240mm height, in 150mm width and in 1500mm length.

Table 3.2. Material properties of adhesive epoxy resin.

Compressive strength (MPa)	Tensile strength (MPa)	Tensile modulus (GPa)
73.5	23.5	3.7

Fig. 3.2. Setting of UFC panel.

To evaluate the influence of concrete strength on the strengthening effect, the compressive strength was set at comparably low values, 10 MPa and 15 MPa (refer to Table 3.3). The specimens in Group 2 and in the bond-slip test (will be introduced in the later session) were designed with the same concrete strength (10 MPa) and were also cast together. On the other hand, the concrete strength of the specimens in Group 1 and Group 3 was 15 MPa. To investigate the influence of rebar type, two types of tensile rebars (D16 and φ16) were used. In Group 1 and Group 2, the longitudinal reinforcement consisted of three D16 for tension, with the tensile strength of 516 MPa and the yield stress of 344 MPa, respectively. The shear reinforcement consisted of φ6 with the yield stress of 415 MPa. As there were many RC bridges reinforced with round rebars in 1960s, three round rebars (φ16) were used as the tensile bars in Group 3. The tensile strength of φ16 was 465 MPa and the yield stress of φ16 was 333 MPa. To measure the strains, the strain gauges were attached in the tensile rebars.

For concrete placing, high-early-strength Portland cement was used to shorten the curing duration. And river sand (density: 2.56g/cm^3, water absorption: 1.50%, fineness modulus: 3.72) and crushed stone (density: 2.62g/cm^3, water absorption: 0.83%, fineness modulus: 6.72) were mixed in as fine aggregate and coarse aggregate,

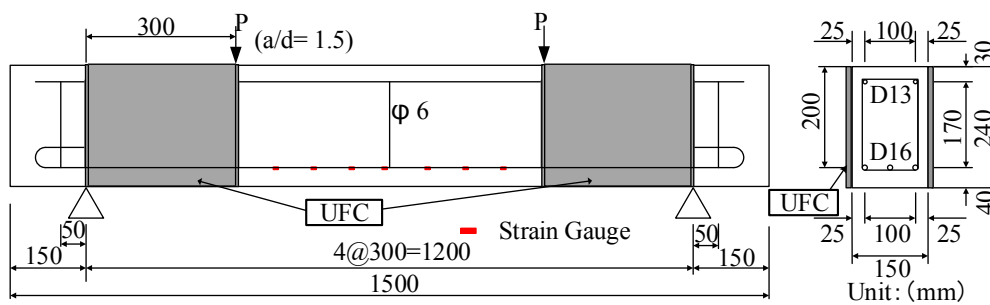Fig. 3.3. Dimensions of RC beams and Locations of UFC panel.

Table 3.3. List of specimens in loading tests.

Group	Specimen	Concrete strength (N/mm^2)	UFC panel	Tensile rebar type
Group 1	N15D	18.5	-	D16
	U15D	18.5	O	D16
Group 2	N10D	13.4	-	D16
	U10D	13.4	O	D16
Group 3	N15R	18.5	-	φ16
	U15R	18.5	O	φ16

39

respectively. AE water reducing agent and AE agent were also added to adjust the liquidity and air volume. Then, the specimens were cured under a wet environment for 28 days. After that, the tests of material properties were conducted. Specimens were loaded with a four points bending configuration in the span of 1200 mm. To simulate the shear failure, the shear-span ratio (a/d) was set as 1.5 in the experiments. And to study the failure mechanism and process, the cracks were marked with load increasing.

3.2.4. Loading test results

The performance of UFC strengthening was evaluated with respect to load-deflection, crack pattern, and rebar strain distribution. Fig. 3.4 shows the photos of the strengthened beam after the loading test, where the red bold mark highlighted the dominant cracks (large width) which led to the failure. After removing the UFC panels along the dominant cracks, the UFC panel and the adjacent concrete were formed into a big block, which was a special failure mode and named as "UFC panel blocking failure" below. The testing results in terms of ultimate load, initial stiffness and failure mode are shown in Table 3.4. In Group 1, the beam U15D strengthened by UFC panels ended with the UFC panel blocking failure, instead of the shear failure which occurred in the un-strengthened beam N15D. As compared to the control beam (N15D), the strengthened beam U15D carried higher ultimate load of 139% and initial stiffness of 115%. The results show that the strengthening technique using UFC panels can significantly enhance the bearing capacity of RC beams with deformed longitudinal rebars. In Group 2, the strengthened beam U10D ended with the UFC panel blocking failure as well and the control beam N10D failed in the shear compression failure. As compared to Group 1, much greater strengthening effect was obtained in the strengthened beam U10D in Group 2. The ultimate load and initial stiffness of beam U10D increased by 56% and 24%, respectively. The results indicate that the concrete strength affects the strengthening performance. The lower the concrete strength is, the better the strengthening effect could be obtained. In Group 3, the strengthened beam U15R failed in an un-predictable anchorage splitting failure, due to the low bond strength. Thus, the expected strengthening results were not achieved. Here, the ultimate load and initial stiffness of beam U15R increased only by 5.2% and 6.3%, respectively. The results show that the anchorage section strengthening should also be taken into account when strengthening the RC beams with round tensile rebars.

40

Table 3.4. Loading test results.

| Group	Specimen	Maximum load P_{max} (kN)	Effective-ness	Stiffness at 30kN (kN/mm)	Effective-ness	Failure mode
Group 1	N15D	189	-	140	-	Shear failure
	U15D	262	38.6%	161	15.0%	UFC panel blocking
Group 2	N10D	131	-	97	-	Shear failure
	U10D	205	56.5%	120	23.7%	UFC panel blocking
Group 3	N15R	196	-	125	-	Shear failure
	U15R	206	5.2%	132	6.3%	Anchorage splitting failure

(a) Bottom of beam

(b) Top of beam

(c) UFC panel blocking

Fig. 3.4. Photos after the loading tests.

The comparisons of the load-deflection relationships of specimens are shown in Fig. 3.5. In Group 1, the beam U15D and N15D performed similarly in the early stage. When the load reached 120 kN, the stiffness of beam N15D decreased significantly, and the inducement can be found from the rebar strain distribution shown in Fig. 3.6. When the load reached at around 120 kN, the debonding occurred at the end of tension rebar of beam N10D as shown in Fig. 3.7. In contrast, the strain of the tension rebar of the strengthened beam U15D was restrained at a low level until the most part of tensile rebar yielded at the load of about 260kN. The experimental results show that, with the UFC panel strengthening, the bond failure along the tensile rebars was restrained and the stiffness and shear capacity were enhanced. In Group 2, different performances were found in beam U10D and N10D after the load reached at about 100 kN. Fig. 3.7 shows the comparison of the rebar strain distribution in Group 2. The debonding in beam N10D (occurred at 100 kN) resulted in the degradation in stiffness. However, the debonding did not occur in beam U10D, and the bond between rebar and concrete was sustained until the maximum load. Furthermore, different from Group 1, the most part of rebar in Group 2 did not yield when the load reached the maximum. Beyond the ultimate load, U10D stabilized at around 120 kN until the tensile rebar yielded finally. Comparing U15D in Group 1 and U10D in Group 2, different failure characteristics were found from the load-deflection relationship, even though they both failed in UFC panel blocking. For beam U15D in Group 1, the rebars yielded almost at the same time when the blocking formed. For beam U10D in Group 2, the most part of rebars didn't
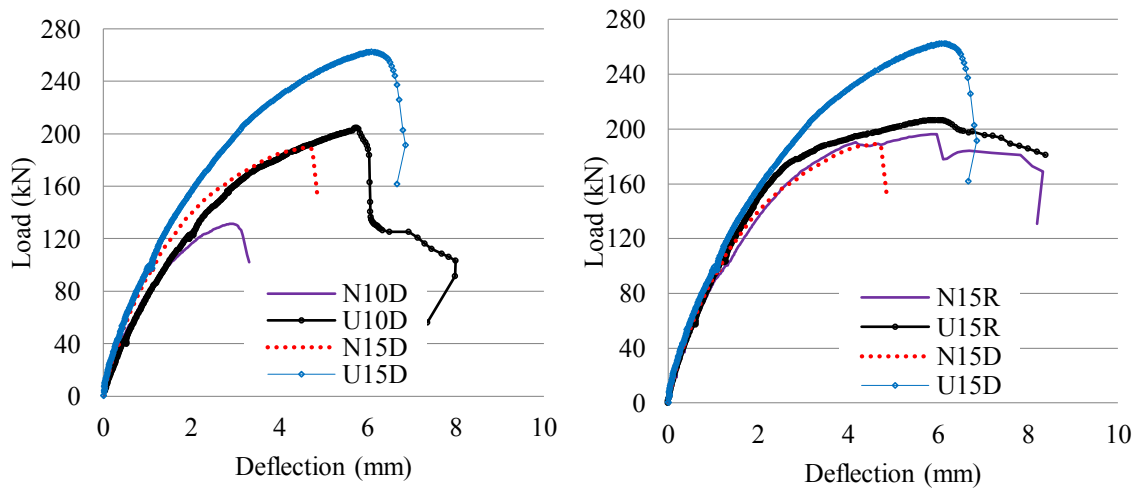
(a) Specimens in Group 1 and Group 2   (b) Specimens in Group 1 and Group 3

Fig. 3.5. The comparisons of Load-deflection relationship
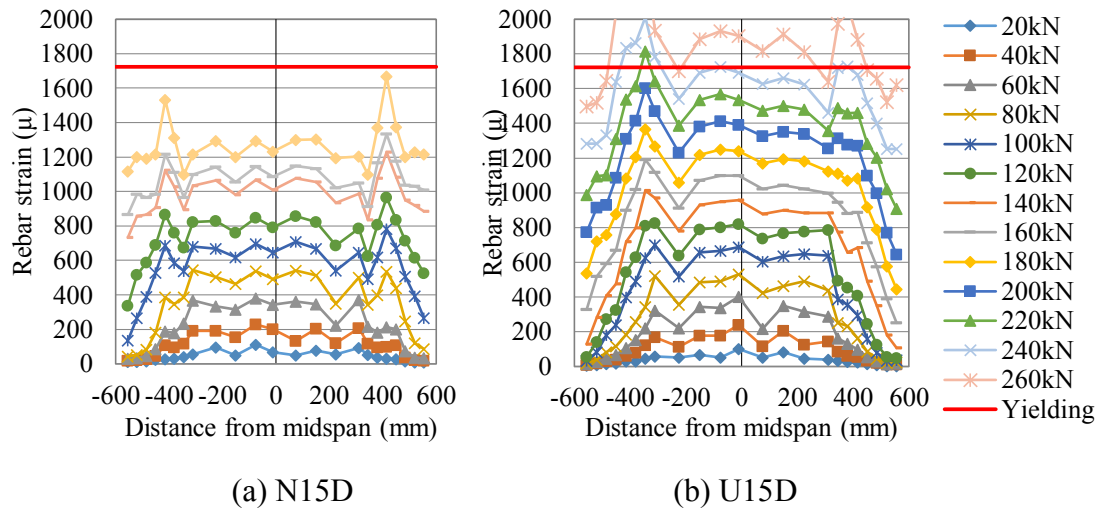
42

(a) N15D (b) U15D

Fig. 3.6. Rebar strain distribution (Group 1).

yield when the UFC panel blocking formed. One possible reason is the concrete strength of the beam U10D is lower than that of U15D. Thus, after reaching at the ultimate load, the U10D beam can still carry the load until the rebars yielded. In Group 3, no difference was found except of the last stage (refer to Fig. 3.5b). For the strengthened beam U15R, the ductile behavior was observed.

Fig. 3.8 shows the crack patterns in the loading tests. With the UFC panel strengthening effect, the crack patterns in the loading tests were different from that occurred in the control RC beams. The crack patterns on the bottoms of strengthened beams are also presented in Fig. 3.8, where the cracks on the beam bottom did not only develop in the transverse direction but also in the longitudinal direction along the edge of UFC panel. In Group 1, for the control beam N15D, the feature of shear compression failure was evident, and the shear cracks obviously appeared in the shear region. For the strengthened beam U15D, the bending cracks opened along the UFC panels after the load level reached at 70 kN and developed longitudinally on the bottom of beam. In Group 2, for the control beam N10D, the shear cracks were obvious between the loading point and the supports. For the strengthened beam U10D, just like what was found in beam U15D in Group 1, the cracks connected together and then the blocking of UFC panel and adjacent concrete formed. Fig. 3.4a shows the cracks on the bottom. From the photo, it can be observed that the longitude cracks led the UFC panel and the adjacent concrete to form into a block. Fig. 3.4b shows the cracks from the top. Similar as the cracks on the bottom, the cracks on the top and side also extended and connected

43

together. Due to the low tensile strength, the RC beam fractured in the blocking of UFC panel and adjacent concrete. Because of the difference of the strength and good bond condition between UFC panel and concrete matrix, cracks tended to occur inside the concrete matrix instead of in the interface surface. Furthermore, due to the high strength of UFC, cracks in the concrete matrix propagated more easily than the shear cracks on the panels. Therefore, the beams did not fail in shear. In Group 3, for the control beam N15R, the crack patterns were very different from what were found in the other two groups. Firstly, the location of the first shear crack was closer to the mid-span, and the splitting cracks along the tensile rebars were more obvious because of the low bond strength of round rebars. Secondly, the dominant shear crack reached the end anchorage section. For the strengthened beam U15R, the UFC panels restricted the development of diagonal cracks. However, due to the insufficient bond strength of round rebars, the dominant cracks occurred in the anchorage section leading the beam U15R to fail in an un-predictable anchorage splitting failure. To avoid the unexpected anchorage splitting failure, an improved strengthening method was proposed where the UFC panel strengthening region was extended to the anchorage section (see chapter 2).

(a) N10D   (b) U10D
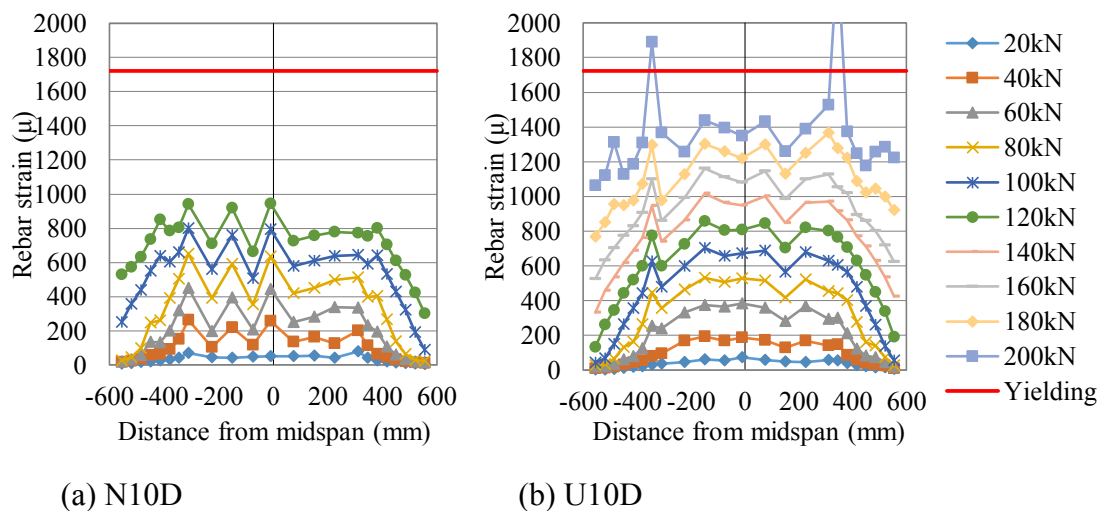
Fig. 3.7. Rebar strain distribution (Group 2).

(a) N15D

(b) U15D

(c) N10D

(d) U10D

(e) N15R

(f) U15R
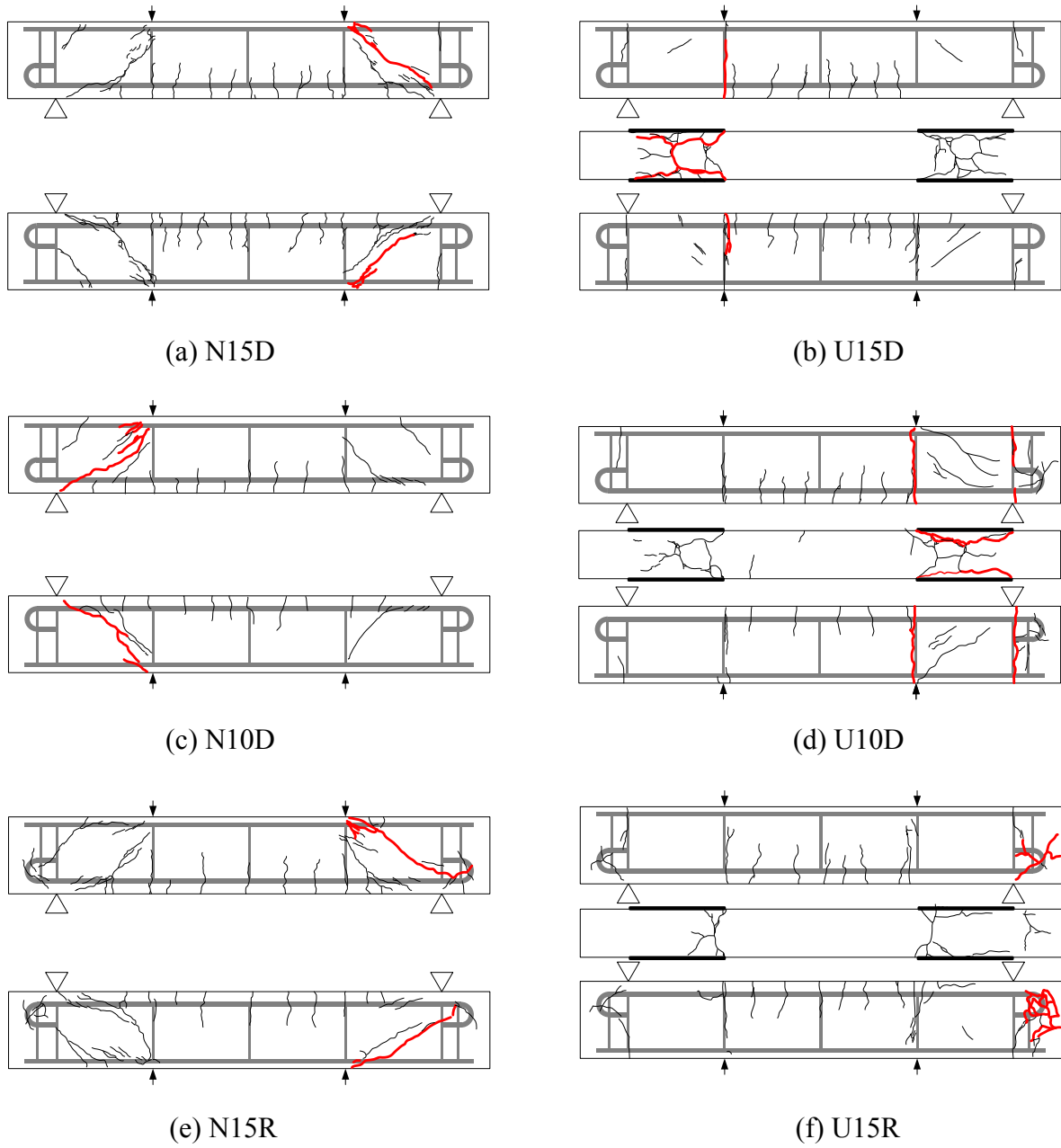
Fig. 3.8. Crack patterns.

3.3. DISCUSSION

3.3.1. Additional experiment

The anchor reinforcement had also been conducted to avoid the anchorage splitting failure in another series[4], where the concrete compressive strength was designed as 20 MPa. Two beams were cast under the same condition as Group 3: one beam was the control beam (N20R) and another one (U20R) was strengthened considering the anchor reinforcement (refer to Fig. 3.9). Fig. 3.10 shows the load-deflection relationships. Similar results were observed as Group 2. For the control beam N20R, the stiffness declined at an early stage and the beam failed in a brittle mode (shear failure). For the strengthened beam U20R, the load bearing capacity was enhanced by about 40% and the failure mode was changed to the ductile mode (similar as beam U10D). The crack patterns in the loading tests were shown in Fig. 3.11. It can be seen that the shear cracks
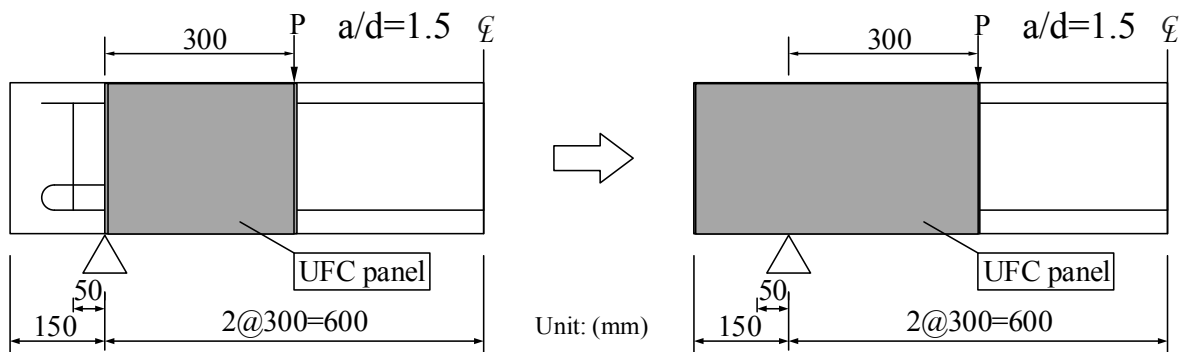
Fig. 3.9. Reformed strengthening scheme.
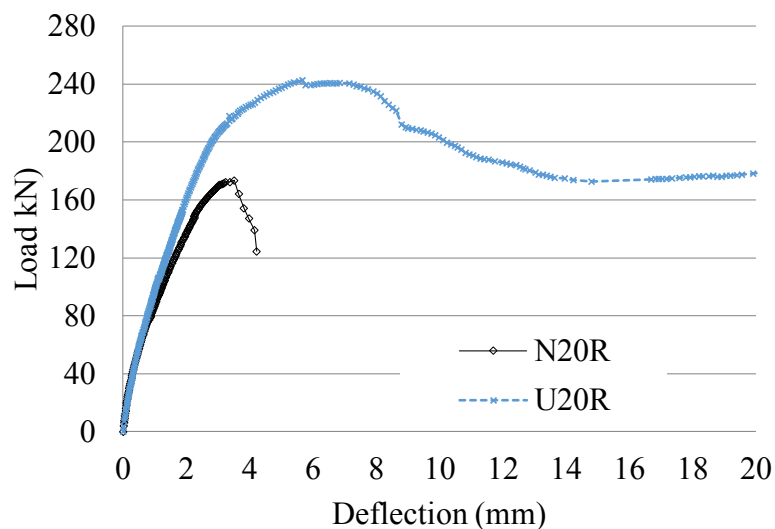
Fig. 3.10. Load-deflection relationship

(a) N20R   (b) U20R
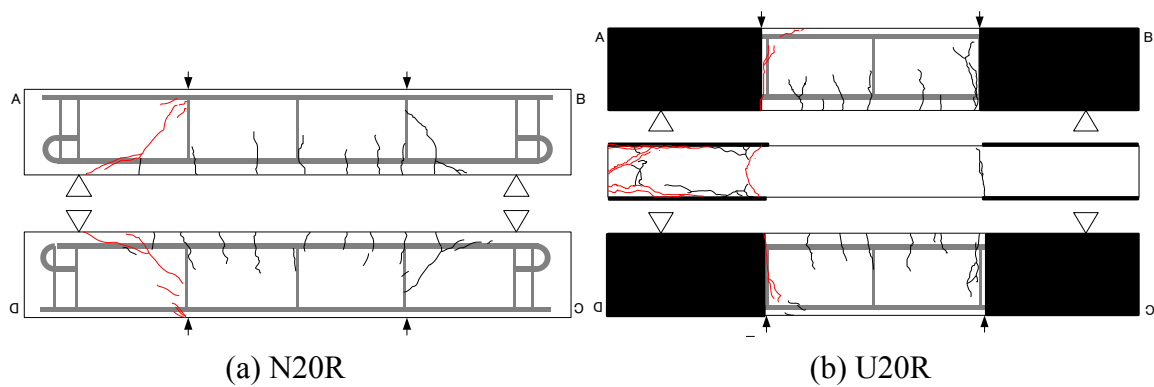
Fig. 3.11. Crack patterns.

in the control beam appeared in the shear zone, while the dominant cracks in the strengthened beam occurred around the UFC panels. The experimental results demonstrated that the ultimate load and the failure mode were ameliorated if the bonding region of UFC panel was extended to the anchorage section.

3.3.2. Influence of concrete strength

When the UFC panel strengthening technique was applied to the low concrete strength beams (refer to Group 2), it was found that much greater strengthening effect can be gained. Especially, the failure mode was changed from the brittle failure to the ductile failure. One explanation for this effect could be that the cracks easily open and develop due to the low concrete strength and the connection of the cracks around the UFC panels tends to form before the tensile rebars yielded. Therefore, this significant strengthening effect on the failure mode can be expected when the UFC panel strengthening technique is applied in the aging RC bridges with low concrete strength or initial defect.

3.3.3. Influence of rebar type

Since the splitting cracks were restricted by UFC panels, the shear capacity and failure mode of the specimens in Group 1 and Group 2 with deformed rebars were improved. However, due to the poor bond of round rebars, the splitting failure occurred in the anchorage section in Group 3. Thus, when upgrading the shear capacity of aging RC

bridges with round rebars, the anchor reinforcement should be taken into account. As demonstrated in the additional experiment, by extending the strengthening region to the anchorage section, the anchorage splitting failure can be avoided and the strengthening effects of the bonding UFC panels be gained.

3.3.4. Shear capacity shared by UFC panels

In order to propose a proper design method for UFC panel strengthening, the calculation means was also investigated to estimate the shear capacity shared by UFC panels. Table 3.5 shows the shear capacities of all the RC beams in the loading tests. It can be seen, except Group 3, all the control beams failed in shear failure and all the strengthened beams failed in the UFC panel blocking. The differences between the shear capacities of the control beam and the strengthened beam in each group were similar, even though the parameters such as the concrete strength and the rebar type were different. The results show that the shear capacity shared by UFC panels may depend on the dimensions of UFC panel and the failure mode, not on the concrete matrix. By far, there are a number of verified calculation formulas to evaluate the shear capacity of normal RC beams, which could be utilized to estimate the shear capacity of the concrete matrix. Here, only the shear capacity shared by UFC panels was investigated. An assumption was made that the difference between the shear capacities of the control beam and strengthened beam can represent the shear capacity shared by UFC panels. The shear

Table 3.5. Shear capacities of specimens

Specimen	Concrete compressive strength (N/mm^2)	Shear capacity $V_{max}(kN)$	Difference of shear capacities (V_U-V_N) $V_{dif}(kN)$	Failure mode	Calculated Shear capacity $V_{ufc}(kN)$
N15D	18.5	94.6	-	Shear failure	-
U15D	18.5	131.2	36.6	UFC panel blocking	30.9
N10D	13.4	65.7	-	Shear failure	-
U10D	13.4	102.3	36.6	UFC panel blocking	30.9
N15R	18.5	98.0	-	Shear failure	-
U15R	18.5	103.2	5.2	Anchorage splitting failure	30.9
N20R	24.5	86.8	-	Shear failure	-
U20R	24.5	121.5	34.7	UFC panel blocking	30.9

capacity shared by UFC panels was calculated based on JSCE Recommendations[5].

$$v_{ufc} = v_{fd} + v_{rpcd} \tag{1}$$

where v_{ufc} is the shear capacity shared by UFC panels, v_{fd} is the shear capacity bore by the part of steel fiber (calculated by Eq. (2)), and v_{rpcd} is the shear capacity bore by the part except steel fiber (calculated by Eq. (3)).

$$v_{fd} = (f_{vd}/\tan \beta_u) \cdot b_w \cdot z \tag{2}$$

where f_{vd} is the tensile strength of UFC panel, β_u is the angle of the diagonal crack and the axial direction, b_w is the width of cross section of UFC panels, and z is equal to $d/1.15$

$$v_{rpcd} = 0.18\sqrt{f'_{cd}} \cdot b_w \cdot d \tag{3}$$

where f'_{cd} is the compressive strength of UFC panel, and d is the effective height.

The calculation results are specified in Table 3.5 where it can be found that the evaluation value was slightly less than the experimental value in all groups, except Group 3 where the anchorage failure occurred. But the small error (slightly less than the experimental value) is still in an acceptable range. Thus, this evaluation method of shear capacity can be used to guide the design of UFC panel strengthening method.

3.4. ANALYSIS

3.4.1. Analysis preparation (Bond-slip test)

So far, many researchers have investigated the material properties of normal concrete, UHPFRC and rebar. However, the bond-slip properties of the rebars, which were embedded inside the RC beam strengthened by bonding UFC panels, have not been studied yet. Here, to evaluate the influence of UFC panels bonding on the bond strength and bond-slip behavior of rebars in RC beams, the bond-slip tests were conducted on the specimens with and without the strengthening of UFC panels.

According to the distance between the rebar and UFC panel and the presence of UFC panel strengthening, the specimens were separated into four groups. In each group, there were three specimens, and the list of specimens is shown in Table 3.6. The details of bond-slip tests are show in Fig. 3.12. The specimens in BN17 and BN42 were kept as the control specimens, where the numbers 17 and 42 mean the concrete cover. On the other hand, the specimens in BU17 and BU42 were strengthened by bonding UFC panels. Here, the compressive strength of concrete was 13.4 MPa which is the same as that of Group 2 in loading test. The bond-slip specimens were cast and cured simultaneously with the specimens in Group 2. So the bond-slip testing results could be used to analyze the specimens of Group 2 as well. Each bond-slip specimen was reinforced by a single deformed rebar (D16) as shown in Fig. 3.12. The length of the deformed rebar (D16) was designed at 1300 mm providing the adequate length for fixing the rebar in the tensile testing machine. To calculate the bond stress caused by rebars, the strain gauge was attached in the center of embedded part. After 28 days' curing, the specimens were polished by the disk grinder, and half of them were roughed and bonded with UFC panel on the surface. Because of the confined surface of the

Table 3.6. List of specimens in bond-slip tests

Specimen	Concrete compressive strength (N/mm^2)	UFC panel strengthening	Concrete cover (mm)	Dimensions (mm)
BN17(-1,2,3)	13.4	-	17	100*100*150
BU17(-1,2,3)	13.4	O	17	100*100*150
BN42(-1,2,3)	13.4	-	42	100*100*150
BU42(-1,2,3)	13.4	O	42	100*100*150

specimens, the anchoring method was not adopted here. Instead, the clamps and washers were used to fix the UFC panel and to control the gaps between the panel surfaces and concrete. Like the specimens in the loading test, the gaps around the panels were sealed except the injection side, and the same type of epoxy resin (shown in Table 3.2) was used.

Before the tensile testing, the set of two CDP displacement transducer was fixed on each side of the rebar. After the specimen was mounted in the tensile testing machine, the other side was pulled axially (refer to Fig. 3.13). The bond-slip testing was applied at a rate of no greater than 20 kN/min. The testing was continuously conducted until the rebars were yielded. The slip s between the rebar and concrete was defined as

$$s = x - \frac{P}{E_S A_S} \times h, \tag{4}$$

where x is the average value of displacements, P is the applied load, E_s is elastic modulus of rebar, A_s is the cross-sectional area of rebar, and h is the range from the fixed position of the displacement transducer to the surface of concrete block.

The average bond stress τ_0 was calculated as

$$\tau_0 = \frac{P - E_S A_S \varepsilon}{u \times \frac{l}{2}}, \tag{5}$$

where ε is the value of the strain gauge in the center of rebar, u is the circumference of rebar, and l is the adhesive length.

(a)BU42   (b)BU17
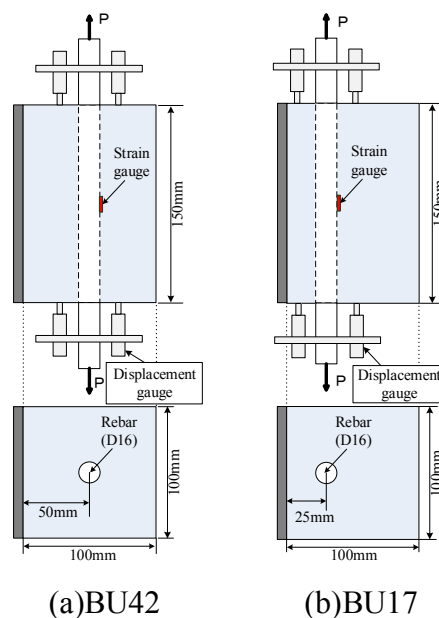
Fig. 3.12. Details of specimen in bond-slip tests.

Table 3.7. Results of bond-slip tests

Specimen	Ultimate bond stress (MPa)			Average value (MPa)	Strengthening effect
	①	②	③		
BN17(-1,2,3)	0.93	0.83	0.83	0.86	-
BU17(-1,2,3)	1.14	1.02	0.87	1.01	1.17
BN42(-1,2,3)	1.01	0.74	0.87	0.87	-
BU42(-1,2,3)	0.99	0.83	0.76	0.86	0.99
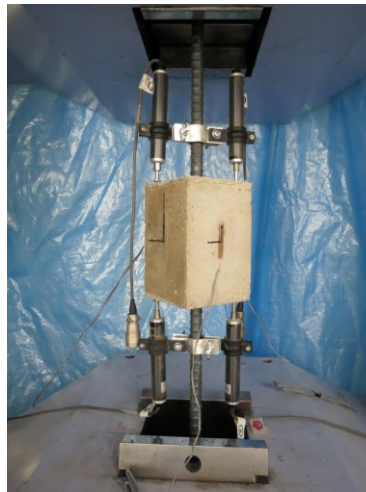
Fig. 3.13. Bond-slip test.

(a) BN17

(b) BU17
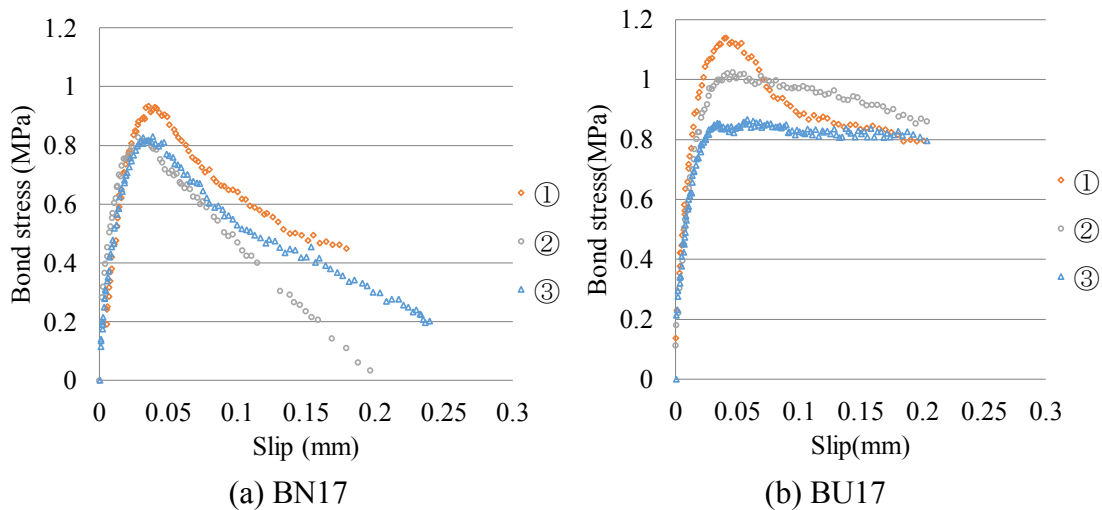
Fig. 3.14. Bond-slip relationships.

Table 3.7 shows the bond-slip testing results. For the case with the cover of concrete of 17 mm, it was found that the bond strength increased by 17%. Fig. 3.14 shows the comparisons between the bond-slip relationship curves of BN17 and BU17. It was observed that the bond-slip curves showed similar tendencies at the beginning stage.

After the bond stress reached at about 40% of the peak value, the stiffness of these curves continuously decreased along with the increase of load level. After reached at the maximum bond stress, different characteristics were observed from the diagram. For the curve of the control specimens (BN17-1.2.3),   the bond stress decreased after the peak stress. On the other hand, for the curve of the strengthened specimens (BU17-1.2.3), the softening was restrained and the bond stress stayed at a high level until the rebars yielded. The obtained results show that the UFC panel strengthening method improved the bond strength of rebars and also significantly restrained the stress softening.

Fig. 3.15 shows the photos of BN17 and BU17 after the bond-slip tests. For the control specimen (BN17), the dominant crack occurred in the surface where the cover was the minimum among the four side surfaces. For the strengthened specimen (BU17), the UFC panel bonding restricted the crack in that surface. As UFC panels can restrict cracks from opening and developing, its remarkable strengthening effect on the bond-slip has been demonstrated.

For the case with the cover of concrete of 42 mm (refer to Table 3.7), the bond strength was recorded at almost the same level. Moreover, there was no distinct difference between the bond-slip relationships of BN42 and BU42 (refer to Fig. 3.16). Along with the increase of load level, the slopes of the bond-slip curves decreased until the maximum bond stress reached. Beyond the peak, the curves descended and became parabola in form again. It was noted that there were some fluctuations of the bond stress, while the maximum bond stress for BN42 and BU42 were nearly at the same level. The

(a)BN17   (b)BU17

Fig. 3.15. Photos after bond-slip tests.

(a) BN42   (b) BU42
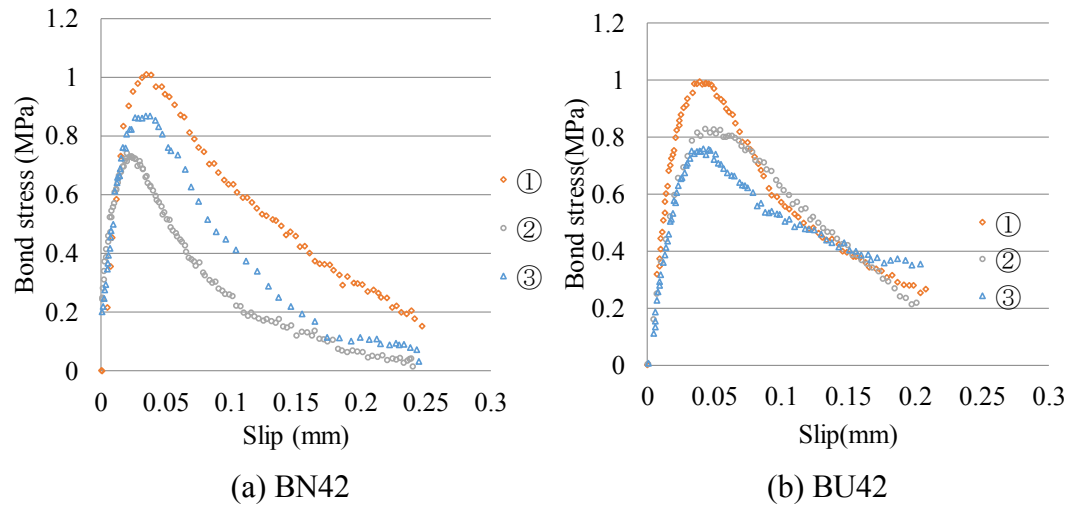
Fig. 3.16. Bond-slip relationships.

results show that the UFC strengthening method has little influence on the bond-slip relationship at the concrete cover of 42 mm. Moreover, comparing to the results obtained in BU17, there exists an influence range of UFC panel strengthening with respect to the cover of concrete.

3.4.2. Analysis introduction

To estimate the bond-slip properties obtained from the bond-slip tests and to evaluate the shear resisting mechanism of beam N10D and U10D in Group 2, the nonlinear Finite Element (FE) analyses were conducted by using the program DIANA 9[6]. The 3D model and boundary conditions are elaborated in Fig. 3.17. Due to the symmetry of RC beams, only half of RC beam was considered here, and the elements on mid-span cross section were bounded in the axis direction.

The 8-node solid brick element was used for concrete. The stress-strain relationship in compression was modeled based on JSCE code[7] (refer to Fig. 3.18). The tensile response was specified as a linear elastic relationship at the first stage. After the tensile stress reached at the maximum value, the softening branch and fracture energy were adopted to represent the post-peak tension, to consider the effect of micro cracks. The compressive strength and the tensile strength of concrete in the strength test were 13.4 MPa and 1.7 MPa, respectively. The fracture energy G_f was calculated according to the JSCE code.

54

$$G_f = 10(d_{max})^{1/3} \cdot f'_c{}^{1/3} \qquad (6)$$

where d_{max} is the maximum dimension of coarse aggregate (20 mm), and f'_c is the compressive strength of concrete.

The 8-node solid brick element was also used for UFC panel. The stress-strain relationship in compression was corresponding to JSCE Recommendations[5] (refer to Fig. 3.19). The tensile properties were empirically determined from the tensile test whose results are shown in Fig. 3.20. Moreover, the peeling failure of the bonding surface of UFC panels has not been observed by now. Therefore an assumption can be made here as that the interface between UFC panel and concrete matrix was the perfect bond.

The line truss element was used for rebars. Here, the young's modulus was set as 200 GPa, and the yield strength was measured in the tensile tests. The double line element was used to model the interface layer between the concrete and rebar. The bond-slip models of rebars used in the analyses are shown in Fig. 3.21. Beyond the maximum bond stress, the softening branch was referred to the CEB-FIP Model Code[8], and the slip value at the softening ending ($S_{3,Non}$) was 1 mm. Before the maximum bond stress reached, the bond-slip model modified by Shima et al. was used to model the nonlinear relationship[9]. It is because that different from the CEB-FIP Model Code, the factors of concrete cover, rebar's diameter and concrete strength were concerned in Shima's formula.
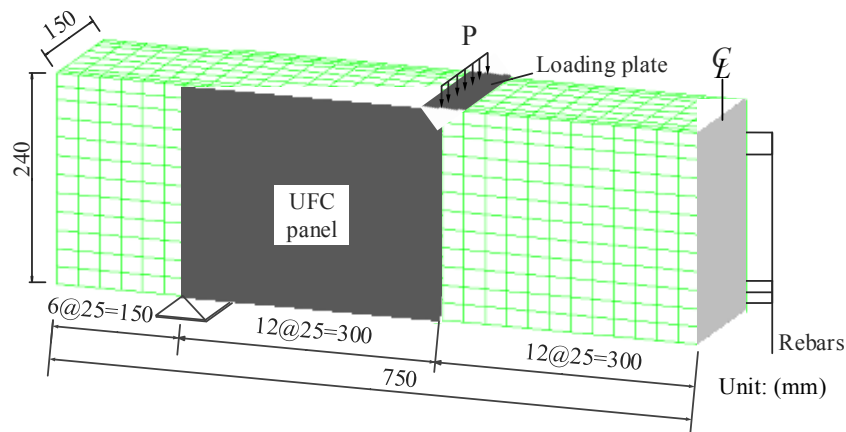

Fig. 3.17. Details of analyses model.
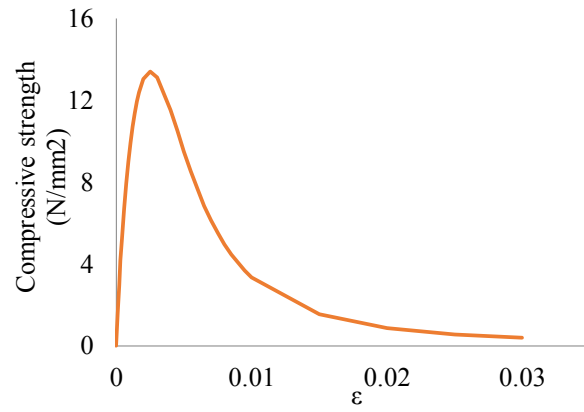
Fig. 3.18. Stress-strain relationship in compression
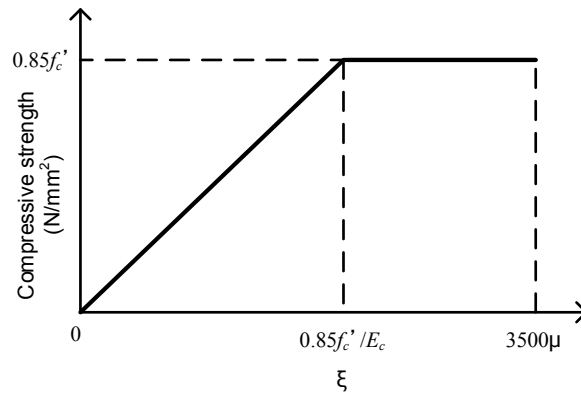
Fig. 3.19. Stress-strain relationship in compression
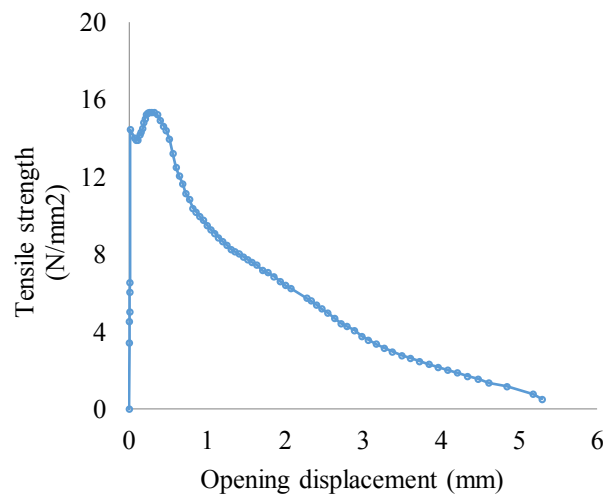
Fig. 3.20. Tensile test of UFC panel.

The bond stress τ and the corresponding slip S_1 were calculated as

$$\tau = 0.4 \times 0.9(f'_c)^{2/3}\left[1 - \exp\{(S/D)^{1/2}\}\right] \tag{7}$$

$$S_1 = 0.09 \times (C/D) \tag{8}$$

where f'_c is the compressive strength of concrete, S is slip, D is the diameter of rebar, and C is concrete cover.

For the strengthened beam U10D, two bond-slip models were considered. One was the same as beam N10D with an assumption that there was no influence of UFC panels on the rebars embedded in concrete matrix. And another bond-slip model was the modified model. The bond-slip testing results show that the bond-slip properties would not be influenced by UFC panels when the distance between UFC panel and rebar exceeds about 50 mm. In the RC beams, except the center tensile rebar, all the other rebars were located in the distance of about 20 mm to the UFC panels (refer to the dimensions in Fig. 3.3). Therefore, the modified model was applied on all the rebars except the center tensile rebar. A comparison of the modified bond model and the original bond model is shown in Fig. 3.21. The modified points were the maximum bond stress and softening branch. According to the bond-slip testing results, the maximum value was increased to 1.17 times and the inhibitory effect of UFC panel on softening branch was also concerned in the modified model.
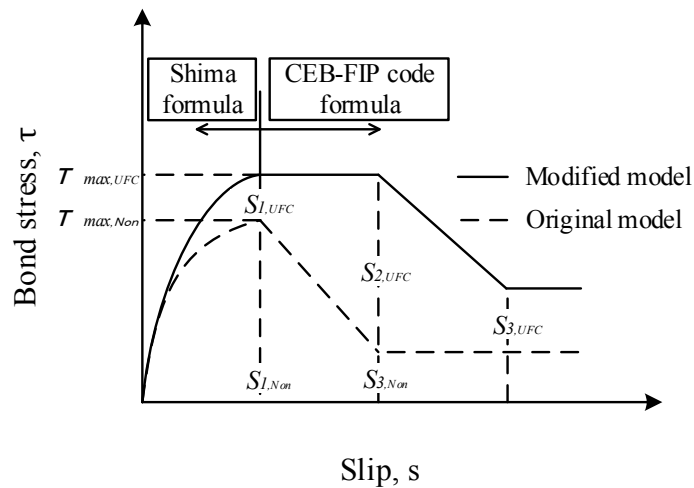
Fig. 3.21. Bond-slip model.

3.4.3. Analytical results

For the control beam N10D, a comparison of the load-deflection relationship between the analytical and experimental results is shown in Fig. 3.22. It shows a good agreement between analytical result and experimental result, which indicates that the used models were capable of simulating the shear mechanism of the normal RC beams. Fig. 3.23 shows the crack patterns in experimental and analytical results. The analytical results show that the obtained feature was similar as that obtained in the experiments. For example, the shear cracks and splitting cracks appeared at almost the same area. Fig.3.23 also indicates that the constitutive models of concrete, rebars and UFC panel can capture the shear resisting behavior of RC beam.

For the strengthened beam U10D, Fig. 3.24 shows the load-deflection curves of analytical (two types of models) and experimental results. From the comparison of load-deflection curves, the original model and the modified model both show a good agreements with the experimental result before the load reached at 120 kN. After the load exceeded 120 kN, the curve of original bond model started to diverge from the experimental curve, with a lower stiffness. On the other hand, as the maximum
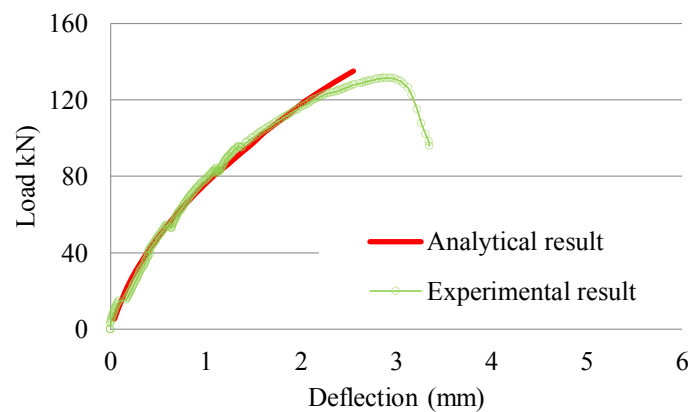
Fig. 3.22. Load-deflection relationship (N10D).

(a) Analytical result   (b) Experimental result
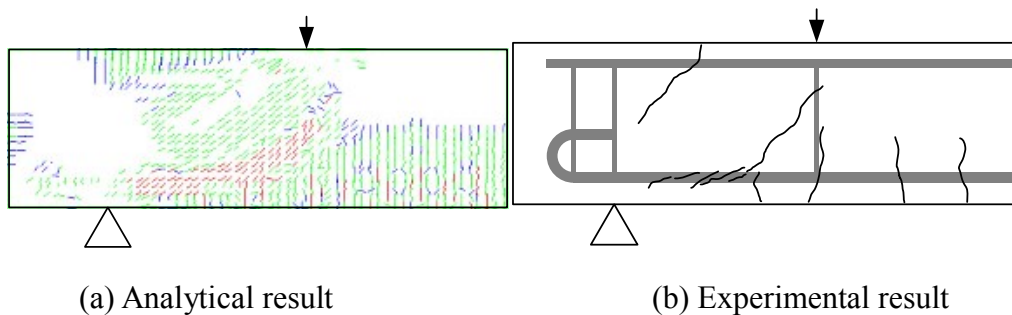
Fig. 3.23. Crack patterns of beam N10D. (Load=125kN)

bond stress and softening branch in the modified bond model were refined, the result of modified bond model was in the similar trend as the experimental results, which captured the shear resisting behaviors of the strengthened RC beam. The difference between the two bond-slip models' results demonstrates that the modified bond-slip model is capable of representing the bond-slip properties of rebars in the RC beam strengthened with UFC panels.

Fig. 3.25 shows the crack patterns of the experiment and analysis. In the analytical results of the modified bond model, cracks around the UFC panels were represented well compared with experiment. For the distinct feature of cracks in the strengthened RC beams, the longitudinal cracks in the bottom were also well captured by FE analysis. From the comparisons between the analytical and experimental results, the validity of the modified bond model was verified, which implies that the modified bond model can represent the shear resisting behavior and the crack pattern in the strengthened RC beams.

Fig. 3.24. Load-deflection relationship (U10D).

(a) Analysis (Lateral of beam)　　　　(b) Experiment (Lateral of beam)

(c) Analysis (Bottom of beam)　　　　(d) Experiment (Bottom of beam)

Fig. 3.25. Crack patterns of beam U10D. (Load=200kN)

59

3.5.   CONCLUSIONS

In this chapter, a new shear strengthening method was proposed to upgrade the shear capacity of the aging RC bridges. The experiments and analyses were conducted to investigate the strengthening effects using UFC panels on the shear resisting mechanism and bond-slip properties of RC members. Following conclusions can be drawn from this study described above.

1.   By using the proposed shear strengthening method (bonding the UFC panels), a very positive effect on the load bearing capacity was obtained in Group 1 and Group 2. Furthermore, comparing to Group 1, a higher increase of the ultimate load (56%) and the initial stiffness (24%) were gained in Group 2, because of the lower concrete strength. And the brittle failur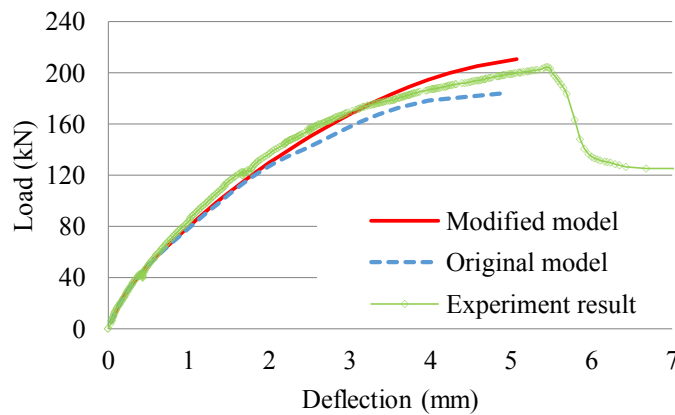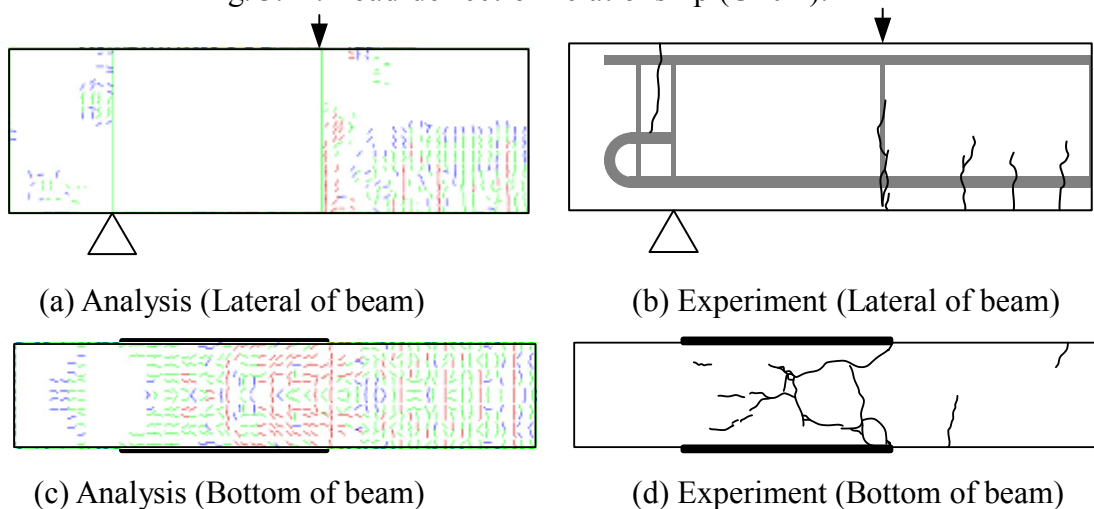e mode (shear failure) was also changed to the ductile mode (UFC panels blocking) in Group 2. Thus, a significant strengthening effect can be expected when using the proposed UFC panel strengthening method to strengthen the aging RC bridges with low concrete strength or initial defect.

2.   When strengthening the RC bridges with round rebars, both shear region and anchorage section should be concerned. In Group 3, the strengthening effect was not obtained in the strengthened beam due to the unpredictable anchorage splitting failure. After extending the strengthening region to the anchorage section, the desirable results were gained. The load bearing capacity and stiffness were enhanced and the failure mode was also changed to the ductile mode, like the beams in the other groups.

3.   From the experimental results, the shear capacity shared by UFC panels does not rely on the concrete matrix, which can be evaluated separately from the matrix. The evaluation result shows that the shear capacity shared by UFC panels can be estimated within an acceptable error range. Furthermore, more effort is still needed to verify and improve the design method of UFC panel strengthening on more specimens.

4.   According to the bond-slip testing results, it was found that the proposed UFC panel strengthening method affects the bond-slip properties of rebars. The maximum bond stress and softening behavior were both improved in case of small cover. Moreover, there exists an influence range of UFC panel strengthening on the bond-slip properties.

5.   From the comparison of experimental and analytical results, the validity of the modified bond model (modified according to the bond-slip tests) was verified.

The original model underestimated the stiffness, while the modified model well captured the shear resisting behavior measured in the tests.

REFERENCES

1 Yu, R., Spiesz, P., and Brouwers, H.J.H., Mix design and properties assessment of Ultra-High Performance Fibre Reinforced Concrete (UHPFRC), Cement and Concrete Research, 56, pp. 29-39, 2014.

2 Hassan, A.M.T., Jones, S.W., and Mahmud, G.H., Experimental test methods to determine the uniaxial tensile and compressive behaviour of ultra high performance fibre reinforced concrete (UHPFRC), Construction and Building Materials, 37, pp. 874-882, 2012.

3 Mao, L., Barnett, S., Begg, D., Schleyer, G., and Wight, G., Numerical simulation of ultra high performance fibre reinforced concrete panel subjected to blast loading, International Journal of Impact Engineering, 64, pp. 91-100, 2014.

4 Kohno, F., Wang, J., Morikawa, H., Kawaguchi, T., Shear strengthening of RC members by bonding with UFC panels considering anchor reinforcement, Proceedings of the Japan Concrete Institute, 36(2), pp. 1237-1242, 2014.

5 Japan Society of Civil Engineers, Recommendations for Design and Construction of Ultra High Strength Fiber Reinforced Concrete Structures (draft), September 2004.

6 Manie, J., and Kikstra, W.P., DIANA User's Manual - Rel. 9.4.3, TNO DIANA BV., 2010.

7 Standard Specifications for Concrete Structures (Design), JSCS concrete committee, pp. 39-44, 2007.

8 CEB-FIP, Bulletin No. 213/214, Model Code 1990, London: Thomas Telford, 1993.

9 Shima, H., Chou, L., and Okamura, H., Bond slip strain relationship of deformed bars embedded in massive concrete, Journal of JSCE, 6, pp. 165-174, 1987.

CHAPTER 4

Investigations on Strengthening by UFC Panels and

Patch Repair on RC Beams affected by Chloride Attack

4.1.   INTRODUCTION

Chloride attack is one of the most widespread causes of deteriorating the RC structure, which is usually caused by several reasons such as inadequate design and/or construction, lack of maintenance and/or severe environment. The chloride attack would lead to the destruction of passive film of rebars, the corrosion of rebars, the spalling of concrete cover and so on. Moreover, it would also lead to the loss of reliability, availability and serviceability of RC structures, and affect the load-bearing mechanism. The European Standard confirmed that the patch repair can be used to restore the original properties and the appearance of damaged RC structures[1]. Since then, the patch repair has been widely used to locally replace the deteriorated concrete and corroded reinforcement bars, and to rehabilitate the pervious functions of repairing objects[2,3]. On the other hand, Polymer Cement Mortar (PCM) has several outstanding attributes, such as low permeability and inhibiting effect on the drying shrinkage cracking. The PCM is widely used to replace the damaged concrete after the cleaning corroded reinforcement bars and the anti-corrosive coating[4].

There exist amounts of existing RC structures with corrosion problem, which are needed to be replaced of the corroded rebars and to be upgraded in the load bearing capacity. In the past decades, many studies have been conducted to evaluate the repairing effectiveness using the patch repair method. Some of the results proved that the patch repair method does be beneficial to the flexural strengthening.[5-13]. However, there are few studies which also pointed out the influence of the patch repair method on the shear resisting mechanism. Moreover, the influence of the shear strengthening on the load bearing capacity of repaired RC structures is also needed to be further investigated.

To investigate the influence of the patch repair method on the shear resisting mechanism, the patch repair was carried out on the RC beams in this chapter. Moreover, the strengthening effectiveness of bonding UFC panels on the patch repaired RC beams was evaluated. And the factors such as shear-span ratio, patch repair and the strengthening of UFC panels were also studied here.

4.2. METHODOLOGY

4.2.1. Specimen details

Six identical RC beams were cast in the experiments, which were loaded with a four point bending configuration, with 240mm in height, 150mm in width and 1500mm in length. The span was 1200mm, and the distance between the loads was specified by the shear-span ratio (a/d). The list of specimens is shown in Table 4.1. All the beams were cast in steel molds and were cured in the molds under a wet hessian for two days. As there were many RC bridges reinforced with round steel bars in 1960s, round rebars in tension were used and the influence of rebar type was investigated in this study. In addition, the aim of this experiment was to evaluate the shear strengthening performance for aging or damaged RC bridges with PCM repairs. For this purpose, RC beams were designed to break down in shear failure and a few shear reinforcement stirrups were set. Two groups of specimens, Group 1 and Group 2, were used to evaluate the effects of the shear strengthening of UFC panels under different shear-span ratios (a/d = 2.5, 1.5).

▪ **Group 1**: Beams were designed to have a shear-span ratio of 2.5, since all sorts of failure modes would occur when the shear-span ratio is equal to 2.5. There were three beams including one control specimen N2.5, one repaired beam P2.5 and one repaired and strengthened beam P2.5UFC. To prevent flexural failure, all beams were further strengthened by using CFRP sheets. Fig. 4.1 shows the details of RC beams. The longitudinal reinforcement consisted of three φ16 for tension and two D13 for

Table 4.1. List of specimens in loading tests.

Group	Specimen	Concrete strength (MPa)	Compressive strength of PCM (MPa)	UFC	CFRP	a/d
	N2.5	18	-	-	O	2.5
Group 1	P2.5	18	20	-	O	2.5
	P2.5UFC	18	20	O	O	2.5
	N1.5	18	-	-	-	1.5
Group 2	P1.5	18	17	-	-	1.5
	P1.5UFC	18	17	O	-	1.5

compression. The yield strength of them were 320 MPa and 375 MPa, and the tensile strength of them were 465 MPa and 545 MPa. The patch repair was conducted on beams P2.5 and P2.5UFC, where PCM was adopted to replace the matrix concrete in the tension zone with 70mm depth.

▪ **Group 2**:   Beams were designed to have a shear-span ratio of 1.5, simulating the girder end of a strengthened RC bridge or the RC deep beam girder. The purpose of this group was to compare the strengthening influence under different shear-span ratios. There were three beams including one control specimen N1.5, one repaired beam P1.5 and one repaired and strengthened beam P1.5UFC. All the beams had the same shear-span ratio (=1.5). Fig. 4.2 shows the details of RC beams. The longitudinal reinforcement consisted of three φ16 for tension and two D13 for compression. The tensile strength of them were 333 MPa and 335 MPa, and the yield strength of them were 465 MPa and 564 MPa. The patch repair by using PCM was also carried out in this group.
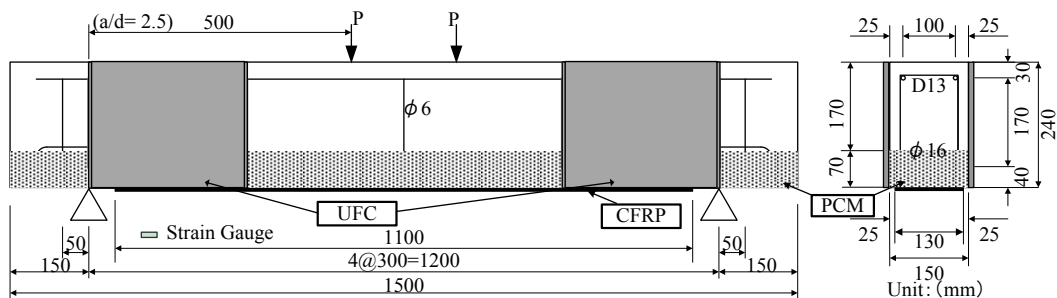

Fig. 4.1. Dimensions of RC beams and Locations of UFC panel (Group 1).
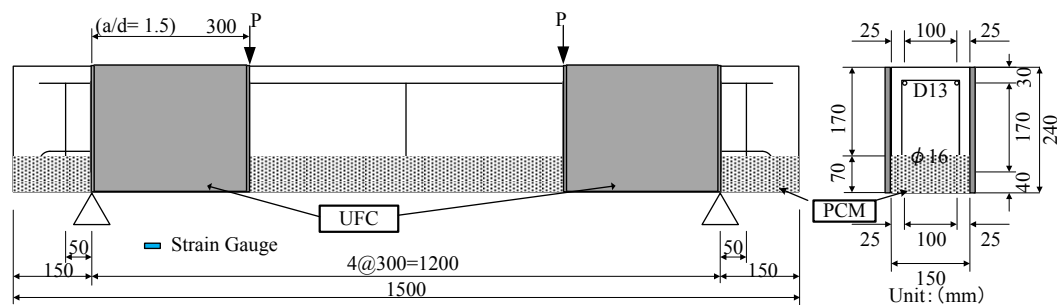
Fig. 4.2. Dimensions of RC beams and Locations of UFC panel (Group 2).

4.2.2. UFC properties

In the experiment, the UFC was molded into panels. The volume of mixed steel fibers was set at around 5%, the steel fibers had the diameter of 0.1~0.25 mm, the length of 10~20 mm and the tensile strength of 2×10^3 MPa. The water-cement ratio was below 0.24. And other components were silica fume, ground quartz, super-plasticizer, and high amount of Portland cement (up to 1000 kg/m^3). The thickness of UFC panels was set as 7 mm. To prevent the stress concentration, the edge of UFC panel was molded to be a 45° taper. The properties of the UFC panel are specified in Table 4.2 and one of the used UFC panels is shown in Fig. 4.3.

4.2.3. UFC panel bonding

The surfaces of concrete matrix and UFC panel were polished and roughed by disk grinder firstly, and then the UFC panels were fixed by anchor bolts at the designed strengthening positions.　Fig. 4.4 shows the positions of the anchoring holes where no rebar passed through. During anchoring, the washers of 3 mm thickness were interposed between concrete matrix and UFC panel. The gaps around the panels were sealed except the injection side (preparing for the injection of the epoxy resin). Table 4.3 shows the material properties of the adhesive epoxy resin.

Table 4.2. Material properties of UFC panel.

Density (g/cm^3)	Compressive strength (N/mm^2)	Flexural strength (N/mm^2)	Tensile strength (N/mm^2)	Elastic modulus (kN/mm^2)
2.55	210	43	10.8	54

Fig. 4.3. The photo of UFC panel used.

4.2.4. CFRP sheets bonding

The procedure of bonding the CFRP sheets was explained below. Firstly, the bonding surface of RC beams was polished by the disc sander. Secondly, the putty with the thickness of 1 mm was applied after the day of surface coating with epoxy primer. On the putty, the CFRP sheet was impregnated and bonded with epoxy resin and deaerated by roller. Thirdly, the surface was covered with a release sheet and was flatted, and then was cured for days. The properties of CFRP sheet are given in Table 4.4.

Fig. 4.4. Setting of UFC panel.

Table 4.3. Material properties of adhesive epoxy resin.

Compressive strength (N/mm^2)	Tensile strength (N/mm^2)	Tensile modulus (kN/mm^2)
73.5	23.5	3.7

Table 4.4. Material properties of CFRP sheet.

Fiber weight per unit area (g/m^2)	Design thickness (mm)	Tensile strength (MPa)	Tensile modulus (GPa)
600	0.333	4490	263

4.2.5. Patch repair

The patch repair has been widely used to locally replace the deteriorated concrete, remove the rust and implement the corrosion protection, rehabilitating the pervious functions of repairing objects. In this chapter, the depth of repairing layer was set as 70mm, so as to expose the tensile rebars out. The matrix concrete was cast to the location designed. Then, 2 hours later, the retardant was used to prolong the concrete setting time. On the second day, after cleaning the surface of matrix concrete, the repairing layer was cast with PCM.

4.3. EXPERIMENTAL RESULTS (GROUP 1)

The test results in terms of ultimate load, initial stiffness and failure mode are given in Table 4.5. Compared with the control beam N2.5, the maximum load and initial stiffness of P2.5 were increased slightly by 7% and 10%, respectively. Furthermore, the greater strengthening effectiveness was observed in P2.5UFC. The maximum load (51%) and initial stiffness (35%) were upgraded significantly by bonding UFC panels. In addition, the PCM interfacial debonding occurred in P2.5. It showed that the integrity between the matrix concrete and repairing layer is still a problem when implementing the patch repair. On the contrary, for the strengthened beam P2.5UFC, the interfacial debonding was restricted and the beam finally failed in shear compression failure.

The load-deflection relationships of Group 1 are shown in Fig. 4.5. For P2.5, a high stiffness was observed at the early stage. However, when the load reached at 80kN, the stiffness dropped. On the other hand, the great stiffness was obtained in P2.5UFC.

Table 4.5. Loading test results.

Specimen	Maximum load P_{max} (kN)	Effective-ness	Stiffness at 50kN (kN/mm)	Effective-ness	Failure mode
N2.5	104.7	-	67.9	-	Shear tension failure
P2.5	112.5	7%	74.4	10%	PCM interfacial debonding
P2.5UFC	157.6	51%	91.8	35%	Shear compression failure

Fig. 4.6 shows the rebar strain distribution. For the control beam N2.5, the debonding occurred at the early stage (load = 80kN). For the repaired beam P2.5, the debonding was delayed, which occurred at 100kN. In previous studies, as compared with the plain concrete, the relatively good bond with rebars was observed in PCM specimens from the pull-out testing, which was considered as the reason of the difference between N2.5 and P2.5. By comparison, due to the UFC panels strengthening, the strain value of end region of tensile rebars in P2.5UFC was kept at a low level, and the debonding was restricted.

Fig. 4.7 shows the crack patterns. For the control beam N2.5, due to poor bonding of round rebars, the splitting cracks occurred along the tensile rebars, and the beam resulted in shear tensile failure. For the beam P2.5, the cracks occurred on the interface of matrix concrete and repairing layer, which led the beam to break down. On the contrary, due to the benefits of bonding UFC panels, the splitting cracks and interfacial layer cracks were restrained. The beam resulted in shear compression failure.
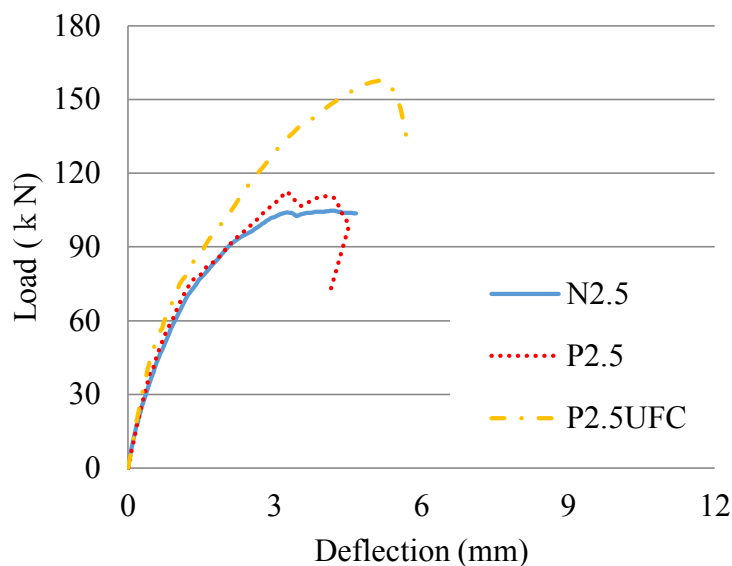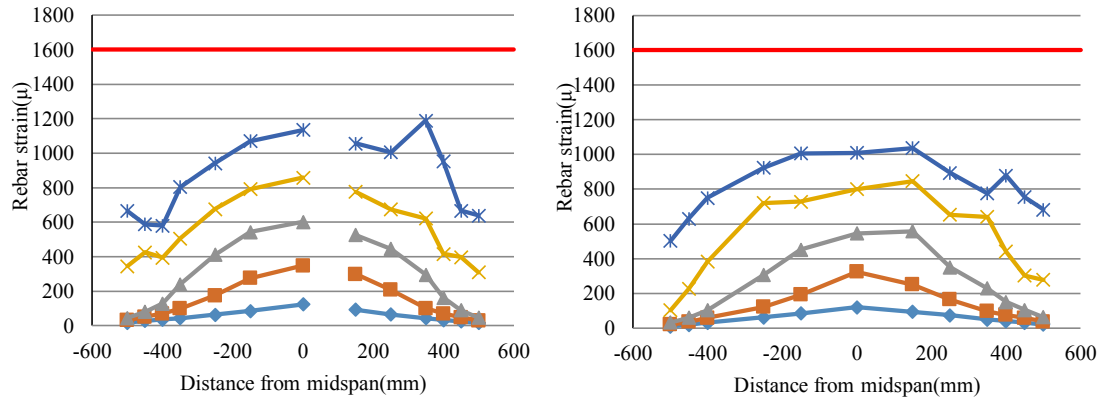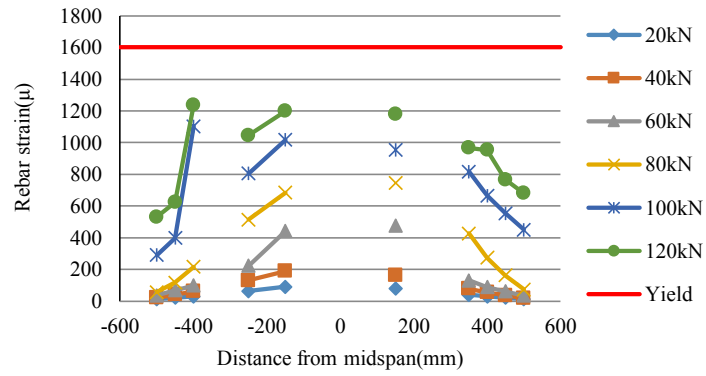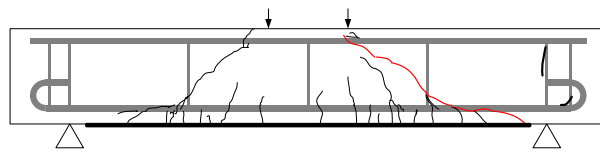

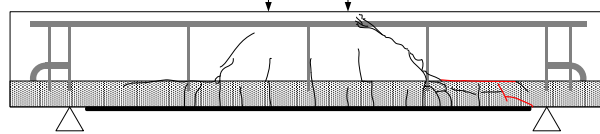Fig. 4.5. Load-deflection relationships.

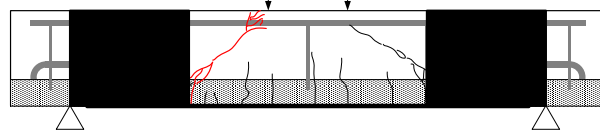(a) N2.5

(b) P2.5

(c) P2.5UFC

Fig. 4.6. Rebar strain distribution.

(a) N2.5

(b) P2.5

(c) P2.5UFC

Fig. 4.7. Crack patterns.

4.4.   EXPERIMENTAL RESULTS (GROUP 2)

The testing results of Group 2 are shown in Table 4.6. It was found that the control beam N1.5 resulted in the shear compression failure (with arch mechanism), the repaired beam P1.5 resulted in the shear compression failure (without arch mechanism), and the strengthened beam P1.5UFC failed in flexure. The results showed that the strengthening method by bonding the UFC panels would affect the failure mode of RC beams. In addition, compared with the control beam N1.5, the minus strengthening effect was observed in repaired beam P1.5. The maximum load was decreased by 14%. It was noticed that the patch repair with improvement of bond strength of rebars, might reduce the shear strength of RC beams due to change in failure mode, especially the beams with the low shear-span ratio. On the contrary, the obvious improvement was obtained in P1.5UFC.

Fig. 4.8 shows the load-deflection relationships. For the repaired beam P1.5, the higher stiffness was observed at the early stage. However, after the load reached at about 70kN, the stiffness declined and the load sharply decreased after reached at the peak. It showed the highly brittle behavior. The minus effects of patch repair on load-bearing capacity and failure mode should be paid attention to when designing. For the strengthened beams P1.5UFC, it can be seen that the failure mode was ameliorated by using the UFC panels strengthening method. The beam failed in ductile flexure. Fig. 4.9 shows the rebar strain distribution. For the control beam N1.5, the debonding at the end of the tensile rebars occurred at 120kN. For the beam P1.5, the abrupt debonding at one side occurred. On the other hand, in the beam P1.5UFC, the strain of the tension rebar was restrained at a low level.

Table 4.6. Loading test results.

Specimen	Maximum load P_{max} (kN)	Effectiveness	Stiffness at 50kN (kN/mm)	Effectiveness	Failure mode
N1.5	196.1	-	108.5	-	Shear compression failure (arch)
P1.5	169.2	-13.7%	177	63.1%	Shear compression failure
P1.5UFC	273.6	39.5%	173	59.4%	Flexural failure

Fig. 4.10 shows the crack patterns. For the control beam N1.5, the first shear crack occurred close to the mid-span, and extended along the tensile rebars. It was because of the low bond strength of the round rebars. Then, the dominant shear crack reached the end anchorage section, and the arch mechanism was formed. For the beam P1.5, due to the good bonding of PCM and rebars, the splitting cracks were restricted. Consequently, the arch mechanism did not form, and the beam broke down abruptly due to the dominant shear crack occurred at about 150kN. For the strengthened beam P1.5UFC, the beam resulted in the flexural failure.
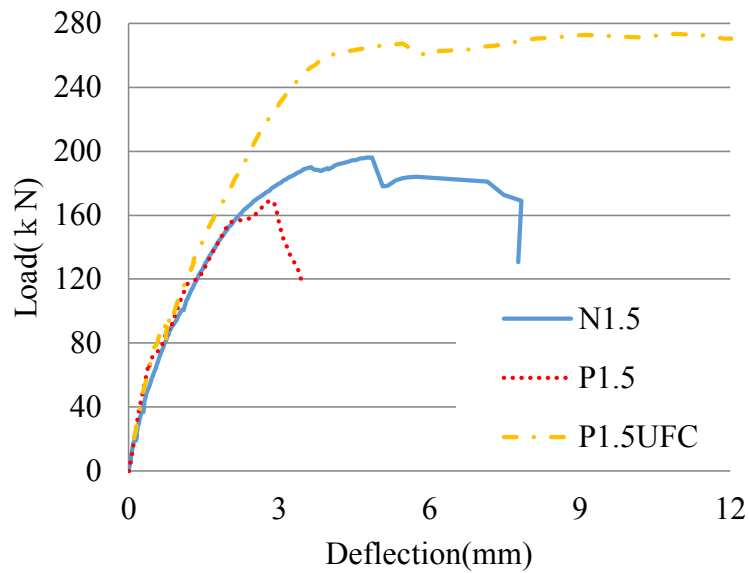
Fig. 4.8. Load-deflection relationships.
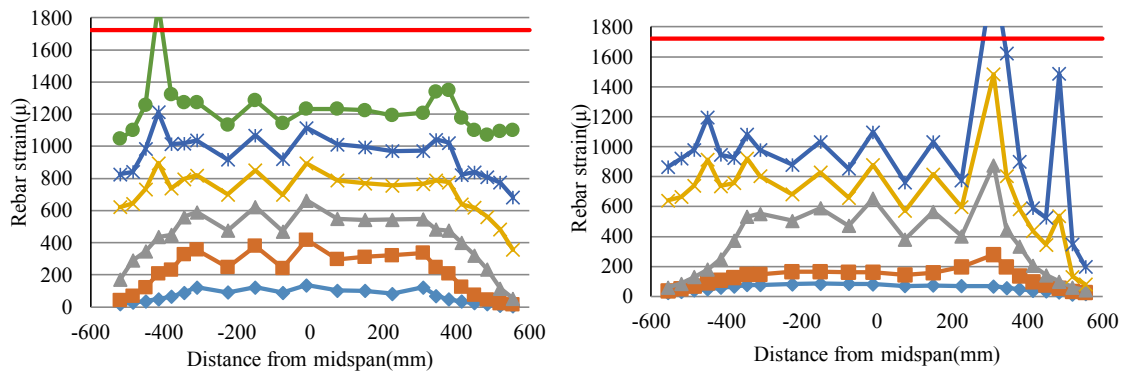
(a) N1.5   (b)P1.5
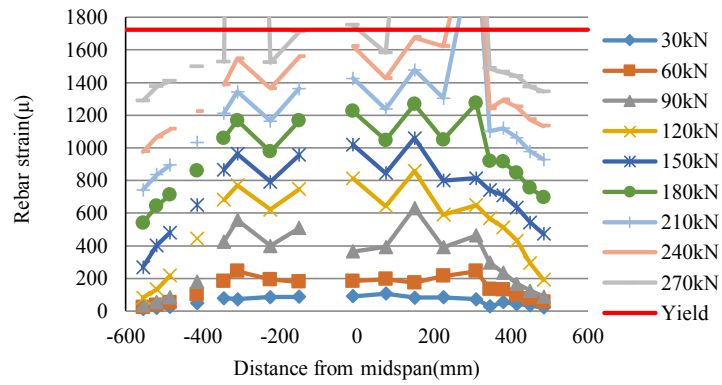
(b) P1.5UFC

Fig. 4.9. Rebar strain distribution.
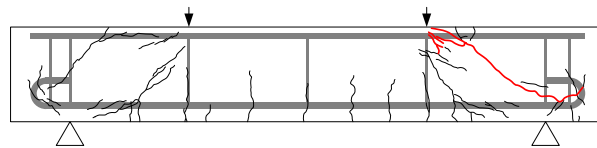
(a) N1.5
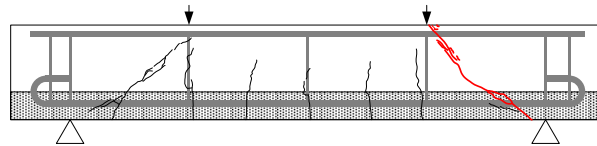
(b) P1.5
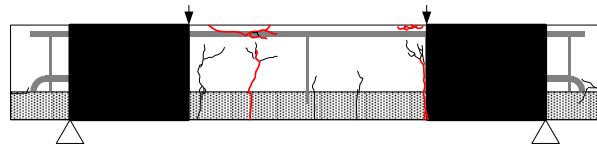
(c) P1.5UFC

Fig. 4.10. Crack patterns.

4.5. DISCUSSION

4.5.1. Influence of PCM on the shear resisting mechanism

With respect to the normal shear-span ratio (a/d = 2.5), the patch repair slightly improved the load bearing capacity and initial stiffness, and restricted the debonding of tensile rebars. However, the PCM interfacial debonding occurred in the repaired RC beam, which implied that the integrity between the matrix concrete and repairing layer was hard to be secured for the patch repair. Moreover, in the case of low shear-span ratio (a/d = 1.5), shear flexural cracks and splitting cracks were restricted. Consequently, the arch mechanism was not formed, and the beam failed in a brittle manner. Therefore, the strengthening effectiveness of patch repair should not be expected, especially for the beams with low shear-span ratio.

4.5.2. Influence of bonding UFC panels on repaired beams

When implementing the patch repair on the beams with normal shear-span ratio (a/d = 2.5), the integrity between the matrix concrete and repairing layer was insufficient in the loading test results. Due to the UFC panels strengthening, the interfacial failure was restricted. The UFC panels improved the integrity of repaired RC beams. In the case of the beams with low shear-span ratio (a/d = 1.5), the load-bearing capacity of the repaired beam by PCM dropped, and the beam resulted in the brittle failure. On the contrary, for the strengthened beam by UFC panels, the improvement of the load-bearing capacity and stiffness were obtained, and the beam resulted in the ductile failure. The great effectiveness of bonding UFC panels on repaired RC beams were gained.

4.6.   CONCLUSIONS

This chapter experimentally investigated the influence of the patch repair on the shear resisting mechanism of RC beams, and evaluated the effectiveness of bonding UFC panels on the patch repaired RC beams. The results are summarized below.

1.   When a/d was equal to 2.5, the load bearing capacity and stiffness were enhanced by applying the patch repair. The concrete splitting around tensile rebars was delayed due to the relatively good bonding of PCM and rebars. However, the beam broke down in the interfacial debonding, which showed the integrity between the matrix concrete and PCM was hard to be secured.

2.   When repairing the RC beams with low shear span ratio (1.5) using PCM, an un-predictable brittle failure occurred. Besides, the decrease in load bearing capacity was observed. The side effect of applying patch repair on the structural performance should be paid attention to especially for the RC beams with low shear span ratio.

3.   Due to the strengthening effect of bonding UFC panels, the shear capacity and stiffness of RC beams were enhanced and the failure mode was ameliorated. Especially the problems such as the interfacial debonding, the decrease in shear capacity and the brittle failure observed in the repaired RC beams were all prevented. It can be said that the integrity and safety of repaired RC beams can be secured by bonding UFC panels.

REFERENCES

1 British Standard Institution, European Standard (ENV 1504, Part 9), 1998.

2 COMETT Project, 7352/Cb, Concrete repair technology, *Proceedings of the short course at Taywood Engineering*, 1995.

3 Keer, J.G., Chadwick, J.R., Thompson, D.M., Protection of reinforcement by concrete repair materials against chlorideinduced corrosion, *Proceedings of the 3rd International Symposium on 'Corrosion of Reinforcement in Concrete Construction' held at Wishaw*, 1990.

4 Sohanghpurwala, A.A., Manual on service life of corrosion-damaged reinforced concrete bridge superstructure elements. *National Cooperative Highway Research Program*, *National Research Council* (US), *Transportation Research Board*, 2006.

5 Hughes, B.P., Evbuomwan, N., Polymer-modified ferrocement enhances strength of reinforced concrete beams, *Construction Building Matererails*, 7, pp. 9-12, 1993.

6 Raoof, M., Structural characteristics of RC beams with exposed main steel. *Structures and Buildings*, 1997.

7 Cairns. J,, Zhao, Z., Behaviour of concrete beams with exposed reinforcement, *Structures and Buildings*, 1993.

8 Almusallam, A.A., Al-Gahtani, A.S., Maslehuddin, M., Kahan, M.M., Aziz, AR., Evaluation of repair materials for functional improvements of slabs and beams with exposed reinforcement, *Structures and Buildings*, 1997.

9 Mays, G.C., Barnes, R.A., The structural effectiveness of large volume patch repairs to concrete structures, *Structures and Buildings*, 1995.

10 Dristos, S., Pilakoutas, K., Kotsira, E., Effectiveness of flexural strengthening of RC members, *Construction and Building Materials*, 1995.

11 Nounu, G., Chaudhary, Z.U.H., Reinforced concrete repairs in beams, *Construction and Building Materials*, 13, pp. 195-212, 1999.

12 Jorge, S., Dias-da-Costa, D., Julio E.N.B.S., Influence of anti-corrosive coatings on the bond of steel rebars to repair mortars, *Engineering Structures*, 36, pp. 372-378, 2012.

13 Kobayashi, K., Rokugo, K., Mechanical performance of corroded RC member repaired by HPFRCC patching, *Construction and Building Materials*, 39, pp. 139-147, 2013.

CHAPTER 5

Introduction Investigations on Shear Behavior and Strengthening

by UFC Panels of RC Beams Affected by Alkali-Silica Reaction

5.1. INTRODUCTION

Alkali-Silica Reaction (ASR), a heterogeneous chemical reaction between the highly alkaline cement paste and reactive non-crystalline silica, is one of the most recognized deleterious phenomena in concrete and will lead to the premature deterioration such as serious expansion and deleterious cracking. ASR was recognized as a durability challenge. Now, how to maintain the RC structure subjected to ASR damage has gained more and more attention. Since ASR problem was first pointed out in 1940[1], many RC structures affected by ASR had been reported around the world[2-4]. In the past decades, to evaluate the ASR problem, several international committees and some researchers have proposed various evaluation methods based on the surface cracking, expansion amount, aggregate ingredient and so on. For instance, the crack width and crack distribution investigation were implemented as one of the fundamental inspections to assess the ASR damage[5,6]. In the expansion evaluation method, the ASR deterioration level was analysed by measuring the expansion amount[7]. In another

research, the stiffness damage test[8,9] and the damage rating index[10] were adopted to evaluate the expansion in the concrete affected by ASR damage[11]. Moreover, to evaluate the concrete cores with ASR damage, Rivard et al.[12] compared the effects of ultrasonic wave velocities[13], dynamic Young modulus measured with resonant frequency[14] and electrical resistivity[15]. With the development of technology, some new techniques have been introduced to assess the ASR deterioration of RC structures. For example, Scanning Electron Microscopy Image Analysis (SEM-IA) was one of the newly introduced techniques, which quantified the ASR degree in affected micro bars, mortar and concrete prisms, and investigated the correlation between the ASR degree and macroscopic expansion[16]. Image analysis techniques were also introduced to facilitate the assessment of the reactivity of aggregates[17]. For better differentiating various aggregates with similar levels of reactivity, a novel Nonlinear Impact Resonance Acoustic Spectroscopy (NIRAS) was introduced to identify the reactivity of aggregates. The performance of NIRAS has been demonstrated in a certain samples[18]. Due to the complexity and diversity of the environment (the locations of the ASR affected structures), how to choose suitable evaluation methods, which can meet the requirements in terms of cost, time-consuming, and precision, is very important. In this chapter, some of those non-destructive inspections were used to characterize the ASR deterioration in RC beams before loading tests, which were designed to simulate the bridge girder and T-shaped RC pier beam.

The influence of ASR damage on the load bearing mechanism of RC structures is also an important issue in ASR researches. In Monette et al.'s research, the material tests and loading tests were carried out, where the testing results demonstrated that the stiffness and load-bearing capacities of the beams with ASR damage were not obviously lower than that of the control beam even though the compressive stiffness and flexural strength of the concrete decreased as ASR developed[19]. With respect to the shear capacities, some research findings indicated that there is no significant difference between the RC beams with ASR damage and the normal ones, as long as the stirrup reinforcing ratio is greater than 0.2%[20]. However, it does not mean that there is no need to concern about the potential accidents in the RC structures subjected to ASR. There still exist amounts of existing ASR affected structures needed to be repaired or

79

strengthened due to the poor design and/or construction. In the past years, the main way to strengthen the structures damaged by ASR is to demolish and reconstruct a portion of the whole structure[21]. With the development of the strengthening techniques, such as bonding the steel plates[22-26], bonding Carbon Fiber Reinforced Plastic (CFRP) sheets[27-31] and retrofitting with Ultra high strength Fiber reinforced Concrete (UFC)[32 -34], the newly developed techniques have been also applied in the ASR affected structures. For example, M.E. Williams evaluated and repaired the substructures of a 10 years old highway bridge subject to ASR problem by using the CFRP composite for confinement and anchorage[35]. However, there are few studies to point out the influence of the flexural strengthening (bonding CFRP sheets) on the load bearing mechanism of RC beams with comparatively low shear-span ratio (a/d), like the beam part of T-shaped pier. Here, the influences of some strengthening methods on the load bearing mechanism of ASR affected RC beams (bridge girder and T-shaped RC pier beam) were investigated in this chapter.

In addition, an appropriate numerical analysis method is an important factor to guide the maintenance and strengthening of ASR affected structures. When conducting the numerical analyses, it is essential to investigate the material properties of concrete deteriorated by ASR. So far, various material tests have been conducted to investigate the properties of ASR affected concrete. It was found that different signs would appear when ASR occurred, such as the changes in the elastic properties due to alkali-silica gel[36]. From another perspective, the behaviors of structural materials would also be affected by ASR damage. Currently, some studies have been conducted on the variation of structural material properties of concrete with the development of ASR. At an early stage, Swamy and AI-Asali conducted a detailed concrete characteristic study on the compressive and tensile strength, elastic modulus and pulse velocity, using a naturally occurring Beltane opal and a synthetic fused silica[37]. Later, Jones and Clark explored the concrete properties such as compressive strength, Young's modulus and tensile strength[38]. To measure the influence of the internal crack pattern caused by ASR on the strength and rheological properties, Giaccio et al. conducted comparisons between the mechanical response of a reference concrete at different ages

(without reactive aggregates), where concretes were prepared with three different types of reactive aggregates (with the same mixture proportions)[39]. The stress strain behavior in compression and the load-deflection response in flexure were measured. Those properties of concrete damaged by ASR in terms of the concrete strength, elastic modulus, ultrasonic pulse velocity and the stress strain behavior, were also tested and similar results were found by the authors [40]. On the other hand, due to the uncertainty and complexity of ASR, it is not sufficient to represent the ASR in the experiments by using those material properties. In this paper, the expansion feature of ASR deterioration is considered as a breakthrough point to set up an appropriate analysis model.

In this chapter, two series (A and B) of RC beams were cast to simulate the ASR affected bridge girder and T-shaped RC pier beam, respectively. Except the control beams, the slow reactive aggregates and alkali additives were added to induce ASR. Also, they were exposed in exterior environment for years and watered regularly to keep the suitable humidity. In the T-shaped RC pier beam, the tensile rebars were located on the top which were easy to contact the rainwater. Thus, the beams in Series B were overturned to keep the tensile rebars on the top. As the accidents that the anchor of tensile rebars fractured due to ASR have been reported recently, the influence of fractured rebars on the load bearing of ASR affected structures was also investigated here[41] (refer to Fig. 5.1).

Fig. 5.1. Fracture of tensile rebar anchor

Before the loading tests, the non-destructive inspections (crack investigation, expansion amount measurement and ultrasonic wave inspection) were adopted to evaluate the differences between the different ASR deterioration states. Moreover, in order to investigate the influence of several strengthening methods on the load bearing mechanism, some of the beams were strengthened by bonding CFRP sheets and the others were strengthened by bonding UFC panels. In addition, the nonlinear Finite Element (FE) analyses were conducted to help better understanding of the ASR damage, and an analysis model was proposed to simulate the expansion caused by ASR.

5.2. BEAM GEOMETRY AND DESCRIPTION

Eleven identical RC beams were used in the experiments, which were loaded with a four point bending configuration, with 240-mm of height, 150-mm of width and 1200-mm of length. The span was 1000 mm, and the distance between the loads was 200 mm. The longitudinal reinforcement consisted of three D16 rebars for tension with yield strength of 342 MPa, and two D13 rebars for compression with yield strength of 359 MPa. The shear reinforcement consisted of D6 rebars with yield strength of 347 MPa. Two experimental series (A and B) were conducted to evaluate the influence of different exposure conditions and alkali additives on the degradation state and shear behavior of ASR affected RC beams. The lists of specimens in series A and B are shown in Table 5.1 and Table 5.2, respectively. Fig. 5.2 shows the dimensions of RC beams. The shear span ratio is 2.0.

Table 5.1. List of specimens in Series A.

Specimen	Simulated Objects	ASR damage	Exposure time	CFRP sheet	UFC panel
GN	Bridge girder	-	-	-	-
GA1(-a)	Bridge girder	O	1 year	-	-
GA1(-b)	Bridge girder	O	1 year	-	-
GA1(-c)	Bridge girder	O	1 year		
GA3_Cs	Bridge girder	O	3 years	O	-
GA3_CsUp	Bridge girder	O	3 years	O	O

Table 5.2. List of specimens in Series B.

Specimen	Simulated Objects	ASR damage	Exposure time	CFRP sheet	UFC panel	Rebar anchor
TN_Cs	T-shaped pier	-	-	O	-	O
TA1_Cs	T-shaped pier	O	1 year	O	-	O
TA1_Cs_Ft	T-shaped pier	O	1 year	O	-	-
TA1_CsUp	T-shaped pier	O	1 year	O	O	O
TA1_CsUp_Ft	T-shaped pier	O	1 year	O	O	-
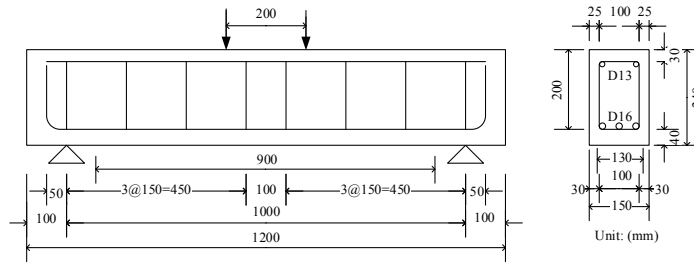
(a) GN, GA1(-a,-b,-c).
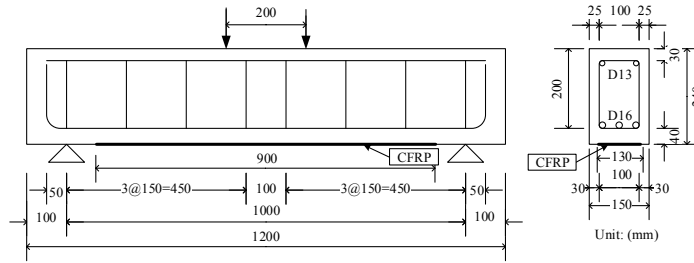
(b) GA3_Cs, TN_Cs, TA1_Cs.
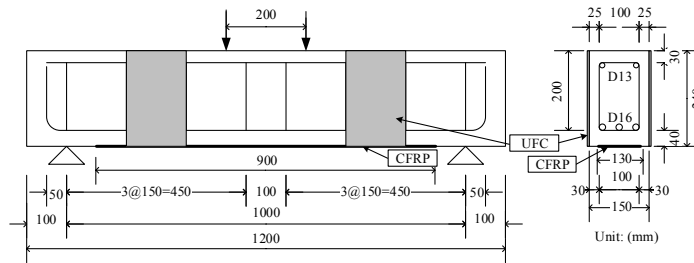
(c) GA3_CsUp.
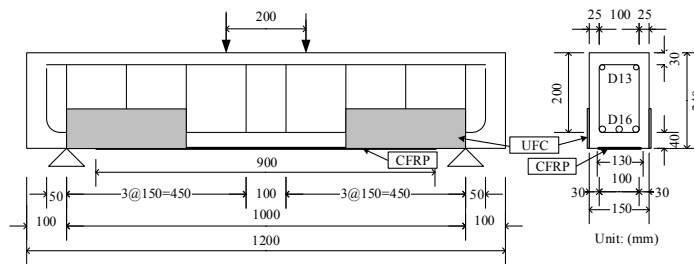
(d) TA1_CsUp.
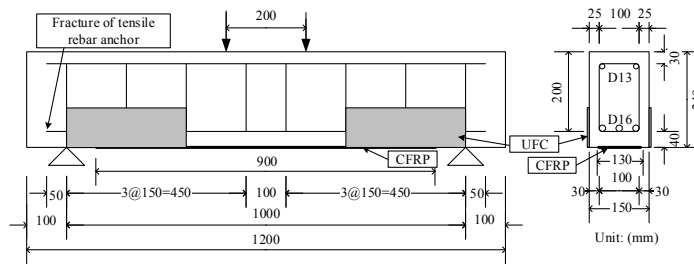
(e) TA1_CsUp_Ft.

Fig. 5.2. Dimensions of RC beams.

84

Series A was designed to simulate the bridge girder affected by ASR damage. It consisted of six RC beams: one control RC beam and five deteriorated RC beams. The ends of tensile rebars were bended to be 90° hooks and additional stirrups were used in the anchorage region. Table 5.3 shows the specific mix proportion of Series A. NaOH was added for ASR triggering with 8.45 kg/m^3, and 50% mixture ratio of reactive aggregate to total aggregate quantity including non-reactive aggregate was used. For all the beams, they were cast in the steel molds and cured under a wet hessian for four weeks. Five beams, which were added the ASR reactive aggregate, have been exposed in exterior environment for one year and three years, respectively. The influence of strengthening techniques on the load-bearing capacity and mechanism was investigated in Series A.

In Series B, the beams with reactive aggregates were exposed in exterior environment for one year under the condition that the tension sides were turned up. The aim is to simulate the ASR affected beam member of T-shaped pier. There were one control RC beam and four deteriorated RC beams. Table 5.4 shows the specific mix proportion of Series B. Different from Series A, NaCl was added as alkali additives with 12.4

Table 5.3. Specified mix proportion (Series A).

| Unit Quantity(kg/m^3)						AE additive (kg/m^3)	NaOH (kg/m^3)
Water	Cement	Sand (Noreactive)	Sand (reactive)	Gravel (Noreactive)	Gravel (reactive)		
183	290	399	411	495	493	2.9	8.5

Table 5.4. Specified mix proportion (Series B).

Unit Quantity(kg/m^3)						AE additive (kg/m^3)	NaCl (kg/m^3)
Water	Cement	Sand (Noreactive)	Sand (reactive)	Gravel (Noreactive)	Gravel (reactive)		
181	287	423	462	431	474	5.7	12.4

kg/m³, and 50% mixture ratio of reactive aggregate to total aggregate quantity was used for the four deteriorated beams. Recently, the fracture of the tensile rebar anchor due to ASR expansion was reported. Thus, in Series B, the tensile rebars without 90° hooks were used in the anchorage region of beams TA1_Cs_Ft and TA1_CsUp_Ft. The purpose is to simulate the fracture damage of the tensile rebar anchor (see Fig. 5.2). Also, the strengthening investigations were carried out in Series B.

5.3.   NON-DESTRUCTIVE TESTING

5.3.1.   Crack investigation

To study the deterioration state, the crack investigation was conducted. The cracks were traced using magic markers. The width of cracks was measured by the crack scale, and the length of cracks was processed by image analysis software. A comparison based upon the crack properties and the area density of cracks along the tensile rebar was conducted between Series A and Series B (see Fig. 5.3 and Table 5.5).

Similar tendency was found in the two Series. Due to the state of ASR expansion, the extending crack was along the axial direction and tended to develop in the direction with small restraint effect by rebars. On the other hand, for the cracks on the side, the positions were different in the two experimental Series. For Series A, cracks occurred where there was no longitudinal rebar. For Series B, cracks appeared directly above the rebar. Moreover, comparing the area density of cracks along the tensile rebar, the area densities of cracks along the tensile rebar in Series B were significantly larger than that in Series A (see Table 5.5). There are two possible reasons to explain this difference. One is that the side of tensile rebars was turned up in Series B, which resulted that the tensile rebar was easier to contact the rainwater and sunlight. Another reason is because of the ASR alkali additives. In Series A, NaOH was used, which would delay the hydration reaction. While in Series B, NaCl was used, which would promote the hydration reaction.
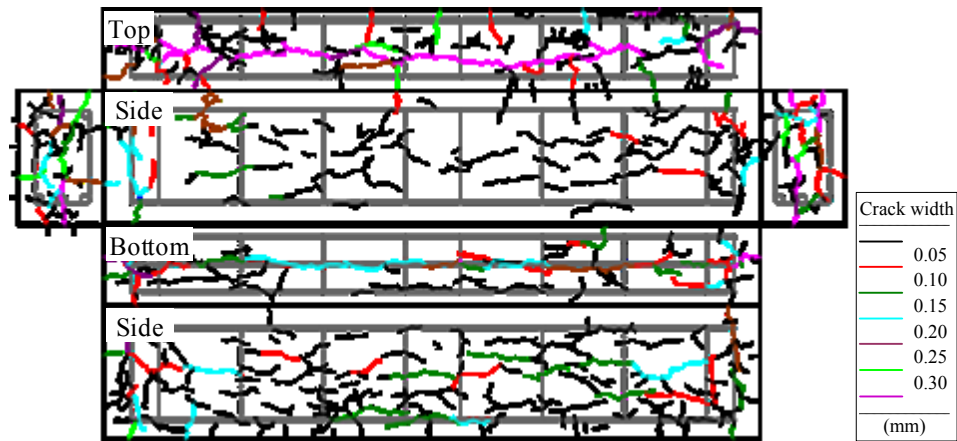
(a) GA1(-a)
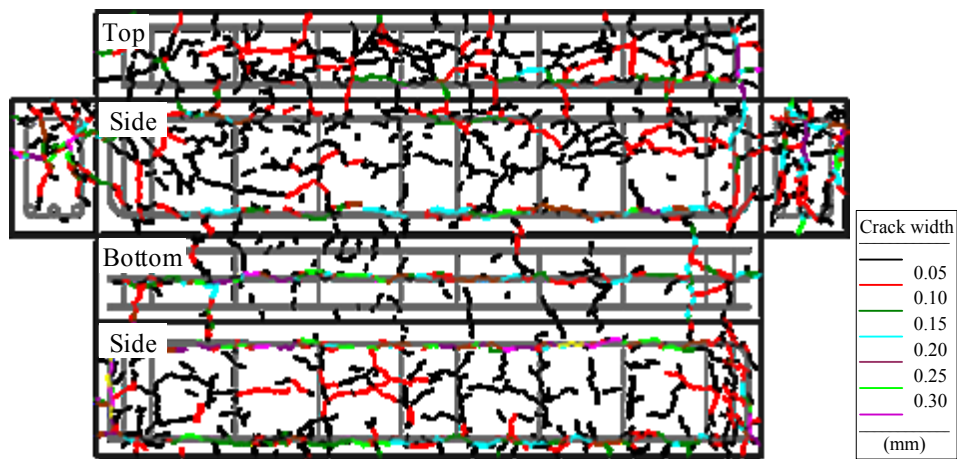
(b) TA1_Cs

Fig. 5.3. Crack condition due to ASR.

Table 5.5. Crack area density of surface concrete at tensile rebars.

	Specimen	Exposure time	Area density of cracks (mm^2/mm^2)
Series A	GA1(-a)	1 year	0.00128
	GA1(-b)	1 year	0.00171
	GA1(-c)	1 year	0.00083
	GA3_Cs	3 years	0.00175
	GA3_CsUp	3 years	0.00174
Series B	TA1_Cs	1 year	0.00342
	TA1_Cs_Ft	1 year	0.00212
	TA1_CsUp	1 year	0.00385
	TA1_CsUp_Ft	1 year	0.00331

5.3.2. Expansion amount investigation

The expansion amount was measured by contact gauge in different directions: vertical direction, upper axial direction and lower axial direction. Fig. 5.4 shows the positions of contact tips. The results of expansion amount are shown in Table 5.6. For the specimens GA1(-a, -b, -c), it can be seen that the degradation level differs greatly from each other, even if they were cast and cured under the same conditions. Furthermore, the greatest values were obtained in the vertical direction. It is because that the restraint of rebars was weakest in that direction.
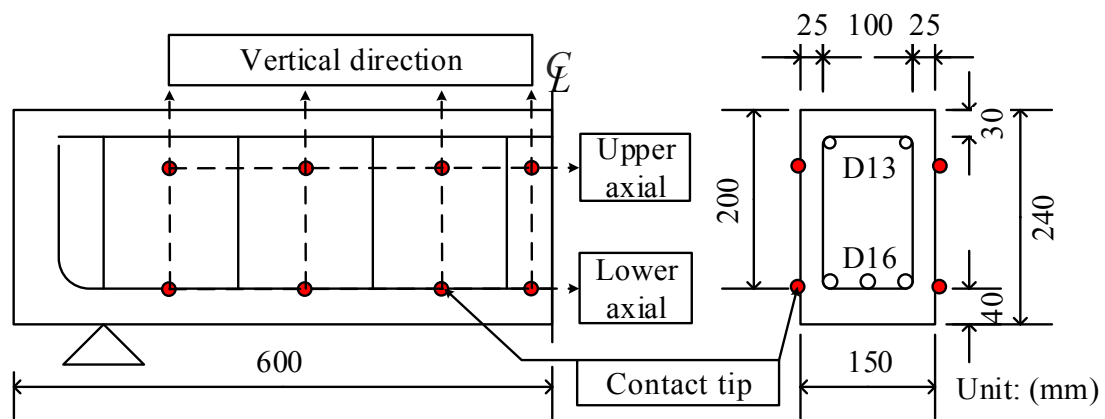
Fig. 5.4. Positions of contact tips.

Table 5.6. Expansion amount.

	Specimen	Expansion amount (μ)		
		Vertical	Upper axial	Lower axial
Series A	GA1(-a)	4325	2550	1050
	GA1(-b)	5055	1060	745
	GA1(-c)	2330	895	355
	GA3_Cs	3325	1050	930
	GA3_CsUp	3465	1295	1340
Series B	TA1_Cs	5632	2645	1417
	TA1_Cs_Ft	5117	1431	1187
	TA1_CsUp	6074	2605	571
	TA1_CsUp_Ft	6867	786	924

5.3.3. Ultrasonic wave velocities

The ultrasonic investigations were carried out to evaluate the degradation state and concrete strength. The ultrasonic wave velocities were measured in two directions: transverse direction and longitudinal direction. The measurement positions are shown in Fig. 5.5. The results of ultrasonic wave velocities are given in Table 5.7. The results indicated that the values in the longitudinal direction were greater than that in the transverse direction. It is because that the constraint effect of rebars in the transverse direction is lower than that in the longitudinal direction.
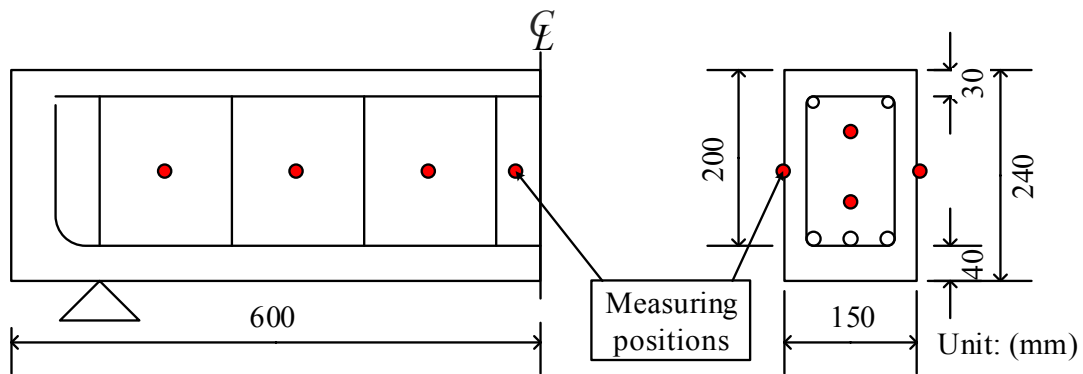
Fig. 5.5. Measuring positions of ultrasonic wave velocities.

Table 5.7. Expansion amount.

	Specimen	Ultrasonic wave velocities (m/s)	
		Longitudinal direction	Transverse direction
Series A	GA1(-a)	3853	3420
	GA1(-b)	3800	3331
	GA1(-c)	3934	3682
	GA3_Cs	3893	3400
	GA3_CsUp	3465	3550
Series B	TA1_Cs	4350	3831
	TA1_Cs_Ft	4485	3953
	TA1_CsUp	4436	3960
	TA1_CsUp_Ft	4449	3898

Furthermore, the fluctuation was found among GA1(-a,-b,-c), even though they were exposed in the same environment. Therefore, considering the different restraint conditions of rebars in beams and cylinders, the strength testing based on the cylinder specimens is not reliable. According to the previous research (a large amount of concrete core tests and ultrasonic wave investigations were conducted), the relationship between the ultrasonic wave velocity and concrete strength was modeled by the Morikawa et al[40]. Here, the material properties of specimens in this study were estimated by the ultrasonic wave velocities. Compressive strength and ultrasonic wave velocity relationship is shown in Fig. 5.6. The compressive strength $f_c{'}$ and the elastic modulus E_c are calculated as

$$f_c{'} = 0.5494 \times e^{0.9873 \times V_u} \tag{1}$$

$$E_c = 0.951 \times e^{0.814 \times V_u} \tag{2}$$

where V_u is the ultrasonic propagation velocity (m/s).
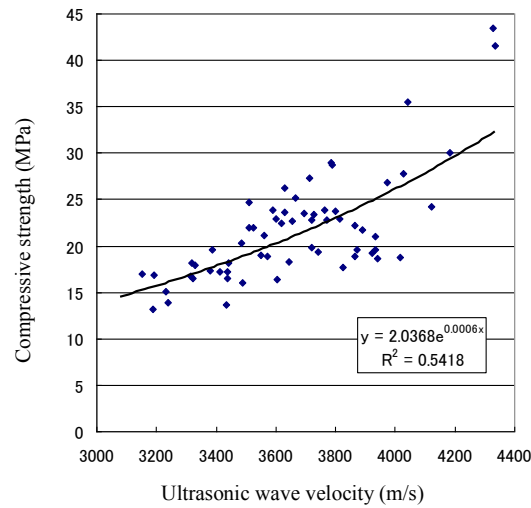
Fig. 5.6. Compressive strength and ultrasonic wave velocity relationship

5.4. LOADING TESTS

5.4.1. Influence of ASR damage on the bearing mechanism

The loading tests were conducted in Series A (consisting of the control beam GN and ASR affected beams GA1(-a,-b,-c)). Table 5.8 and Fig. 5.7 show the loading test results and the load-deflection relationship, respectively. In Table 5.8, the evaluation values were calculated according to Strut-tie theory and JSCE Specification [42]. In the experiments, the control beam resulted in the diagonal tension failure, while the ASR affected beams resulted in the flexural failure. It is inferred that, the opening and development of loading cracks were easy to be affected by the preceding cracks
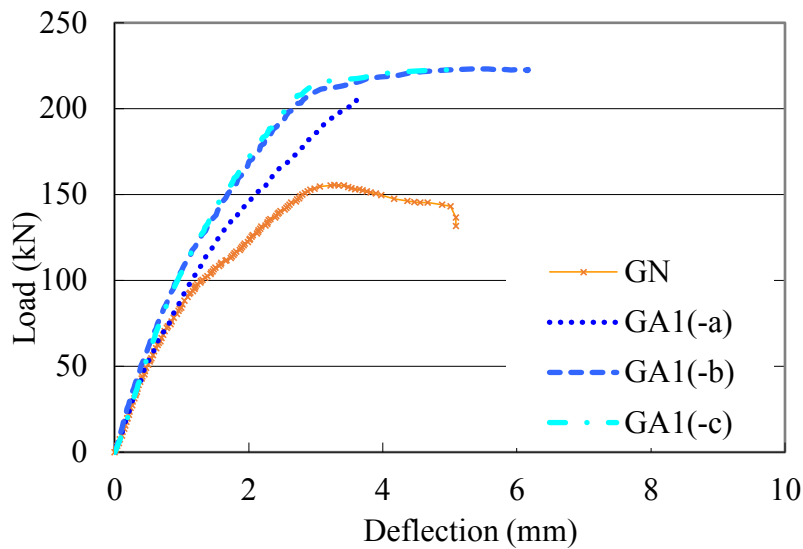
Fig. 5.7. Load-deflection.

Table 5.8. Loading tests results.

Specimen	Concrete strength (MPa)	Evaluation Shear strength (JSCE) (kN)	Evaluation Strut-tie strength (Strut-tie) (kN)	Maximum load (kN)	Stiffness (load=40kN) (kN/mm)	Failure mode
GN	36.5	137.2	-	155.6	108.9	Diagonal tensile failure
GA1(-a)	24.7	(128.0)	239.4	203.8	109.0	Flexural failure
GA1(-b)	23.4	(126.9)	237.6	223.1	131.6	
GA1(-c)	26.7	(129.8)	248.5	222.6	112.7	

91

caused by ASR, which accelerated the flexural cracks and bond-split cracks development at the early stage. When the slipping of rebar occurred, the bond stress of tensile rebar decreased and the load-bearing mechanism changed to arch mechanism. As shown in Table 5.8, the results demonstrated that the maximum loads of GA1 (-a,-b,-c) were much greater than the evaluation values of shear strength by JSCE, but were close to the evaluation values of strut-tie strength. It is because that the change of load bearing system from the diagonal tensile resisting mechanism to the arch mechanism significantly raised the load bearing strength. Besides, due to the concrete expansion cause by ASR, the pre-stress occurred inside the beams with ASR damage, which influenced the resisting mechanism and led to the increase of the load bearing capacity. In addition, even though the three beams of GA1 were cast and exposed in the same conditions, different maximum load and stiffness were obtained in the loading tests. The uncertainty and complexity of ASR damage were confirmed.

Fig. 5.8 shows crack patterns. The diagonal cracks were observed between the loading point and the support in GN. On the other hand, due to the influence of preceding cracks caused by ASR, the load bearing mechanism was different from the control beam. In GA1(-a,-b,-c), the dominant cracks occurred in the mid-span and did not extend to the supports.
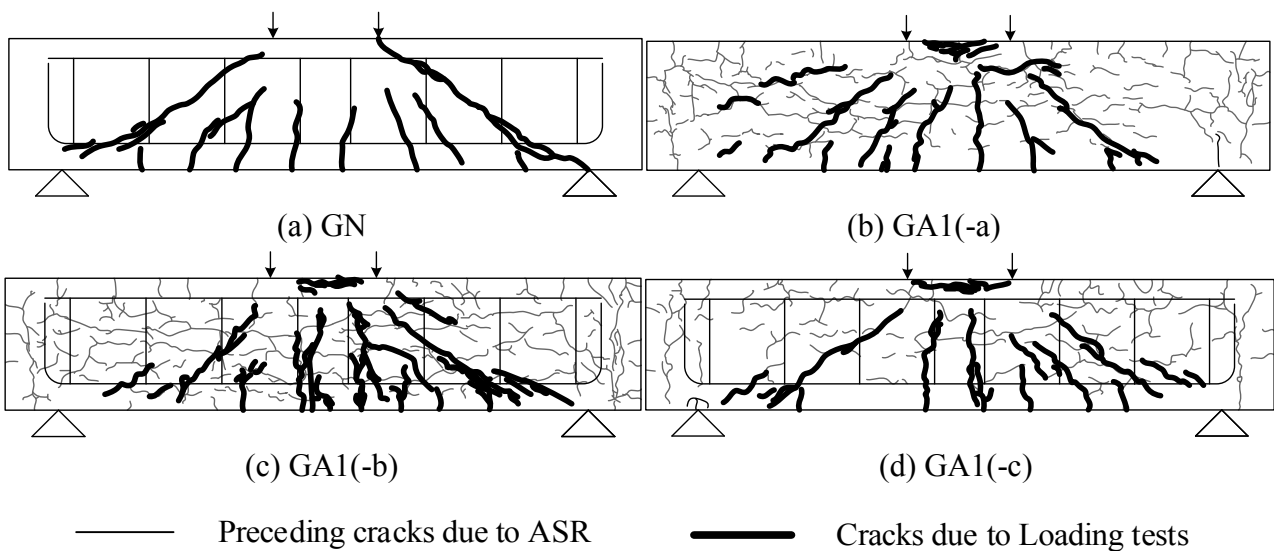

(a) GN   (b) GA1(-a)

(c) GA1(-b)   (d) GA1(-c)

——— Preceding cracks due to ASR   ▬▬ Cracks due to Loading tests

Fig. 5.8. Crack patterns.

5.4.2. Influence of strengthening by bonding CFRP sheets on ASR affected beams

Due to the poor design and/or construction, sometimes the existing ASR affected structures are needed to be repaired or strengthened to upgrade the design load and avoid the accident events. Therefore, in this chapter, the influence of strengthening by bonding CFRP sheets on flexural bearing mechanism was also investigated. The properties of CFRP sheet are given in Table 5.9.

(1) Bonding CFRP sheets

The procedure to bond the CFRP sheets was explained below. Firstly, the bonding surface of RC beams was polished by the disc sander. Secondly, the putty with the thickness of 1 mm was applied after the day the surface coated with epoxy primer. On the putty, the CFRP sheet was impregnated and bonded with epoxy resin, and deaerated by roller. Thirdly, the surface was covered with a release sheet and was flattened, and then was cured for days.

(2) Experimental results in Series A

In Series A, the ASR affected beam GA3_Cs was strengthened by CFRP sheets. The influence of CFRP sheet on the bearing mechanism in the bridge girder with ASR damage was investigated. The testing results in terms of maximum load, initial stiffness and failure mode are shown in Table 5.10.

It can be seen that the strengthened RC beam resulted in diagonal tensile failure, while the un-strengthened beams GA1(-a,-b,-c) resulted in flexural failure. For the stiffness, the initial stiffness of strengthened beam was much greater than that of un-

Table 5.9. Material properties of CFRP sheet.

Fiber weight per unit area (g/m^2)	Design thickness (mm)	Tensile strength (MPa)	Tensile modulus (GPa)
600	0.333	4490	263

strengthened beams due to the strengthening of CFRP sheets. However, the maximum load was even lower than the weakest one among GA1(-a,-b,-c), that is, the maximum load was not raised.

Fig. 5.9 shows the load-deflection relationships of specimens. At the early stage, the great stiffness can be seen on the strengthened beam. When the load reached at 150 kN, the stiffness of strengthened beam decreased significantly, and ended up in the brittle failure. The inducement can be found from crack patterns shown in Fig. 5.10. Comparing the crack patterns of the un-strengthened beams and the strengthened beam, it can be found that the flexural cracks were restrained by CFRP sheet. While, the preceding cracks in the shear region significantly developed along the diagonal direction. Due to the strengthening effect using CFRP sheets, the stiffness of ASR affected RC beam was enhanced and the flexural cracks were restrained obviously. In addition, the shear cracks along the diagonal direction developed and led the beam to fail in a brittle manner. Thus, when strengthening the RC structures with ASR damage, the secondary effect of flexural strengthening should be paid more attention.

(3) Experimental results in Series B

In Series B, the normal RC beam and ASR affected beams were all strengthened by CFRP sheets. The influence of CFRP sheet on the bearing mechanism in the T-shaped pier beam with ASR damage was investigated. In addition, the artificial fracture damage of the tensile rebar anchor was introduced in TA1_Cs_Ft.

The experimental results are shown in Table 5.11. The control beam (TN_Cs) resulted in the diagonal tensile failure. Both of the ASR affected RC beams (TA1_Cs and TA1_Cs_Ft) resulted in the bond-split failure. The maximum loads of ASR affected beams were higher than that of the control beam, while the initial stiffness of ASR affected beams was much lower than that of the control beam. To explore the reasons, the load-deflection relationships and crack patterns were studied as shown in Fig. 5.11 and Fig. 5.12.

Table 5.10. Loading tests results.

Specimen	Compressive strength (MPa)	Maximum load (kN)	Stiffness (load=40kN) (kN/mm)	Failure mode
GA1(-a)	24.7	203.8	109.0	
GA1(-b)	23.4	223.1	131.6	Flexural failure
GA1(-c)	26.7	222.6	112.7	
GA3_Cs	25.7	212.5	156.9	Diagonal tensile failure
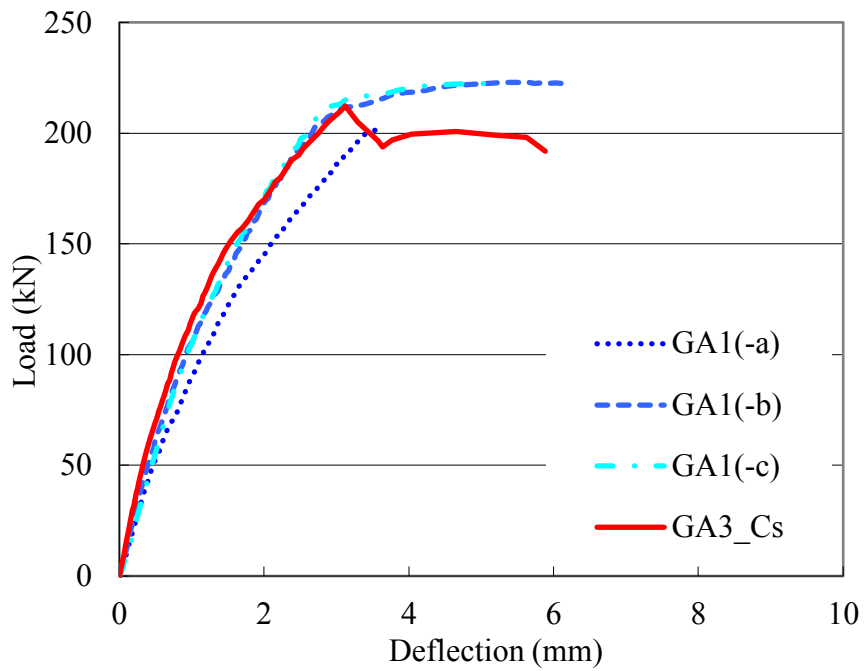
Fig. 5.9. Load-deflection.
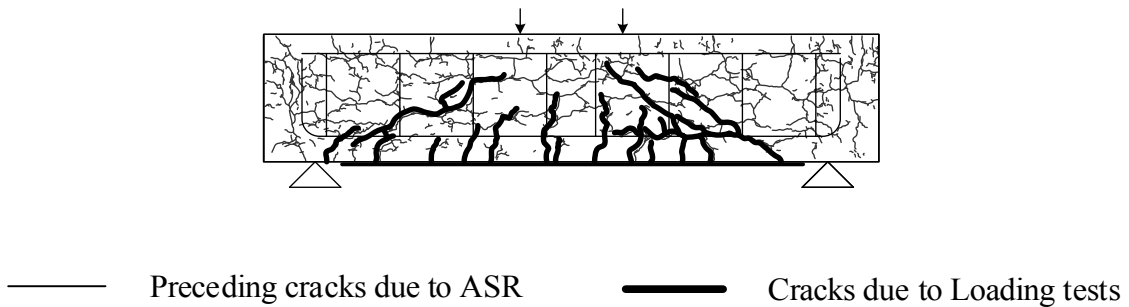
Fig. 5.10. Crack patterns (GA3_Cs)

Table 5.11. Loading tests results.

Specimen	Concrete strength (MPa)	Maximum load (kN)	Stiffness (load=60kN) (kN/mm)	Failure mode
TN_Cs	46.9	238.4	247.7	Diagonal tensile failure
TA1_Cs	40.3	259.5	182.6	Bond-split failure
TA1_Cs_Ft	46.0	245.0	140.5	
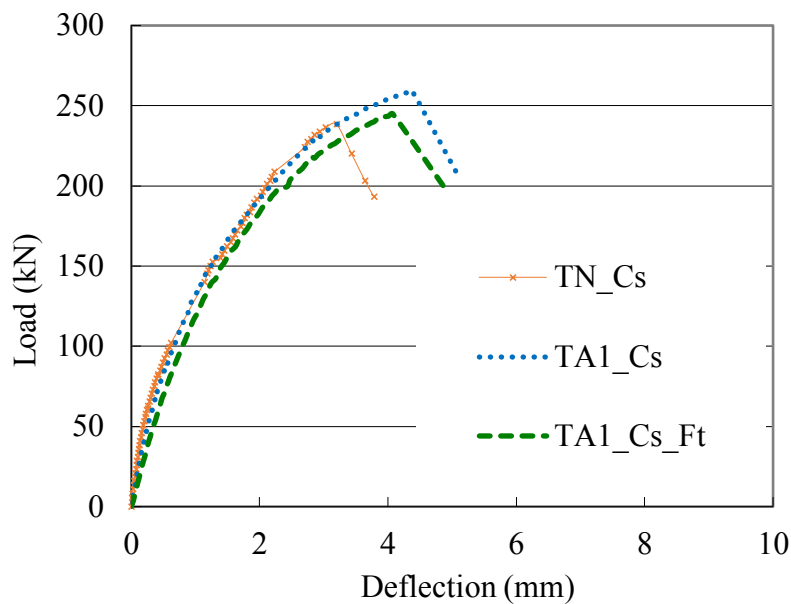
Fig. 5.11. Load-deflection.

From the load-deflection relationships, it can be seen that the stiffness of the control beam was greater than that of the other two beams, especially at the early stage. The RC beam with fracture damage of the tensile rebar anchor showed the lowest stiffness. As the specimens in Series B were designed to simulate the T-shaped RC pier beam and the bottom surface close to tensile rebar was exposed to sunshine and rainwater, the preceding cracks were easy to occur along the tensile rebars. Moreover, due to the preceding cracks, the bond-split cracks occurred at the early stage, and leaded to a lower stiffness comparing to the control beam. On the other hand, the features of brittle failure were observed on the all three beams.

For the crack patterns, the dominant cracks can be seen in the diagonal direction in the control beam. In the ASR affected beams, the obvious bond-split cracks can be seen along the tensile rebars. The results showed that, even though the exposure time and strengthening method were the same, different bearing characteristics were obtained from Series A and B. When strengthening the RC structures with ASR damage, diagonal cracks for bridge girder and bond-split cracks for T-shaped RC pier beam should be noticed.

(a) TN_Cs

(b) TA1_Cs   (c) TA1_Cs_Ft

——— Preceding cracks due to ASR   ▬▬▬ Cracks due to Loading tests
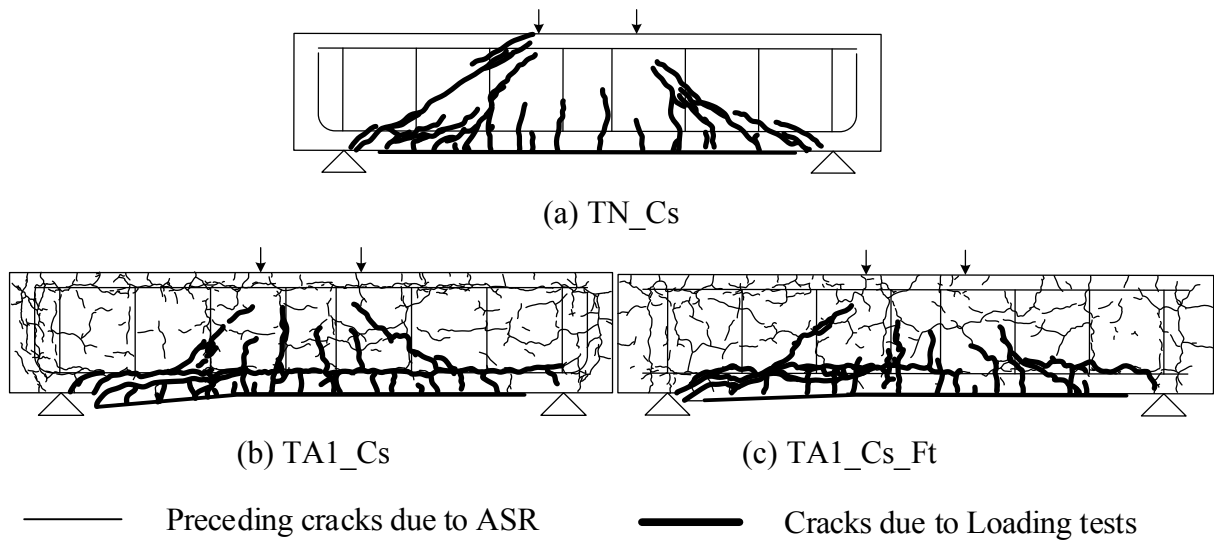
Fig. 5.12. Crack patterns.

5.5. FINITE ELEMENT ANALYSIS

For better understanding of the strengthening influence of CFRP sheets on the shear resisting mechanism in RC beams, the numerical analyses were also conducted in the beams of TN_Cs and TA1_Cs. An analysis method was proposed in this study to represent the experimental results of ASR affected RC beams. To measure the pre-strain generated in the rebar caused by ASR expansion, a survey of the rebar strain was conducted in the two RC beams. The boundary conditions and FEM model used in this study are illustrated in Fig. 5.13.

5.5.1. Material Properties
(1) Concrete

To model the concrete behavior, an elastic plastic model was used with an assumption that the two main failure modes were tensile cracking and compressive crushing. Under uni-axial tension, the stress-strain response was a linear elastic relationship, until the failure stress value was reached. Considering the post-peak tension failure behavior of the concrete, the fracture energy method (the area under the softening curve) was employed. In the experiments, the fracture energy was given as 98 J/m^2 and 87 J/m^2, and Poisson's ratio was 0.2. For the concrete failure, The Mohr-Coulomb
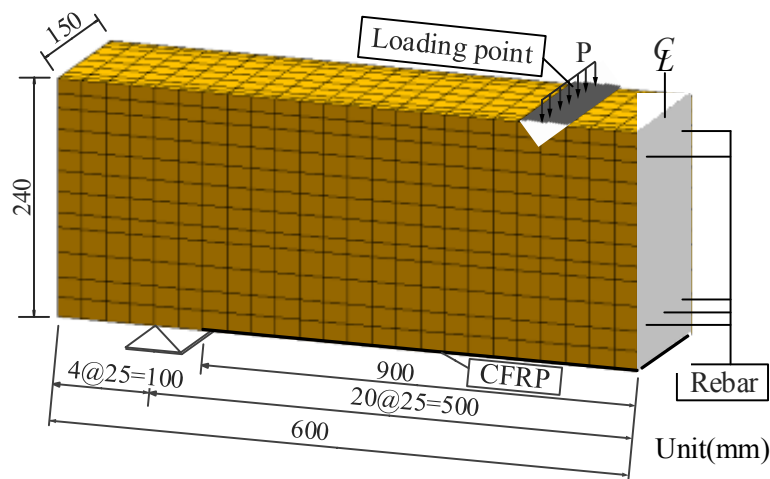
Fig. 5.13. Boundary conditions and FEM model

98

yield criterion was adopted. Also, the stress-strain relationship was used to stimulate the uni-axial compressive stress-strain curve. Fig. 5.14 shows the stress-strain relationship for concrete, and Fig. 5.15 shows the tension softening model.

Based on the experimental results, the tensile strength of TN_Cs and TA1_Cs was 3.3 MPa and 2.3 MPa, respectively. For the compressive strength, the differences of the states of degradation between the cylinder (without the restraint of rebars) and the RC beams (the concrete expansion was constrained by the steel bars) were considered. Here, the material properties were estimated from the ultrasonic propagation velocity.

(2) Steel reinforcement

The rebar was assumed as an elastic–perfectly plastic material and was identical in tension and compression. The elastic modulus E_s and the yield stress f_y were measured in the experimental study. The bond law according to CEB-FIP Model Code 90[43] was used.

(3) CFRP

Considering the CFRP material was linear elastic isotropic until failure, the elastic modulus was specified as 262 GPa and the tensile strength in the fiber direction of the unidirectional CFRP material was specified as 3.8 GPa.

A cohesive zone model was used to model the interface between the concrete and CFRP. Fig. 5.16 shows a graphic interpretation of a simple bilinear bond stress-slip
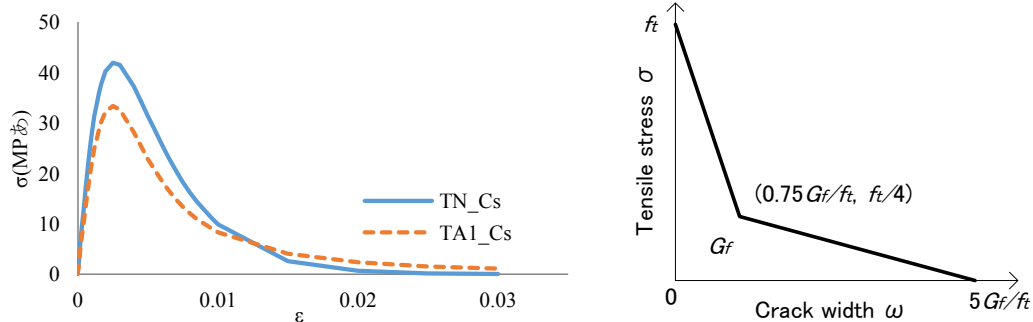
Fig. 5.14. Stress–strain relationship for concrete Fig. 5.15. Tension softening model (1/4)

law in terms of the effective traction and effective opening displacement[44]. More modeling details of the interface are available in Guo et al.'s publication[45].

(4) Considering of ASR deterioration

ASR deterioration was considered in the thermal strain model corresponding to the chemical pre-strain. To measure the pre-strain generated in rebar caused by ASR expansion, a survey of rebar strain was conducted. Here, a thermal strain analysis method was proposed to simulate the concrete expansion caused by ASR degradation. This method utilized the linear thermal expansion coefficient of concrete element. A series of temperature values were used as the inputs, which would be the factors of the expansion of concrete elements. A group of outputs of the pre-strain of rebars was obtained. Comparing to the experimental data, the equivalent thermal strain corresponding to the chemical pre-strain was specified as about 500μ. On the other hand, the FE analysis was conducted on the loading test to assess the shear mechanism and shear resisting performance of the concrete members due to the initial defect and ASR. For further comparison, the normal FE analysis without consideration of concrete expansion was also conducted here.
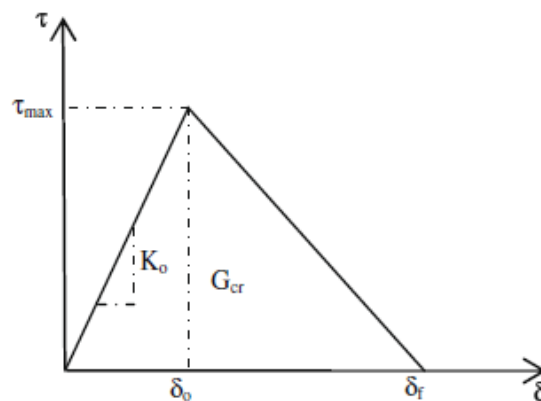
Fig. 5.16. Bond slip law of CFRP sheet.

5.5.2. Analytical results

(1) Load-Deflection Relationship

The compared load-deflection curves of the analytical and experimental results between TN_CS and TA1_Cs are compared in Fig. 5.17.

For TN_CS, there was a good agreement between analytical and the experimental results, especially the maximum load value. This good agreement indicated that the constitutive models used for concrete and reinforcement can well capture the fracture behavior. The predicted stiffness value in FE analysis was slightly lower than the experimental result after the load reached at 150 kN. It is considered that the error was caused by the accuracy of the ultrasonic propagation velocity. For TA1_Cs, the no expansion model significantly underestimated the stiffness and load-bearing capacity. As the concrete expansion was not considered, the stiffness and load-bearing capacity in the analysis was lower than the experimental results. However, the chemical pre-stress model showed a good agreement with the experimental results, as the chemical pre-stress due to ASR was considered.

(a) TN_Cs   (b) TA1_Cs
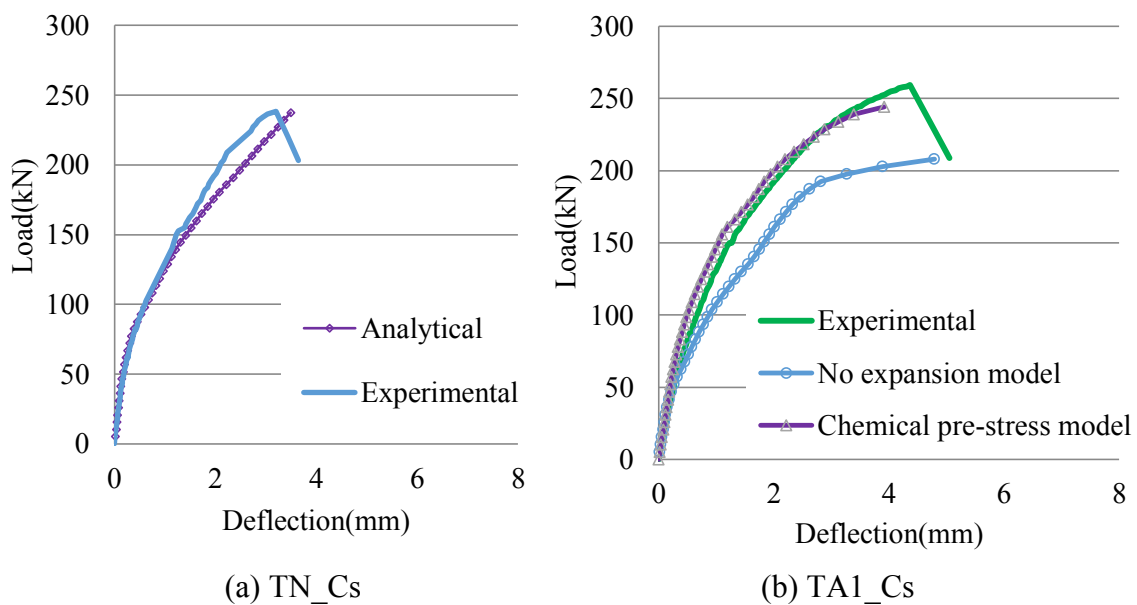
Fig. 5.17. Load-deflection curves of beams.

(2) Rebar Strain Distribution

The rebar strain distributions of analytical and experimental results of TN_CS and TA1_Cs are shown in Fig. 5.18. In the experimental results of TN_CS, the bond at the ends of rebars was secured until 120kN. Then, the bond-slip failure occurred at the edge of tensile rebar. Similar results were obtained in the FE analysis, which predicted that the bond in the rebar end zone of the RC beam was secured with a load of 120kN.
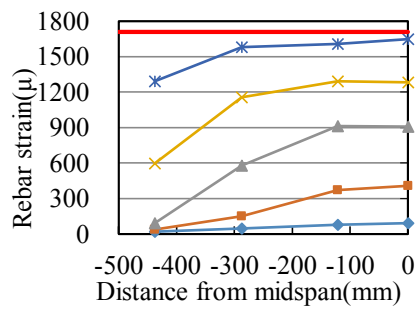
(a) Analytical result (TN_Cs).　　　　(b) Experimental result (TN_Cs).
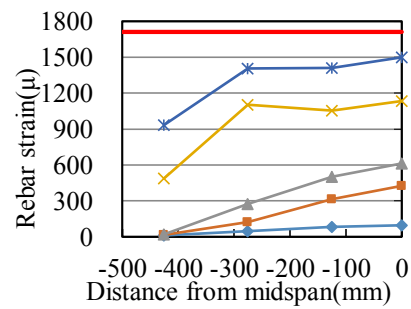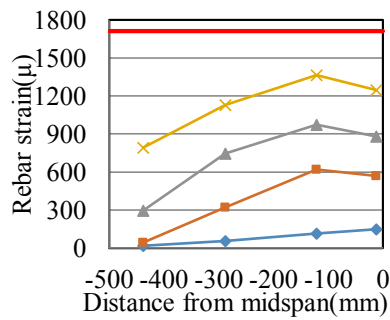
(c) Analytical result of no expansion model. (d) Analytical result of chemical pre-strain model.
　　(TA1_Cs)　　　　　　　　　　　　　　(TA1_Cs)
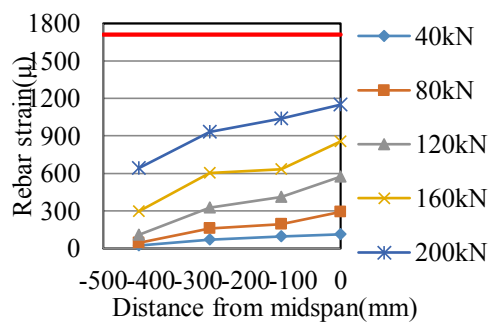
(e) Experimental result (TA1_Cs).

Fig. 5.18. Rebar strain distribution.

In the experimental results of TA1_Cs, the slipping occurred at the end of the tensile rebar at a load of 160kN, which further expanded until the beam broke down. On the other hand, in the no expansion model, different load values of bond-slip failure were obtained. The load value 120kN obtained in FE analysis is much lower than the load value 160kN obtained in the experimental results. It showed that the strain of the tensile rebar was overestimated, when the concrete expansion was not considered. Conversely, when the chemical pre-stress was considered, the analytical results well captured the timing when the bond-slip failure occurred.

(3) Crack Patterns

Fig. 5.19 shows the crack patterns obtained in the experimental results of RC beams. In the experiment of TN_Cs, after the flexural/shear cracks occurred, the shear cracks expanded to connect the supports with the loading points, leading to a collapse in diagonal tensile failure. The analytical result showed similar crack behavior as in the experiments, where the opening of the crack started in the same location and finally the stirrup yielded after the flexural/shear cracks expanded.

In the experiment of TA1_Cs, the RC beams broke down and resulted in bond-split failure due to the flexural/shear and bond-slip cracks. However, the no expansion model showed different behaviors compared with the experimental results. In the no expansion model, the diagonal cracks were obviously observed. In the analytical results of the chemical pre-stress model, the cracks obtained in the experiment and in the simulation were similar, which proved that the model can well capture the mechanisms of fracture in the beams. Considering the chemical pre-stress induced by the expansion in concrete due to ASR, the FE analysis was adopted to simulate one of the experimental results. The analysis results showed a good agreement with the experimental data with respect to the load-deflection response, crack pattern and rebar strain distribution.
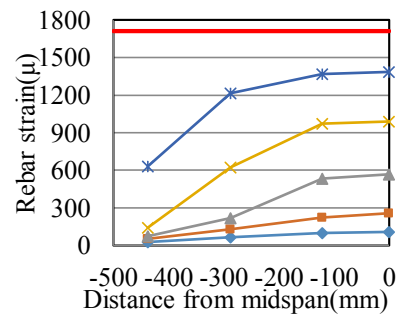
(a) Analytical result (TN_Cs).   (b) Experimental result (TN_Cs).
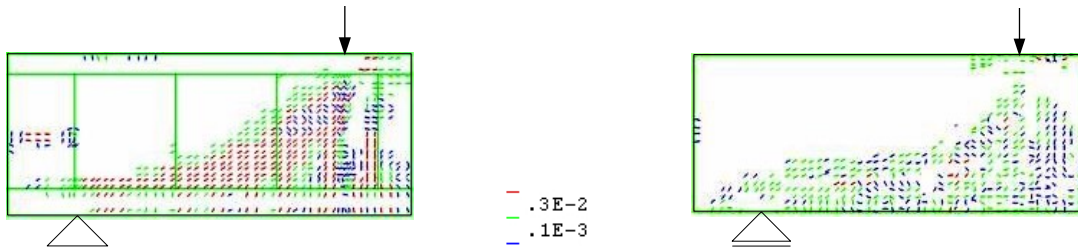
(c) Analytical results of no expansion model. (d) Analytical result of chemical pre-stress model.

    (TA1_Cs)   (TA1_Cs)
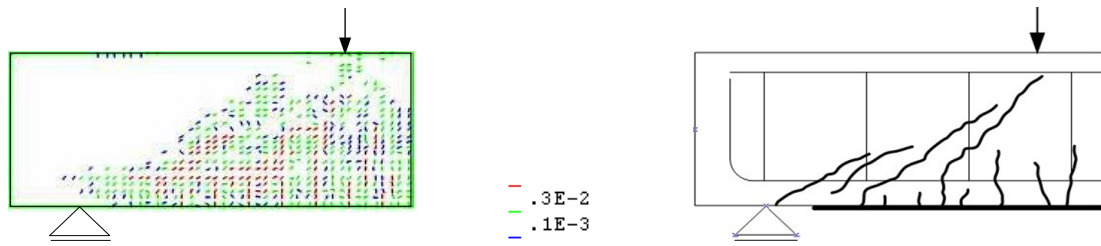
(e) Experimental result s (TA1_Cs)

Fig. 5.19. Crack patterns. (Load=200kN).

5.6. SHEAR STRENGTHENING BY UFC PANELS

In the experimental results, the degradation states were different in terms of the bridge girder (Series A) and T-shaped RC pier beam (Series B) with ASR damage, which resulted in different bearing mechanisms formed. For example, the dominant cracks were diagonal cracks in Series A, while the fatal cracks were the bond-slip cracks in Series B. Then, a shear strengthening method, bonding the panels made of UFC on the RC beams, was proposed. Moreover, two different strengthening schemes were adopted in this study to restrict the shear cracks in both Series A and B (see Fig. 5.2).

5.6.1. Material properties of UFC

In this experiment, UFC was molded into panels. The volume of mixed steel fibers was set at about 5%, with the diameter of 0.1~0.25mm, the length of 10~20mm and the tensile strength of 2×10^3 MPa. In addition, the water-cement ratio was below 0.24, and the other components were silica fume, ground quartz, super-plasticizer, and high amount of Portland cement (up to 1000 kg/m^3). According to the previous research results, the thickness of UFC panels was set as 7mm in the experiments to ensure the good cohesion between concrete matrix and UFC panel. To prevent the stress concentration, the edge of UFC panel was molded to be a 45° taper. The properties of the UFC panel are specified in Table 5.12.

5.6.2. UFC panel bonding

The surfaces of concrete matrix and UFC panel were polished and roughed by disk grinder firstly, and then the adhesive surfaces were coated with epoxy resin. After that, the bracket was used to fix UFC panels in the designed strengthening positions, and the specimens were cured for two weeks. Table 5.13 shows the material properties of the adhesive epoxy resin and the photo of UFC panel bonding is shown in Fig. 5.20.

5.6.3. Experimental results in Series A

To restrict the diagonal cracks, the UFC panel was designed to strengthen the stirrups as shown in Fig. 5.2 (c). The ASR affected beam GA3_CsUp was strengthened by CFRP sheets and UFC panels simultaneously.

The results of loading tests are shown in Table 5.14. Compared with beam GA3_Cs, the maximum load and initial stiffness of GA3_CsUp were enhanced by using UFC panels strengthening method. On the other hand, the failure mode was still the same as GA3_Cs.

Table 5.12. Material properties of UFC panel.

Compressive strength (MPa)	Flexural strength (MPa)	Tensile strength (MPa)	Elastic modulus (GPa)
210	43	10.8	54

Table 5.13. Material properties of adhesive epoxy resin.

Compressive strength (N/mm^2)	Tensile strength (N/mm^2)	Tensile modulus (kN/mm^2)
73.5	23.5	3.7

Fig. 5.20. The photo of UFC panel bonding.

Table 5.14. Loading tests results.

Specimen	Concrete strength (MPa)	Maximum load (kN)	Stiffness (load=40kN) (kN/mm)	Failure mode
GN	36.5	155.6	108.9	Diagonal tensile failure
GA3_Cs	25.7	212.5	156.9	
GA3_CsUp	16.8	240.3	164.0	

The load-deflection relationships of specimens are shown in Fig. 5.21. Due to the strengthening effect of UFC panels, the stiffness was kept at a comparatively higher value. In addition, at the last stage, the ductile failure was observed in GA3_CsUp. From the crack patterns shown in Fig. 5.22, it is found that the diagonal cracks on one side were significantly restrained by UFC panels. However, the diagonal cracks on the other side led to the failure finally.

Therefore, for the bridge girder affected by ASR damage, the strengthening method, which restrains the diagonal cracks, can upgrade the load bearing capacity and stiffness, and to some extent, can prevent the brittle failure.

Fig. 5.21. Load-deflection.

——— Preceding cracks due to ASR　　■■■■■ Cracks due to Loading tests
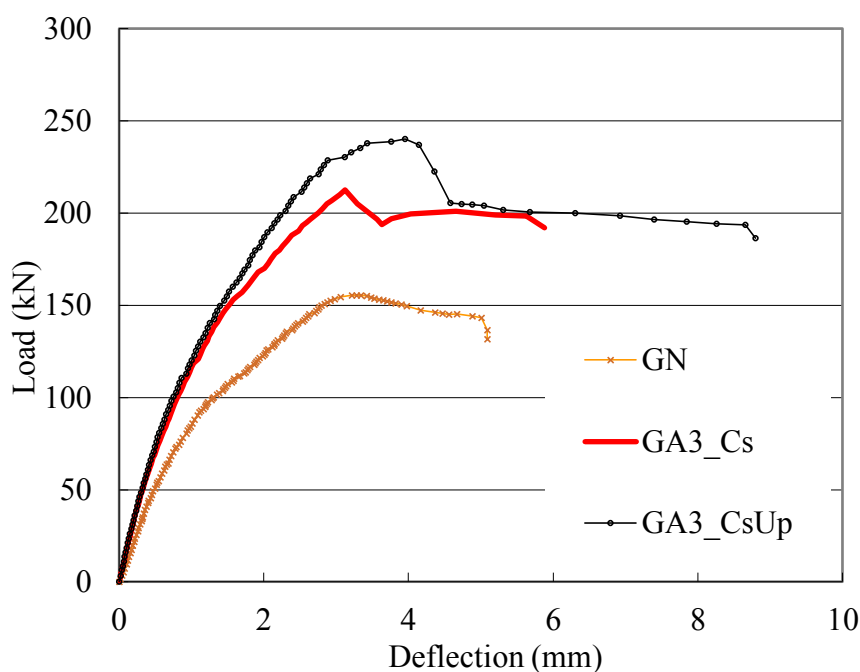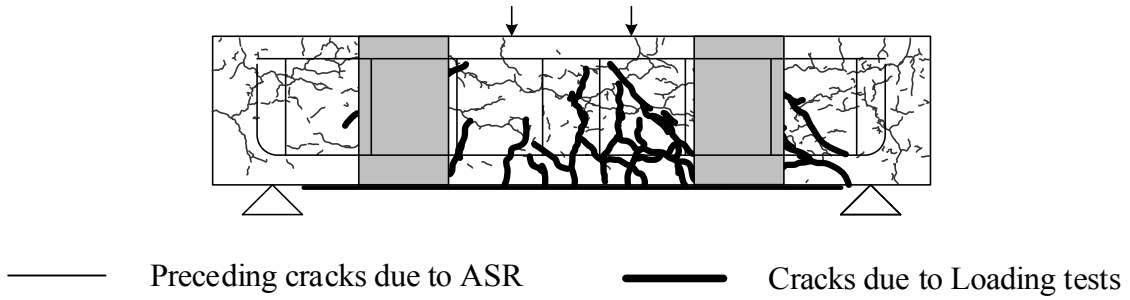
Fig. 5.22. Crack patterns.

5.6.4. Experimental results in Series B

The strengthening scheme of restricting the bond-split cracks was adopted (refer to Fig. 5.2 (d, e)). The ASR affected beams TA1_CsUp and TA1_CsUp_Fc were bonded with UFC panels. The experimental results are given in Table 5.15. Fig. 5.23 shows the load-deflection relationships. It can be seen that the stiffness dropped significantly when the load reached at about 220 kN. The insufficient bond strength between concrete and CFRP sheet should be considered as the main reason.

From the crack patterns shown in Fig. 5.24, the peeling failure of CFRP sheet on one side can be observed in both of two beams. The results showed that the UFC panel can restrict the bond-split cracks. But the failure occurred in the weak part where the enough bond was not provided by CFRP sheet.

Table 5.15. Loading tests results.

Specimen	Concrete strength (MPa)	Maximum load (kN)	Stiffness (load=60kN) (kN/mm)	Failure mode
TA1_Cs	40.3	259.5	182.6	
TA1_Cs_Ft	46.0	245.0	140.5	Bond-split failure
TA1_CsUp	43.8	273.6	173.9	
TA1_CsUp_Ft	44.4	263.3	192.1	
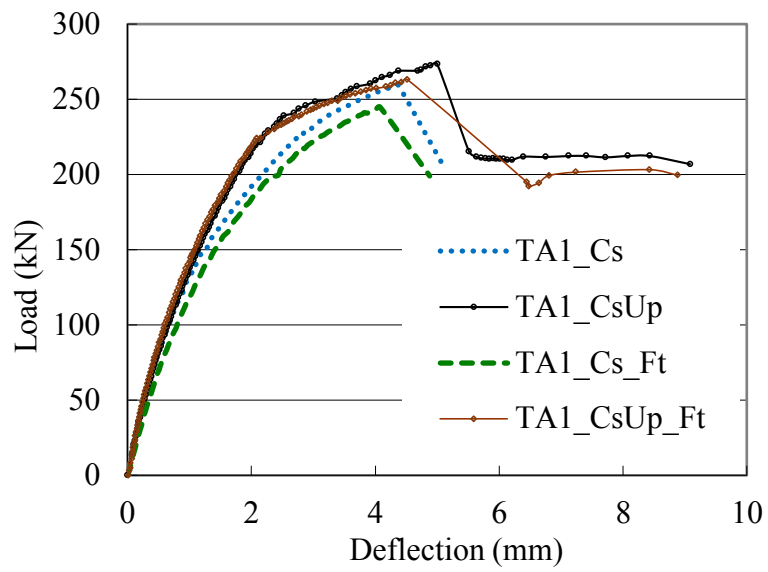
Fig. 5.23. Load-deflection.
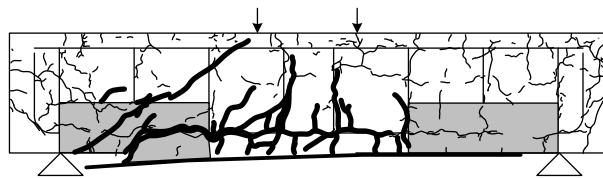
(a) TA1_CsUp
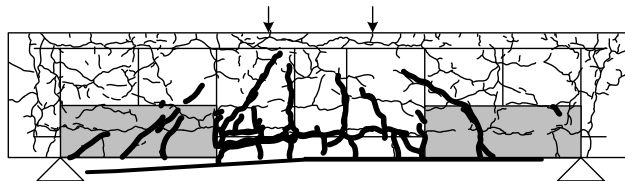
(b) TA1_CsUp_Ft

———— Preceding cracks due to ASR   ▬▬▬ Cracks due to Loading tests

Fig. 5.24. Crack patterns.

5.7.   CONCLUSIONS

This chapter describes ASR related studies on two experimental series, including different exposure methods, different exposure times and different strengthening methods. The influences of ASR deterioration on shear failure mechanism and the shear resisting performance of RC beams were evaluated.   Following conclusions can be drawn:

1.   According to the non-destructive testing, it is found that the rebar restraint ratio and the exposure condition affected the degradation state in RC structures with ASR damage, which led to the different failures in loading tests.

2.   In the loading tests, due to the influence of preceding cracks and pre-stress, the load bearing mechanism changed from the diagonal tensile resisting mechanism to the arch mechanism, and the bearing capacity was enhanced consequently. In addition, even though some specimens were cast and exposed in the same conditions, different maximum load and stiffness were obtained in the loading tests. The uncertainty and complexity of ASR damage were confirmed.

3.   When repairing or strengthening the ASR affected RC beams with CFRP sheets, an increase of bearing capacities may not be obtained, since the specimens failed in shear failure.

4.   Comparing the experimental and analytical results, the validity of FE analysis method proposed for ASR was verified. For ASR affected specimen, the no expansion model significantly underestimated the stiffness and load-bearing capacity. Conversely, the chemical pre-stress model showed a good agreement with the experimental results, in which the chemical pre-stress due to ASR was considered.

5.   Based on the different failure modes in Series A and Series B, different strengthening schemes were proposed to restrain the diagonal cracks or bond-split cracks. Using the proposed shear strengthening method (bonding the UFC panels) led to a very positive effect on the load bearing capacity in both Series A and Series B. Furthermore, the brittle failure mode was also changed to the ductile mode.

REFERENCES

1 Stanton, T.E., Expansion of concrete through reaction between cement and aggregate, Proceeding American Society of Civil Engineers, 66, pp. 1781-1811, 1940.

2 Baillemont, G, Delaby, J.B., Brouxel, M., and Remy, P., Diagnosis, treatment and monitoring of a bridge damaged by AAR, Proceedings of the 11th International Conference on Alkali-Aggregate Reaction (ICAAR), pp. 1099-1108, 2000.

3 Institution of Structural Engineers, Structural Effects of Alkali-Silica Reaction: Technical Guidance on the Appraisal of Existing Structures, London: SETO Ltd, 1992.

4 Nishibayashi, S., Okada, K., Kawamura, M., Kobayhashi, K., Kojima, T., Miyagawa, T., Nakano, K., and Ono, K., Alkali-silica reaction - Japanese experience, in: The Alkali-Silica Reaction in Concrete, pp. 333, R.N. Swamy (Blackie and Son, London), 1992.

5 ISE, Structural effects of ASR: technical guidance on the appraisal of existing structures, London (UK): The Institution of Structural Engineers (ISE), 1992.

6 Fournier, B., Berube, M.A., Alkali-aggregate reaction in concrete: a review of basic concepts and engineering implications, Can J Civil Eng, 27(2), pp. 167-91, 2000.

7 Fan, S., and Hanson J.M., Length expansion and cracking of plain and reinforced concrete prisms due to Alkali-Silica Reaction, ACI Structural Journal, 95(4), pp. 480-487, 1998.

8 Chrisp, T.M., Wood, J.G.M., and Norris, P., Towards quantification of microstructural damage in AAR deteriorated concrete, Proceedings of the International Conference on Recent Developments on the Fracture of Concrete and Rocks, pp. 419-427, 1989.

9 Chrisp, T.M., Waldron, P., and Wood, J.G.M., Development of a non-destructive test to quantify damage in deteriorated concrete, Magazine of Concrete Research, 45(165), pp. 247-256, 1993.

10 Grattan-Bellew, P.E., and Danay, A., Comparison of laboratory and field evaluation of AAR in large dams, Proceedings of the International Conference on Concrete Alkali–Aggregate Reactions in Hydroelectric Plants and Dams, pp. 1-23, 1992

11 Smaoui, N., Berube, M.A., Fournier, B., Bissonnette, B., and Durand, B., Evaluation of the expansion attained to date by concrete affected by alkali-silica reaction. Part 1: Experimental study, Can J Civil Eng, 31, pp. 826-845, 2004.

12 Rivard, P., and Saint-Pierre, F., Assessing alkali-silica reaction damage to concrete with non-destructive methods: From the lab to the field, Construction and Building Materials, 23(2), pp. 902-909, 2009.

13 Bungey, J.H., Ultrasonic testing to identify Alkali-Silica reaction in concrete, British Journal of Non-Destructive Testing, 33(5),   pp. 227-231, 1991.

14 Chrisp, T.M., Waldron P., and Wood J.G.M., Development of a non-destructive test to quantify damage in deteriorated concrete, Mag Concrete Res, 45(165), pp. 247-256, 1993.

15 Tashiro, C., and Yamada, K., Study of relationship between alkali-aggregate reaction and electrical resistivity, Proceedings of the eighth International Conference on AAR in concrete, pp. 381-383, 1989.

16 Ben Haha, M., Gallucci, E., Guidoum, A., and Scrivener, K.L., Relation of expansion due to alkali silica reaction to the degree of reaction measured by SEM image analysis, Cement and Concrete Research, 37(8), pp. 1206-1214, 2007.

17 Ben Haha, M., Gallucci, E., Guidoum, A., and Scrivener, K.L., Relation of expansion due to alkali silica reaction to the degree of reaction measured by SEM image analysis, Cement and Concrete Research, 37(8), pp. 1206-1214, 2007.

18 Chen, J., Jayapalan, A.R., Kim, J.Y., Kurtis, K.E., and Jacobs, L.J., Rapid evaluation of alkali-silica reactivity of aggregates using a nonliear resonance spectroscopy technique, Cement and Concrete Research, 40(6), pp. 914-923, 2010.

19 Monette, L., Gardner, J., and Grattan-Bellew, P., Residual Strength of Reinforced Concrete Beams Damaged by Alkali-Silica reaction - Examination of Damage Rating Index Method, ACI Materials Journal, 99(1), pp. 42-50, 2002.

20 Institution of Structural Engineers, Structural Effects of Alkali-Silica Reaction: Technical Guidance on the Appraisal of Existing Structures, London: SETO Ltd, 1992.

21 Blight, G.E., and Lampacher, B.J., Repair of reinforced concrete portal frame damaged by alkali-silica reaction-strains after 5 1/2 years, Magazine of Concrete Research, 50(4), pp. 293-296, 1998.

22 CEB Bulletin d'Information 162, Assessment of concrete structures and design procedures for upgrading (redesign), Losanne: CEB, 1983.

23 Sharif, A.M., Al-Sulaimani, G.J., and Hussain, M., Strengthening of shear damaged RC beams by external plate bonding of steel plates, Magazine of Concrete Research,

47(173), pp. 329-334, 1995.

24 Swamy, R.N., Jones, R., and Charif, A., Contribution of externally bonded steel plate reinforcement to the shear resistance of reinforced concrete beams, ACI Special Publication, 165, pp. 1-24, 1996.

25 Subedi, N.K., and Baglin, P.S., External plate reinforcement for concrete beams, Journal of Structural Engineering, 124(12), pp. 1490-1495, 1998.

26 Adhikary, B.B., Mutsuyoshi, H., and Sano, M., Shear strengthening of reinforced concrete beams using steel plates bonded on beam web: experiments and analysis, Construction and Building Materials, 14(5), pp. 237-244, 2000.

27 Valivonis, J., and Skuturna, T., Cracking and strength of reinforced concrete structures in flexure strengthened with carbon fiber laminates, Journal of Civil Engineering and Management, 13(4), pp. 317-323, 2007.

28 Yeong-soo, S., and Chadon, L., Flexural behavior of reinforced concrete beams strengthened with carbon fiber-reinforced polymer laminates at different levels of sustaining load, Structural Journal, 100(2), pp. 231-239, 2003.

29 Ashour, A.F., El-Refaie, S.A., and Garrity, S.W., Flexural strengthening of RC continuous beams using CFRP laminates, Cement and Concrete Composites, 26, pp. 765-775, 2004.

30 Esfahani, M., Kianoush, M., and Tajari, A., Flexural behavior of reinforced concrete beams strengthened by CFRP sheets, Engineering Structures, 29(10), pp. 2428-2444, 2007.

31 Chajes, M.J., Januska, T.F., Mertz, D.R., Thomson, Jr T.A., and Finch Jr, W.W., Shear strengthening of reinforced concrete beams using externally applied composite fabrics, ACI Structural Journal, 92(3), pp. 295-303, 1995.

32 Iskhakov, I., Ribakov, Y., Holschemacher, K., and Mueller, T., High performance requiring of reinforced concrete structures, Materials and Design, 44, pp. 216-222, 2013.

33 Martinola, G., Meda, A., Plizzari, G.A., and Rinaldi, Z., Strengthening and repair of RC beams with fiber reinforced concrete, Cement and Concrete Composites, 32(9), pp. 731-739, 2010.

34 Wirojjanapirom, P., Matsumoto, K., Kono, K., and Niwa, J., Shear resistance mechanisms of RC beams using U-shaped UFC permanent formwork with shear keys and bolts, Proccedings of International Conference on Sustainable Construction Materials and

Technologies, e-35, pp. 1-10, 2013.

35 Williams, M.E., Repair of deteriorated bridge substructures using carbon fiber-reinforced polymer (CFRP) composites, Advanced Composites in Bridge Construction and Repair, pp. 265-286, 2014.

36 Phair, J.W., Tkachev, S.N., Manghnani, M.H., and Livingston, R.A., Elastic and structural properties of alkaline-calcium silica hydrogels, Journal of Materials Research, 20(2), pp. 344-349, 2005.

37 Swamy, R.N., and AI-Asali, M.M., Engineering properties of concrete affected by alkali-sikica reaction, Materials Journal, 85(5), pp. 367-374, 1988.

38 Jones, A.E.K., and Clark, L.A., The effects of ASR on the properties of concrete and the implications for assessment, Engineering Structures, 20(9), pp. 785-791, 1998.

39 Giaccio, G., Zerbino, R., Ponce, J.M., and Batic, O.R., Mechanical behavior of concretes damaged by alkali-sikica reaction, Cement and Concrete Research, 38, pp. 993-1004, 2008.

40 Fuchi, Y., Morikawa, H., Iwata, T., and Peng, F., Evaluation of Strengthening Effect of RC Beams with ASR Deterioration by CFRP Sheet Bonding, Proceedings of the Concrete Structure Scenarios, JSMS, 9, pp.389-396, 2009.

41 Miyagawa, T., Fracture of reinforcing steels in concrete damaged by ASR, International Symposium on Cement and Concrete Material, Cement Construction and Building Materials, 39, pp. 105-112, 2006.

42 Standard Specifications for Concrete Structures (Design), JSCS concrete committee, pp. 39-44, 2007.

43 CEB-FIP, Bulletin No. 213/214, Model Code 1990, London: Thomas Telford, 1993.

44 Lu, X.Z., Ten, J.G., Ye, L.P., and Jaing, J.J., Bond-slip models for FRP sheets/plates bonded to concrete, Engineering Structures, 24(5), pp. 920-37, 2005.

45 Guo, Z.G., Cao, S.Y., Sun, W.M., and Lin, X.Y., Experimental study on bond stress-slip behaviour between FRP sheets and concrete, Proceedings of the International Symposium on Bond Behaviour of FRP in Structures, pp. 77-84, 2005.

CHAPTER 6

Size Effect on Shear Strengthening of RC Beams by

Bonding UFC Panels for Practical Study

6.1.   INTRODUCTION

In order to meet the requirements of high durability, efficiency, reliability, short-duration and low-cost, the authors proposed a shear strengthening method by bonding the UFC panels on RC beams[1-4]. To evaluate the influence of concrete strength, tensile rebar type, shear-span ratio and patching repair on the strengthening effects and the shear resisting mechanism, the experimental investigations of the UFC panels strengthening on RC beams with 1/4 depth of real bridge girder were conducted in previous chapters[1-3]. The experimental results demonstrated that the shear resisting capacity of RC beams and bond-slip properties of rebars were both improved by bonding UFC panels. Moreover, to better understand the influence of UFC panel strengthening on the shear resisting mechanism in RC beams, the numerical analyses were also conducted[4]. Based on the discussion on the bond-slip behaviors of concrete and rebars, the analytical results of the modified bond-slip model showed the good agreement with the experimental results in terms of load-deflection and crack pattern. However, whether the similar shear

strengthening effects can be gained on the existing bridge girder, becomes an important problem. To realize the practical application, the influence of the factors in terms of size effect and UFC panel thickness has to be evaluated. In this chapter, the experimental investigations were conducted to evaluate the strengthening performance of bonding UFC panels on the large specimens and to evaluate the influence of the factors in terms of size effect and UFC panel thickness. And JSCE recommendation equation was verified to evaluate the shear carried by UFC panels[5].

6.2. METHODOLOGY

6.2.1. Material properties

In this thesis, the proposed shear strengthening method is to retard the development of shear cracks around the ends of the RC beams by bonding UFC panels. As there were many RC bridges reinforced with round steel bars in 1960s, round rebars in tension were used in this chapter. In addition, the aim of this experiment is to evaluate the shear strengthening performance in the aging or damaged RC bridges. For this objective, RC beams were designed to break down in shear failure and a few shear reinforcement stirrups were set.

The list of specimens is shown in Table 6.1. Five identical RC beams were used in the experiments, loading with a four point bending configuration. All the beams were cast in steel molds and were cured in the molds under a wet hessian for two days. The beams were designed to have a shear-span ratio of 1.5. Fig. 6.1 shows the shear damage in the girder end of an aging bridge that was built in 1960s in Japan. Due to the low concrete strength and the excessive load in the girder end, the shear cracks already occurred. Therefore the experiments were designed to evaluate the strengthening influence on the RC beams with low shear-span ratio and to investigate the size effect on the strengthening performance.

Fig. 6.1. Girder end of an aging bridge built in 1960s in Japan.

Table 6.1. List of specimens in loading tests.

Specimen	Concrete strength (MPa)	Tensile rebar	UFC panel	a/d	Beam depth (mm)
1.5RN1/4	24.6	φ16	-	1.5	240
1.5RDA	24.6	φ16	7mm	1.5	240
1.5RN1/2	24.0	φ28	-	1.5	500
1.5RD14A	24.0	φ28	14mm	1.5	500
1.5RD28A	24.0	φ28	28mm	1.5	500

There were total five beams including two control RC beams and three beams strengthened by bonding the UFC panels. To investigate the size effect of RC beams on the strengthening performance, two types of size were used. One was 1/4 depth of real bridge girder, and another was 1/2 depth. All the beams were with the same shear-span ratio (=1.5). For the 1/4 size beams (see Fig. 6.2), the longitudinal reinforcement consisted of three φ16 for tension and two D13 for compression. The tensile strength of φ16 and D13 was 465 MPa and 564 MPa, and the yield strength of φ16 and D13 was 333 MPa and 385 MPa. The shear reinforcement consisted of φ6 with a yield strength of 415 MPa. For the 1/2 size beams (see Fig. 6.2), the longitudinal reinforcement consisted of four φ28 for tension and two φ19 for compression. The tensile strength of φ28 and φ19 was 472 MPa and 464 MPa, and the yield strength of φ28 and φ19 was 333 MPa and 337 MPa. The shear reinforcement consisted of φ12 with a yield strength of 333 MPa.

117
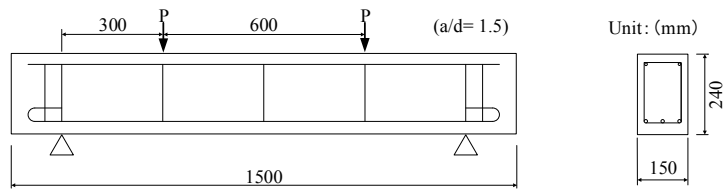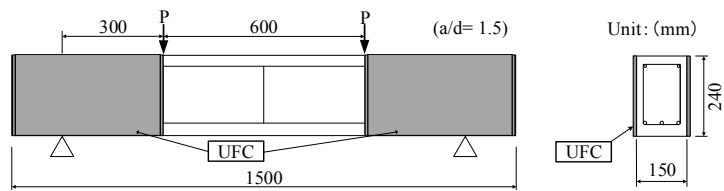
(a) 1.5RN1/4

(b) 1.5RDA
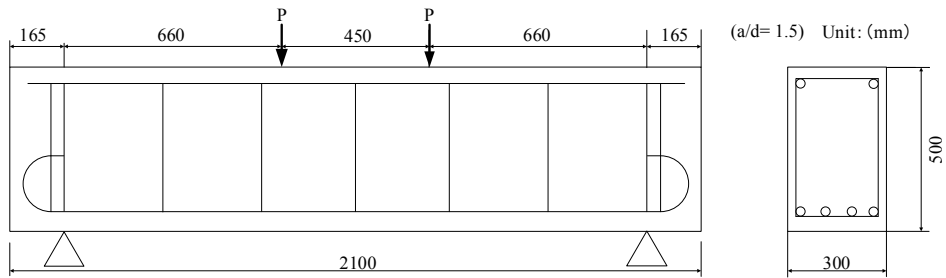
(c) 1.5RN1/2
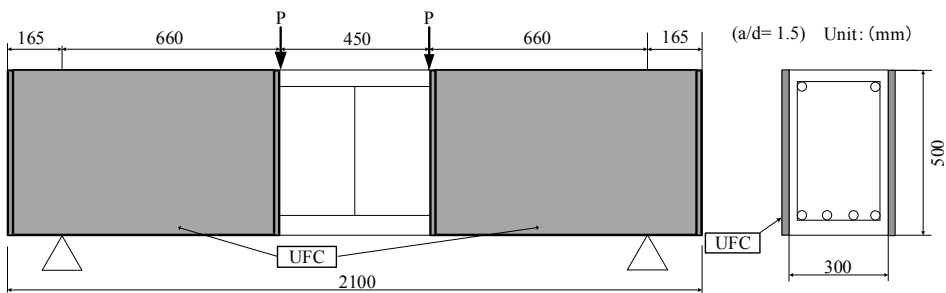
(d) 1.5RD14A & 1.5RD28A

Fig. 6.2. Dimensions of RC beams and Locations of UFC panel.

118

6.2.2. UFC properties

In the experiments, the UFC was molded into panels. The volume of mixed steel fibers was set at around 5%, with the diameter of 0.1~0.25 mm, the length of 10~20 mm and the tensile strength of 2×10^3 MPa. The water-cement ratio was below 0.24. And other components were silica fume, ground quartz, super-plasticizer, and high amount of Portland cement (up to 1000 kg/m^3). For the 1/4 size RC beams, the thickness of UFC panels was set as 7 mm. The reason is to ensure a good cohesion between concrete matrix and UFC panel. For the 1/2 size RC beams, an investigation of the thickness of UFC panels was conducted to evaluate the beam size effect. Here, two types of UFC panel thickness were considered. One was 14mm (1.5RD14A), and another was 28mm (1.5RD28A). To prevent the stress concentration, the edge of UFC panel was molded to be a 45° taper. The properties of the UFC panel are specified in Table 6.2 and one of the used UFC panels is shown in Fig. 6.3.

6.2.3. UFC panel bonding

The surfaces of concrete matrix and UFC panel were polished and roughed by disk grinder firstly, and then the UFC panels were fixed to the designed strengthening positions as shown in Fig. 6.2. During anchoring, the washers of 3 mm thickness were interposed between concrete matrix and UFC panel. The gaps around the panels were sealed except the upper side preparing for the injection of the epoxy resin. Table 6.3 shows the material properties of the adhesive epoxy resin. Fig. 6.4 shows the setting of strengthened RC beam.

Table 6.2. Material properties of UFC panel.

Density (g/cm^3)	Compressive strength (MPa)	Elastic modulus (GPa)	Splitting tensile strength (MPa)	Uniaxial tensile strength (MPa)
2.55	210	54	10.8	16.7

Table 6.3. Material properties of adhesive epoxy resin.

Compressive strength (MPa)	Tensile strength (MPa)	Tensile modulus (GPa)
73.5	23.5	3.7

Fig. 6.3. The photo of UFC panel used.
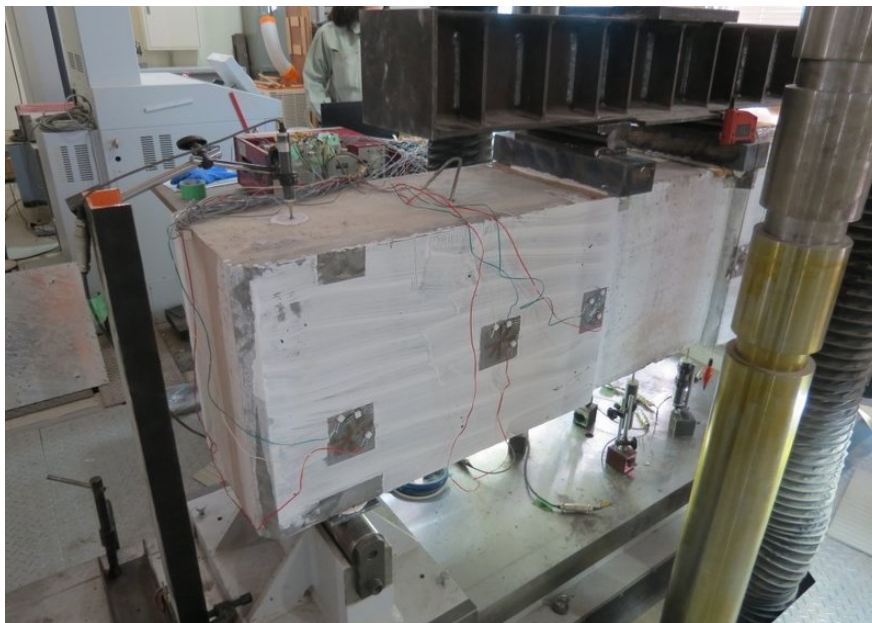
Fig. 6.4. Setting of strengthened RC beam.

6.3. EXPERIMENTAL RESULTS

6.3.1. Experimental results of 1/4 size beams

In chapter 3, the anchorage splitting failure was observed in specimen with low shear-span ratio. Thus an anchorage reinforcement method that the bonding region of UFC panel was extended to the anchorage section, was proposed to prevent the anchorage splitting failure. Two beams (control beam 1.5RN1/4 and strengthened beam 1.5RDA) were cast in this study to verify the improved strengthening method (refer to Fig. 6.2(b)). The loading test results of 1/4 size beams are given in Table 6.4. The load-deflection relationships of 1.5RN1/4 and 1.5RDA are shown in Fig. 6.5. From the figure, the brittle failure occurred in the control beam 1.5RN1/4, where the load declined immediately after

Table 6.4. Loading test results.

Specimen	Maximum Load (kN)	Concrete Strength (MPa)	Effective-ness	Stiffness at 30kN (kN/mm)	Effective-ness	Failure mode
1.5RN1/4	173.5	24.6	-	153.3	-	Shear compression failure
1.5RDA	242.9	24.6	40.0%	138.9	-9.4%	UFC panel peeling failure

(a)

Fig. 6.5. Load-deflection relationships.

it reached at the peak. On the other hand, due to benefits of the anchorage reinforcement and shear strengthening, a significant upgrading effect on bearing capacity was obtained and the maximum load was enhanced by about 40%. Moreover, the failure mode was also ameliorated, and the curve demonstrated the outstanding ductility at the last stage.

Fig. 6.6 shows the crack patterns, where the cracks on the bottom of strengthened beam are also presented. For the control beam 1.5RN1/4, the shear cracks and the compressive splitting cracks can be seen in the shear region, and the beam resulted in the shear compression failure. On the contrary, due to the benefits of the anchorage reinforcement, the anchorage splitting cracks did not occur in beam 1.5RDA. Due to the strengthening effect by bonding the UFC panel, the crack patterns in 1.5RDA were different from that occurred in 1.5RN1/4. The cracks on the beam bottom developed not only in the transverse direction but also in the longitudinal direction along the edge of UFC panel. The beam 1.5RDA resulted in partially peeling failure of UFC panel (refer to Fig. 6.7). The experimental results demonstrated that the ultimate load and the failure mode were ameliorated by implementing the anchorage reinforcement in which the bonding region of UFC panel was extended to the anchorage section.

(a) 1.5RN1/4   (b) 1.5RDA
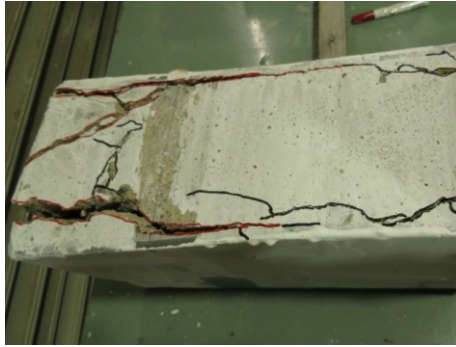
Fig. 6.6. Crack patterns.

Fig. 6.7. Photo of UFC panel partially peeling failure (1.5RDA).

6.3.2. Experimental results of 1/2 size beams

Considering the influence of beam size effect, the thickness of UFC panels was also investigated in this study. Two types of UFC panel thickness were adopted to strengthen the RC beams. The strengthened RC beams were 1.5RD14A and 1.5RD28A, and the thickness of the bonding UFC panel in those specimens was 14mm and 28mm, respectively.

The loading test results are shown in Table 6.5. The shear strength and flexural strength were evaluated based on Standard Specifications for Concrete Structures. $N_{V,cal}$ indicates the load-bearing capacity based on the calculated shear strength, and $N_{Mu,cal}$ indicates the load-bearing capacity based on the calculated flexural strength. The anticipated load-bearing capacities based on the calculated shear strength for strengthened beams (1.5RD14A and 1.5RD28A) are also given in the parentheses. The calculating method for the anticipated load-bearing capacities will be explained in 6.4.3. From the loading test results, the real shear capacity is inferred as about 763.1 kN according to 1.5RN1/2 result (failed in shear failure), and the real flexural capacity is inferred as about 1161.4 kN according to 1.5RN28A result (failed in flexural failure). It is noted that there exist some errors between the calculated results and the experimental results. For the beam 1.5RD14A, the maximum load of the strengthened beams was upgraded significantly. It is because bonding with UFC panels enhanced the shear strength. For the beam 1.5RD28A in which the thicker UFC panels (28mm) were used, higher shear strength was anticipated. However, the beam failed in the flexural failure when the load was raised

beyond the flexural capacity of the substrate concrete. The maximum loads for 1.5RD14A and 1.5RD28A were 45% and 52% higher, respectively, than that for control beam 1.5RN1/2. Their initial stiffness increased by 23% and 66%, respectively. The control beam failed in diagonal tension, but the strengthened RC beams demonstrated a better, relatively ductile failure mode. More significant strengthening effects were obtained with the thicker UFC panels.

Fig. 6.8 shows the load-deflection relationships. For the control beam 1.5RN1/2, the low stiffness can be seen from the graph, and the load sharply decreased after reached at the peak. It showed the highly brittle behavior. For the strengthened beams 1.5RD14A and 1.5RD28A, it can be seen that the failure mode was ameliorated by using the UFC panels strengthening method. Especially in 1.5RD28A, the beam resulted in flexural failure. For the beam 1.5RD14A, although it broke down in shear failure, the panels relieved the drop of load and stiffness and withheld relatively ductility due to the steel fiber mixed in UFC panels. Fig. 6.9 shows the rebar strain distribution. For the control beam 1.5RN1/2, the de-bonding occurred at the early stage (load = 400kN). On the other hand, due to the UFC panels strengthening and the anchorage reinforcement, the strain value of end region of tensile rebars in 1.5RD14A and 1.5RD28A were kept at a low level (load = 400kN). For the beam 1.5RD14A, the de-bonding at the ends of rebars occurred at 500kN. For the beam 1.5RD28A, since the double thick panels were used, the restraint on the de-bonding was sustained until 600kN.

Table 6.5. Loading test results.

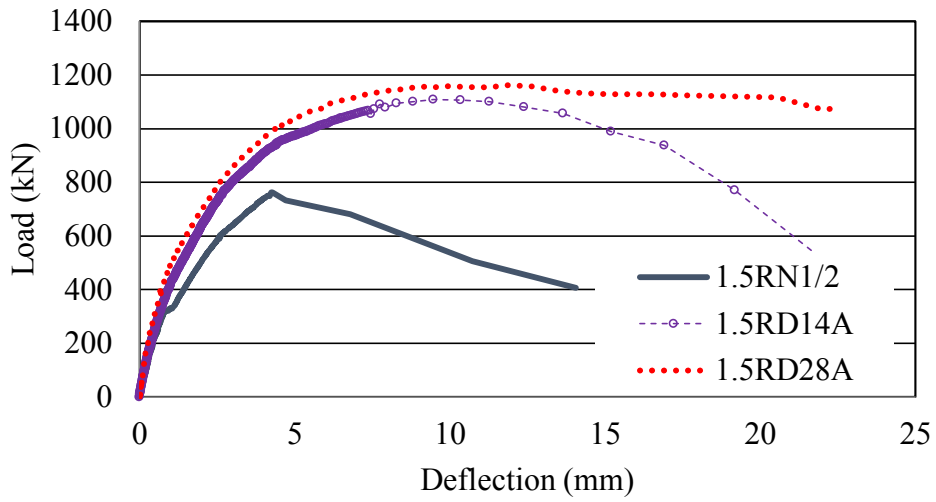| Specimen | Calculated results | | Experimental results | | | | |
	$N_{V,cal}$ (kN)	$N_{Mu,cal}$ (kN)	$P_{max,exp}$ (kN)	Effective-ness	Stiffness at 100kN (kN/mm)	Effective-ness	Failure mode
1.5RN1/2	850.2	1049.8	763.1	-	524.8	-	Diagonal tension failure
1.5RD14A	(1122.2)	1049.8	1109.2	45.4%	643.1	22.5%	Shear compression failure
1.5RD28A	(1394.2)	1049.8	1161.4	52.2%	869.6	65.7%	Flexural failure

Fig. 6.8. Load-deflection relationships.
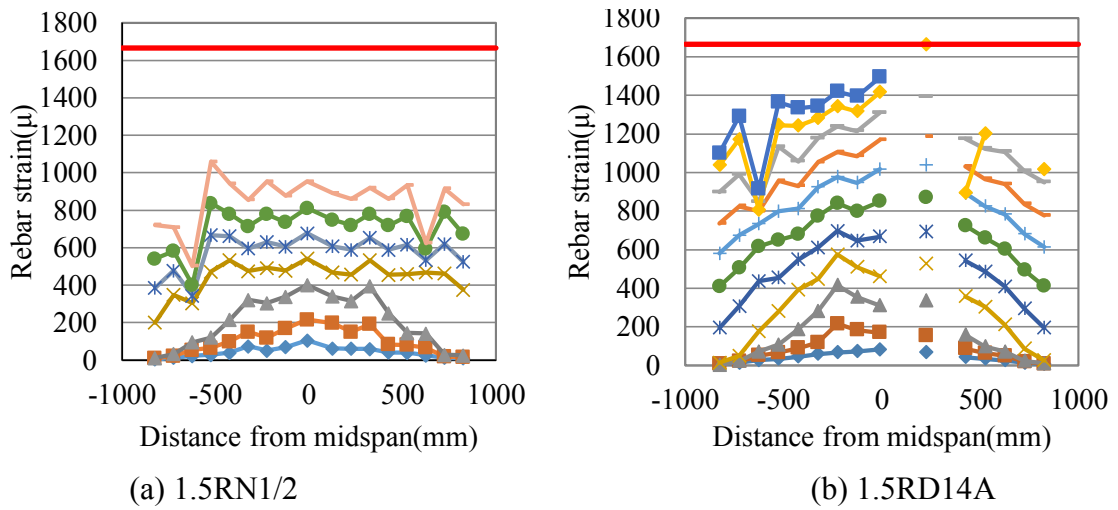
(a) 1.5RN1/2

(b) 1.5RD14A
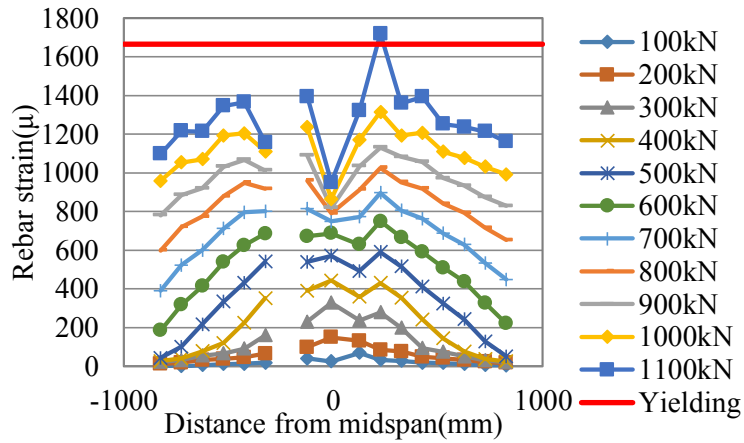
(c) 1.5RD28A

Fig. 6.9. Rebar strain distribution.

Fig. 6.10 shows the crack patterns. In the case of the control beam 1.5RN1/2, shear cracks occurred when the load reached at about 300kN, which caused the decline of stiffness. Then the dominant diagonal cracks spread, and the beam broke down abruptly. For the strengthened beam 1.5RD14A, when the load reached at about 500kN, the shear cracks were observed on UFC panels. Then the dominant shear cracks were formed when the load reached at 1000kN, and the beam finally resulted in the shear compression failure. Compared with the beam 1.5RD14A, the shear cracks were not observed in the beam 1.5D28A that broke down in the flexural mode.

(a) 1.5RN1/2

(b) 1.5RD14A   (c) 1.5RD28A
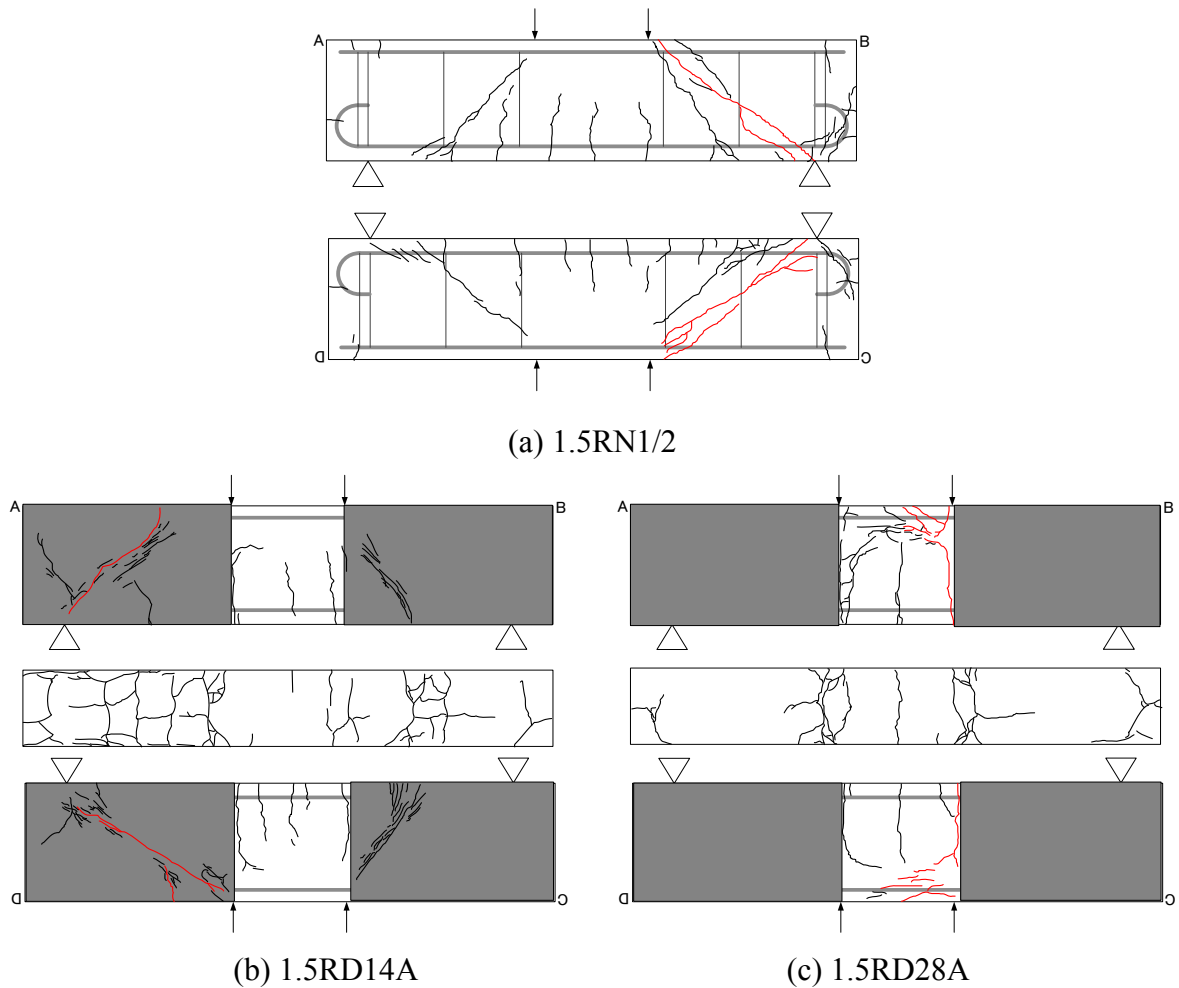
Fig. 6.10. Crack patterns.

6.4. DISCUSSION

6.4.1. Influence of size effect and UFC panel thickness

In the loading tests results, the improvements of the maximum load and failure mode observed in the 1/4 size RC beams were also found in the 1/2 size RC beams. The maximum load of the 1/4 size RC beams was upgraded by 40%, while that of the 1/2 size RC beams was raised by 45%. Moreover, the failure modes in the two beams were both ameliorated, and the ductility properties were also gained. On the other hand, a significant enhancement in the stiffness was only observed in the 1/2 size RC beams, and then, showed similar strengthening effects can be expected in the real size bridge girder, especially in the stiffness.

For the thickness of UFC panels, the integrity of matrix concrete and UFC panels was investigated. Fig. 6.11 shows the photos after removing the UFC panels. In the beam 1.5RD14A, several shear cracks were observed in the bonding area during loading tests.

(a) 1.5RD14A

(b) 1.5RD28A
Fig. 6.11. Photos after removing the UFC panels.

127

On the contrast, in the beam 1.5RD28A, there were no obvious shear crack occurred in the bonding area. Furthermore, it was more difficult to detach the UFC panels from 1.5RD28A than from 1.5RD14A. And an outstanding integrity was observed in the RC beam bonding with 28mm thickness UFC panels. It shows that a proper thickness of UFC panels should be chosen to upgrade the performance of RC beams.

6.4.2. Influence of anchorage reinforcement

According to the experimental results described in Chapter 3, the intensive strengthening on the shear region caused an unexpected failure: the destruction of the rebar anchorage section. Once the anchorage section was also reinforced by extending the region bonded to the UFC panels to the anchorage section, more desirable results were achieved. Fig. 6.12 shows the load strain relationships of the anchorage section. L and R mean the left side and right side respectively. In the control beam, the strain started rising abruptly when the load reached at about 300~400kN. On the contrary, because of the anchorage reinforcement, the value of strain was restricted because of the anchorage reinforcement effect. Until the load reached at 500~600kN, the value of strain increased gradually. Thus, the strengthening effects of the anchorage reinforcement were demonstrated in the loading tests.
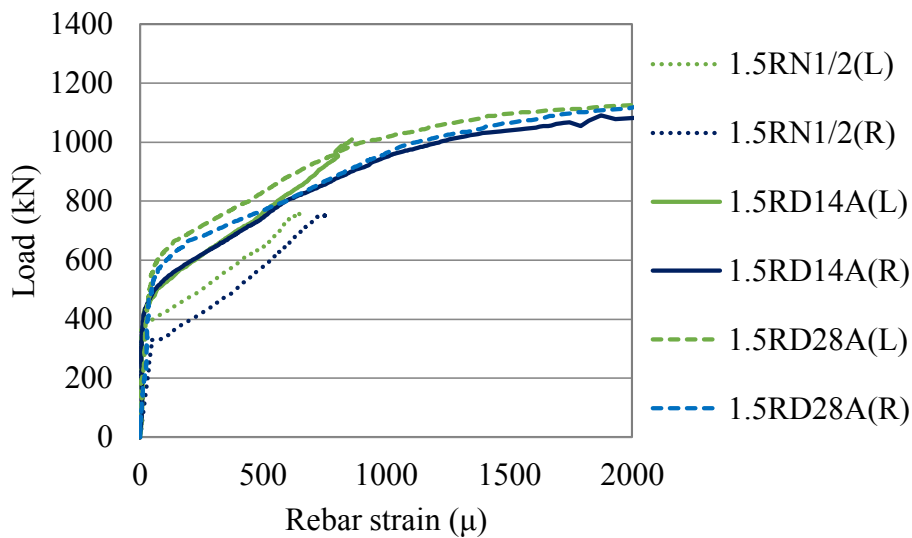

Fig. 6.12. Load strain relationships in the anchorage section.

6.4.3. Evaluation of shear capacity

To propose a proper design method for UFC panels strengthening, a calculation means which will be used to estimate the shear capacity of strengthened RC beams, was investigated. In the plain RC beams, the shear capacities are based on Standard Specifications for Concrete Structures [6]. In regard to the strengthened beams, an assumption will be made that the shear carried by the concrete matrix can approximate the shear capacity of the plain RC beam. Then, the ultimate shear capacity v_u can be calculated as follow:

$$V_u = V_{mat} + V_{UFC} \tag{1}$$

where V_u is the ultimate shear capacity, V_{mat} is the shear carried by concrete matrix, and V_{UFC} is the shear carried by UFC panels. The shear carried by UFC panels was calculated by Eq. (2) according to JSCE Recommendations [5].

$$V_{UFC} = V_{fd} + V_{rpcd} \tag{2}$$

where V_{fd} is the shear carried by the part of steel fiber (calculated in Eq. (3)), and V_{rpcd} is the shear carried by the part except steel fiber (calculated in Eq. (4)).

$$V_{fd} = (f_{vd}/\tan\beta_u) \cdot b_w \cdot z \tag{3}$$

where f_{vd} is the tensile strength of UFC panel (discussed below), β_u is the angle of the diagonal crack and the axial direction, b_w is the width of cross section of UFC panel, and z is equal to $d/1.15$

$$V_{rpcd} = 0.18\sqrt{f'_{cd}} \cdot b_w \cdot d \tag{4}$$

where f'_{cd} is the compressive strength of UFC panel, and d is the effective height.

Since the UFC was cast into a panel shape, the real tensile strength is difficult to determine when evaluating the shear force carried by the UFC panels. As is well known, there are two main types of tensile tests: uniaxial tensile tests ($f_{t,un}$) and splitting tensile tests ($f_{t,sp}$). Neither of these can represent the real tensile strength of the UFC panels due to differences in the orientation of the steel fibers. The orientation of the steel fibers is neither three-dimensional as in the cylinder in splitting tensile tests, nor uniaxial as in specimens used in uniaxial tensile testing. The real value should be between the two types of tensile tests.

The calculation results are given in Table 6.6. $V_{u,1}$ and $V_{u,2}$ are the evaluation values of the ultimate shear capacity based on $f_{t,un}$ and $f_{t,sp}$, respectively. Since the beam 1.5RD28A resulted in the flexural failure, the shear capacity was not evaluated here. For the shear carried by UFC panels (V_{UFC}), the evaluation value $V_{UFC,1}$ calculated by $f_{t,un}$ significantly overestimated the shear capacity of UFC panels ($V_{UFC,exp}$). On the other hand, the evaluation value $V_{UFC,2}$ calculated by $f_{t,sp}$ estimated the shear capacity of UFC panels within an acceptable error.

Comparing the experimental results with the evaluation results of the control beams, the shear capacity of 1.5RN1/4 was estimated on the conservative side, while the evaluation value of 1.5RN1/2 was beyond the experimental value. Consequently the ultimate shear capacity of 1.5RD14A was overestimated slightly.

The results demonstrated that, based on the splitting tensile strength, the shear force carried by UFC panels can be estimated within an acceptable error. Thus, this evaluation method of shear capacity can be expected to guide the design of UFC panel strengthening method. From the evaluation results, it can be seen that there exists some deviation between the evaluation value and the experimental value. The reason is that the changes of the failure mode and shear resisting mechanism due to the UFC panels strengthening were not considered. Thus, adding a safety coefficient would be a practical means to involve the influence from those unconcerned factors.

Table 6.6. Shear capacities of specimens.

| Specimen | Experimental results | | Evaluation results | | | | |
	$V_{max,exp}$ (kN)	$V_{UFC,exp}$ (kN)	V_{mat} (kN)	$V_{UFC,1}$ (by $f_{t,un}$) (kN)	$V_{u,1}$ (kN)	$V_{UFC,2}$ (by $f_{t,sp}$) (kN)	$V_{u,2}$ (kN)
1.5RN1/4	86.8	-	82.1	-	-	-	-
1.5RDA	121.5	34.7	82.1	44.7	126.8	30.9	113.0
1.5RN1/2	381.6	-	425.1	-	-	-	-
1.5RD14A	554.6	173.1	425.1	196.8	621.9	136.0	561.1
1.5RD28A	580.7	N/A	N/A	N/A	N/A	N/A	N/A

6.5.　CONCLUSIONS

The experimental investigations were conducted in terms of strengthening position, size effect and UFC panel thickness, and the loading test results demonstrated that this strengthening method achieved significantly positive effects. More summarized results are reported below.

1.　When strengthening the RC beams with low shear span ratio, an un-predictable failure mode (anchorage splitting failure) was observed. Thus, an anchorage reinforcement method was proposed, which extended the bonding region of UFC panel to the anchorage section. The strengthening results with the proposed anchorage reinforcement method demonstrated that the shear strength has been upgraded by 40% in the loading tests.

2.　The investigation of the size effect influence in the strengthening method is an important step in the practical applications. In this chapter, the strengthening effects on two different sizes beams were discussed. Comparing the 1/2 size and 1/4 size beams, similar strengthening improvements on shear capacity and ductility were obtained in the experimental results. But for the stiffness, the upgrading effect was only observed in the 1/2 size beams. Moreover, the experimental results proved that the shear strengthening effects by bonding UFC panels could be expected in the real size bridge girder.

3.　The JSCE recommendation equation was used to evaluate the shear force carried by UFC panels. The evaluation results showed good agreement with the experimental results. Based on the splitting tensile strength of UFC, the shear carried by UFC panels can be estimated with an acceptable error. This evaluation means of shear capacity of UFC panles can be expected to guide the design of the UFC panel strengthening. Moreover, adding a safety coefficient would be a practical means to involve the influence from the changes of the failure mode and shear resisting mechanism.

REFERENCES

1 Wang, J., Kohno, F., Morikawa, H., Kawaguchi, T., Shear Strengthening by Bonding with UFC Panels on RC Beams with Low Shear-Span Ratio, *Proceedings of the Concrete Structure Scenarios*, vol. 13, pp. 389-396, 2013.

2 Wang, J., Morikawa, H., Kawaguchi, T., Influence of Strengthening by UFC Panels and Patching Repair on Shear Resisting Mechanism of RC Members with Low Concrete Strength, *Proceedings of the Japan Concrete Institute*, 35(2), pp. 1381-1386, 2013.

3 Wang, J., Morikawa, H., Influence of Strengthening by Ultra High Strength Fiber Reinforced Concrete Panels on Shear Resisting Mechanism and Bond-Slip Behavior of Low Strength RC Members, *Proceedings of 3rd International Conference on Sustainable Construction and Technologies SCMT3*, e291, 2013.

4 Wang, J., Morikawa, H., Kawaguchi, T., Analytical Evaluations of Shear Strengthening of Low-strength RC Members by bonding with UFC Panels, *Proceedings of the Concrete Structure Scenarios*, vol. 12, pp. 1-8, 2012.

5 Japan Society of Civil Engineers, Recommendations for Design and Construction of Ultra High Strength Fiber Reinforced Concrete Structures (draft), September 2004.

6 Japan Society of Civil Engineers, Standard Specifications for Concrete Structures (Structural Performance Verification), pp.190-191, 2002

CHAPTER 7

Conclusion and Future Work

7.1. CONCLUSION OF THE THESIS

In order to meet the requirements of high durability, efficiency, reliability, short-duration and low-cost, in this study, a new shear strengthening method, bonding the panels made of UFC on the girder end of aging RC bridges, was proposed. The principle of the proposed shear strengthening method is to retard the opening and propagation of cracks around the ends of the RC beams by bonding UFC panels. There exist amounts of causes to rise the loss of structural performance for RC structures, such as physical damage and chemical deterioration. The strengthening effectiveness of bonding UFC panels on the RC structures with concrete degradation problem, such as the initial defect (low concrete strength), chloride attack and Alkali-Silica Reaction (ASR) damage will be discussed in this study. The conclusions of this thesis are given as follows.

In Chapter 2 (Basic Investigations on Shear Strengthening Effects of Bonding UFC Panels on RC Beams with Low Concrete Strength), when the shear-span ratio (a/d) is

equal to 2.5, the shear capacity of RC beams was enhanced and the failure mode was ameliorated by bonding the UFC panels. Especially when the DB type strengthening (bonding RC beams with round tensile rebars) was applied, the improvement of the structural performance of RC beams was confirmed. Moreover, comparing different types of tensile rebars, the results showed that a greater strengthening effectiveness and significant ductility were obtained in the beam with round tensile rebars. It is considered that a good performance can be expected when the DB type strengthening scheme is applied in the practical applications. When strengthening the RC beams with low shear span ratio, an un-predictable failure mode (anchorage splitting failure) was observed. Thus, an anchorage reinforcement method was proposed to extend the bonding region of UFC panel to the anchorage section. Based on the loading test results, the improvement on the shear strength (40%) and the destruction energy absorption were demonstrated, when the anchorage reinforcement method was applied. From the comparisons between the different shear-span ratios, it is inferred that the strengthening effect varies with the shear span ratios. It demonstrated that greater strengthening effects can be gained in RC beams with low shear span ratio.

In Chapter 3 (Investigations on Strengthening by Bonding UFC Panels on RC Beams with Low Shear-Span Ratio), by using the proposed shear strengthening method (bonding the UFC panels), a very positive effect on the load bearing capacity was obtained. Comparing to Group 1 (concrete strength is 18.5 MPa), a higher increase of the ultimate load (56%) and the initial stiffness (24%) were gained in Group 2 (concrete strength is 13.4 MPa) because of the lower concrete strength. And the brittle failure mode (shear failure) was also changed to the ductile mode (UFC panels blocking) in Group 2. Furthermore, from the experimental results, the shear capacity shared by UFC panels does not rely on the concrete matrix configuration, which can be evaluated separately from the matrix. The evaluation result shows the shear capacity shared by UFC panels can be estimated within an acceptable error range. Furthermore, more effort is still needed to verify and improve the design method of UFC panel strengthening on more specimens. According to the bond-slip testing results, it was found that the proposed UFC panel strengthening method affects the bond-slip properties of rebars. The maximum bond stress and softening behavior were both enhanced in case of small cover. Moreover, from the comparison of

experimental and FE analyses results, the validity of the modified bond model (modified according to the bond-slip tests) was verified. The original model underestimated the stiffness, while the modified model well captured the shear resisting behavior in the experimental results.

In Chapter 4 (Investigations on Strengthening by UFC Panels and Patch Repair on RC Beams Affected by Chloride Attack), two groups of specimens, Group 1 and Group 2 (with different shear-span ratio a/d), were used to evaluate the effects of the shear strengthening of UFC panels under different shear-span ratios (a/d = 2.5, 1.5). When a/d was equal to 2.5, the load bearing capacity and stiffness were enhanced by applying the patch repair. The concrete splitting around tensile rebars was delayed due to the relatively good bonding of PCM and rebars. However, the beam broke down in the interfacial debonding, which showed the integrality between the matrix concrete and PCM was hard to be secured. When repairing the RC beams with low shear-span ratio (a/d = 1.5) using PCM, an un-predictable brittle failure occurred. Besides, the decrease in load bearing capacity was observed. The side effect of applying patch repair on the structural performance should be paid attention especially for the RC beams with low a/d. Due to the strengthening effect of bonding UFC panels, the shear capacity and stiffness of RC beams were enhanced and the failure mode was ameliorated. Especially the problems such as the interfacial debonding, the decrease in shear capacity and the brittle failure observed in the repaired RC beams were all restricted. It can be said that the integrality and safety of repaired RC beams can be secured by bonding UFC panels.

In Chapter 5 (Investigations on Shear Behavior and strengthening by UFC Panels of RC beams affected by Alkali-Silica Reaction), two series of RC beams were cast to simulate the bridge girder (Series A) and T-shaped RC pier beam (Series B), respectively. The rebar restraint ratio and the exposure condition affected the degradation state in RC structures with ASR damage, which leaded to the different failures in loading tests. Due to the influence of preceding cracks and pre-stress, the load bearing mechanism changed from the diagonal tensile resisting mechanism to the arch mechanism, and the bearing capacity was enhanced consequently. In addition, even though some specimens were cast and exposed in the same conditions, different maximum load and stiffness were obtained

in the loading tests. The uncertainty and complexity of ASR damage were confirmed. Comparing the experimental and FE analytical results, the validity of analysis method proposed for ASR was verified. For ASR affected specimen, the no expansion model significantly underestimated the stiffness and load-bearing capacity. Conversely, the chemical pre-stress model showed a good agreement with the experimental results, in which the chemical pre-stress due to ASR was considered. Based on the different failure modes in Series A and Series B, different strengthening schemes were proposed to restrain the diagonal cracks or bond-split cracks. Using the proposed shear strengthening method (bonding the UFC panels) leaded to a very positive effect on the load bearing capacity in both Series A and Series B. Furthermore, the brittle failure mode was also changed to the ductile mode.

In Chapter 6 (Practical Study on Shear Strengthening of RC Beams by Bonding UFC Panels), the investigation of the size effect influence in the strengthening method is an important step in the practical applications. In this chapter, the strengthening effects on two different sizes beams were discussed. Comparing the 1/2 size and 1/4 size beams, similar strengthening improvements on shear capacity and ductility were obtained in the experimental results. But for the stiffness, the upgrading effect was only observed in the 1/2 size beams. Moreover, the experimental results proved that the shear strengthening effects by bonding UFC panels could be expected in the real size bridge girder. The JSCE recommendation equation was used to evaluate the shear force carried by UFC panels. The evaluation results showed a good agreement with the experimental results. Based on the splitting tensile strength of UFC, the shear carried by UFC panels can be estimated within an acceptable error. This evaluation means of shear capacity of UFC panles can be expected to guide the design of the UFC panel strengthening. Moreover, adding a safety coefficient would be a practical means to involve the influence from the changes of the failure mode and shear resisting mechanism.

7.2.   FUTURE RESEARCH DIRECTIONS

More work can be pursued along the directions of this research. Currently only the FE analyses under static loading was conducted. The influence of cyclic loading on RC members strengthened by bonding UFC panels is still needed to be studied. For example, the tests under cyclic loading can be carried out, then the proper analysis method will be investigated. The critical shear-span ratio and the maximum strengthening effectiveness of bonding UFC panels can be found out. Furthermore, the cyclic loading tests can be conducted on the existing RC bridge. The test data is useful to improve the analysis method.

Doctor Thesis, Kobe University

"Study on Shear Strengthening of RC Structures by Bonding Ultra High Strength Fiber Reinforced Concrete Panels", 137 pages

Submitted on Jan, 22nd, 2015

The date of publication is printed in cover of repository version published in Kobe University Repository Kernel.